

AERODYNAMIC STUDY OF AXIAL DIFFUSER

A Thesis Submitted to

Delhi Technological University

For the Award of Degree of

Doctor of Philosophy

In

Mechanical Engineering

By

DEVESH KUMAR

(2K12/Ph.D./ME/11)

Under the Supervision of

Prof. B. B. Arora

Professor, Department of Mechanical Engineering



Department of Mechanical Engineering

Delhi Technological University

(Formerly Delhi College of Engineering)

Delhi-110042, India

JULY-2020

AERODYNAMIC STUDY OF AXIAL DIFFUSER

A Thesis Submitted to

Delhi Technological University

For the Award of Degree of

Doctor of Philosophy

In

Mechanical Engineering

By

DEVESH KUMAR

(2K12/Ph.D./ME/ 11)

Under the Supervision of

Dr. B. B. Arora

Professor, Department of Mechanical Engineering



Department of Mechanical Engineering

Delhi Technological University
(Formerly Delhi college of Engineering)

Delhi-110042, India

JULY-2020

©DELHI TECHNOLOGICAL UNIVERSITY-2020
ALL RIGHTS RESERVED

DECLARATION

I hereby declare that the work which being presented in the major thesis entitled “**Aerodynamic Study of Axial Diffuser**” in the partial fulfilment for the award of degree of Ph.D. in “**THERMAL ENGINEERING**” submitted to **Delhi Technological University Delhi**, is an authentic record of my own work carried out under the supervision of **Prof. B. B. ARORA, Department of Mechanical Engineering, Delhi Technological University, Delhi**. I have not submitted the contents in this thesis for the award of any other Degree or Diploma or any other purpose whatsoever.

Date: July 13, 2020

(Devesh Kumar)

2K16/Ph.D./ME/11

Department of Mechanical Engineering

Delhi Technological University,

Delhi-110042, India

CERTIFICATE

This is to certify that the thesis entitled “**Aerodynamic Study of Axial Diffuser**” being submitted by **Devesh Kumar (Roll No. 2k12/PhD/ME/11)** for the award of the degree of **Doctor of Philosophy** is a record of bonafide research work carried out by him. **Mr. Devesh Kumar** worked under my guidance and supervision and has fulfilled the requirements for the submission of this thesis, which to my knowledge has reached the requisite standard. The results contained herein have not been submitted in part or in full, to any other university or Institute for the award of any degree.

Dr. B. B. Arora

(Supervisor)

Professor

Department of Mechanical Engineering

Delhi Technological University, Delhi

ACKNOWLEDGMENTS

It is a great pleasure to have the opportunity to extend my heartiest felt gratitude to everybody who helped me throughout the Ph.D. work.

It is distinct pleasure to express my deep sense of gratitude and indebtedness to my learned supervisor **Prof. B. B. ARORA, Professor, Department of Mechanical Engineering, Delhi Technological University Delhi**, for their invaluable guidance and encouragement. Their continuous inspiration only has made me able to complete the Ph.D. work. I am thankful to my friends and colleagues for their unconditional support and motivation for complete the Ph.D. work. I would like to thank Mr. Hardial Singh and Mr. Ashish Misra for their kind help, fruitful discussion and wisdom.

Above all, my heartfelt thanks go to my wife and daughter. It was impossible to finish Ph.D. work without their non-stopping encouragement and support. I admire my wife's sincere efforts in providing support at various stages. I also thank all those who helped and supported me directly and indirectly.

Date: July 13, 2020

Place: Delhi

(Devesh Kumar)

2K12/Ph.D./ME/11

Department of Mechanical Engineering

Delhi Technological University,

Delhi-110042, India

ABSTRACT

A diffuser is a device which is generally used to convert the kinetic energy of the moving fluid into pressure energy. When a fluid passes through diffuser it is retarded and diffusion comes into picture. Diffuser is an important member in a power plant, which generally increases the efficiency of the power plant by increasing the pressure. The requirements of fuels and water can be reduced and saved for the society with the help of good design diffuser. So, diffuser is a very important device. Lot of experimental research work has been done on the diffuser, but mathematical modelling is scanty available. Work on annular diffuser is also scanty available. The analysis of flow through annular diffuser are not studied at intermediate areas ratios 2.5, 3.5 and 4.5 etc. The present study involves the Computational Fluid Dynamic (CFD) analysis of annular diffuser with parallel hub and diverging casing. The characteristic quantities such as longitudinal velocity, swirl velocity, pressure recovery coefficient, flow patterns, flow separation and flow reversals have been analyzed graphically and numerically by using FLUENT Code. Variation of longitudinal velocity and Swirl velocity have been analyzed along the different diffuser passages heights at different traverses of $(x/L) = 10\%$, 20% , 40% , 60% , 80% and 90% along the axial direction of the annular diffuser. The variation of pressure recovery coefficient has been also analysed along the walls of Casing and Hub of the annular axial diffuser. We used

second order scheme for momentum, swirl velocity and turbulent kinetic energy and Presto scheme for pressure. The Residual have been taken as 10^{-6} for x-velocity. Different turbulence models were used to obtain the results and finally it was found that the results of RNG k- ϵ turbulent model shows good agreements with the experimental results .So RNG k- ϵ turbulent model have been used to analyse the flow through the annular diffuser. Parametric investigations have been done at different area ratios of (2, 3, 2.5 & 4) and different swirl angles at the inlet (0^0 , 7.5^0 , 12^0 , 17^0 & 25^0). Finally, the results are presented in terms of non-dimensional longitudinal velocity, swirl velocity and Pressure recovery coefficients and with the help of these results separation and development of flow through annular diffuser have been discussed.

LIST OF PUBLICATIONS

- [1] **Devesh Kumar** and B. B. Arora, “Study and Analysis of Parallel Hub and Diverging Casing Axial Annular Diffuser with Area Ratios of 4”, *Journal of Emerging Technologies and Innovative Research* (ISSN-2349-5162), vol. 5, no. 10, pp. 533-542, October 2018 (Available Online).
- [2] **Devesh Kumar** and B. B. Arora, “CFD Analysis of Flow Through Axial Annular Diffuser at Area Ratio 2.5 and Casing Diverging Angle of 6°”, *Journal of Emerging Technologies and Innovative Research* (ISSN-2349-5162), vol. 6, no. 1, pp. 536-544, January 2019 (Available Online).
- [3] **Devesh Kumar** and B. B. Arora, “To Study and Analyse the Variation of Pressure Recovery Coefficient at the Walls of Axial Annular Diffuser at Area Ratio 2.5 and Casing Diverging Angle of 6° By CFD”, *International Journal of Advance Research and Innovation*, (ISSN 2347-3258), vol. 7, no. 3, pp. 269-272, 15 June 2019 (Available online).
- [4] **Devesh Kumar** and B. B. Arora, “Analysis of Flow through Parallel Hub and Diverging Casing Annular Diffuser of Area Ratio 2 with or without Swirl”, *Int. Conf. on Advanced Production and Industrial Engineering* (ICAPIE-2018), Paper ID: ICAPIE-2018-IDA511, October 5, 2018 (Accepted and Presented).
- [5] **Devesh Kumar** and B. B. Arora “To Study and Analyse the Variation of Pressure Recovery Coefficient at the Walls of Axial Annular Diffuser at Area Ratio 2.5 and Casing Diverging Angle of 6° By CFD”, *Int. Conf. on Advanced Research and Innovation* (ICARI-2019), January 20, 2019 (Accepted and Presented, ISBN-978-93-5346-324-3).

TABLE OF CONTENTS

ACKNOWLEDGMENTS	v
ABSTRACT.....	vi
LIST OF PUBLICATIONS	viii
TABLE OF CONTENTS.....	ix
LIST OF FIGURES	xiii
LIST OF TABLES.....	xvi
NOMENCLATURE.....	xvii
LIST OF SYMBOLS.....	xviii
LIST OF SUBSCRIPTS.....	xix
AUTHOR BIOGRAPHY	xx
CHAPTER1: INTRODUCTION.....	1-11
1.1 Introduction.....	1
1.2 Classification of diffusers.....	4
1.2.1 Axial Diffuser.....	4
1.2.2 Radial Diffuser.....	4
1.2.3 Curved wall Diffuser.....	5
1.3 Performance of Diffuser	5
1.3.1 The geometric parameters.....	5
1.3.2 Dynamical parameters.....	6

1.3.3	Flow parameters.....	6
1.3.4	Boundary Layer Parameters.....	6
1.4.	Performance Calculation Parameters.....	7
1.4.1	Static Pressure Recovery Coefficient.....	7
1.4.2	Diffuser Effectiveness.....	7
1.4.3	Total Pressure Loss Coefficient.....	8
1.5	The design requirements for a good diffuser.....	8
1.6	Limitation of diffuser design.....	9
1.7	Overview of the thesis	9
CHAPTER 2: Literature Review.....		12-28
2.1	Introduction.....	12
2.2	Geometry of the diffuser	12
2.3	Effect of flow parameters.....	18
2.3.1	Inlet swirl flow.....	18
2.3.2	Inlet turbulence and working fluid.....	22
2.3.3	Mach Number Influence.....	24
2.3.4	Reynold Number Influence.....	24
2.4	Aerodynamic Blockage.....	25
2.5.	Boundary layer parameter.....	26
2.5.1	Boundary Layer Suction.....	27
2.5.2	Blowing and Injection.....	27
2.6	Research Gap	28

2.7 Objectives	28
----------------------	----

CHAPTER 3: Experimental Setup and Investigation.....29-43

3.1 Introduction.....	29
3.2 Experimental set up.....	30
3.3 Swirl generation and Specifications.....	32
3.4 Geometry of the Test-Diffusers	33
3.5. Description of Geometry of the diffuser.....	33
3.6 Dimensional details of the annular diffuser	35
3.7 Diffuser Inlet Location	35
3.8 Instrumentation.....	36
3.8.1 Three tube impact pressure prove (cobra probe).....	36
3.8.2 Traversing Mechanism.....	36
3.8.3 Manometers.....	37
3.9 Inlet conditions.....	38
3.10 Experimental Procedure.....	38
3.10.1 Measurement of the wall static pressure.....	39
3.10.2 Measurement of the mean velocity field.....	39
3.10.3 Flow visualization.....	40
3.11 Uncertainty Measurement.....	41

CHAPTER 4: Computational and Mathematical Modelling44-62

4.1 Introduction	44
4.2. Planning of CFD Analysis.....	45
4.2.1 Geometry Creation.....	45
4.2.2 Grid Generation and its Independence.....	45
4.2.3 Boundary Conditions	46

4.2.3.1 Inlet boundary condition	46
4.2.3.2 Outlet boundary condition.....	46
4.2.3.3 Surface or wall boundary conditions.....	47
4.2.4 Choice of Physical Models.....	47
4.2.5 Determination of the Solution Procedure.....	47
4.3. Mathematical Modeling.....	48
4.4 Conservation principals.....	49
4.4.1 The Mass Conservation Equation (Continuity Equation).....	49
4.4.2 Momentum Conservation Equations.....	50
4.5 Turbulence Modelling.....	52
4.5.1 Selection of a Turbulence Model.....	52
4.5.2 The Standard k- ϵ Model.....	53
4.5.3 The RNG k- ϵ Model	55
4.5.4. Realizable k- ϵ Model	57
4.5.5 Turbulence Modeling in Swirling Flows.....	59
4.6 Simulati on Procedure.....	59
4.7 Methodology adopted	61
CHAPTER 5: Validation.....	63-68
5.1 Introduction.....	63
5.2 Grid Independence	63
5.3 Validation of different turbulence model.....	66
CHAPTER 6: Results and Discussion.....	69-95
CHAPTER 7: Conclusions and Future Scope.....	96-97
CHAPTER 8 References.....	98-110

LIST OF FIGURES

Figure 3.1 : Block diagram of Experimental setup.....31

Figure 3.2 : Traversing mechanism for experimental setup..... 29

Figure 3.3 : Centrifugal blower used for experimental set up..... 30

Figure 3.4 : Geometry of the annular diffuser with parallel hub and diverging casing.
 34

Figure-4.1: Flow-Chart for CFD Modeling and Simulation.....61

Figure-5.1: Grid independence test at different mesh size for longitudinal velocity
 versus non-dimensional height at axial position $(x/L) = 10\%$
64

Figure-5.2: Validation of Turbulence Model with Experimental Results of Longitudinal
 Velocity of annular diffuser of AR=2, equivalent cone angle 20° at different non-
 dimensional diffuser passage length at axial location of 80% and 90%
 respectively.....66

Figure-5.3: Validation of Turbulence Model with Experimental Results of Swirl
 Velocity of annular diffuser of AR=2, equivalent cone angle 20° at different non-
 dimensional diffuser passage height along the length *i.e.* $x/L = 0.6$ to 0.9 ...67

Figure-6.1(a): Variation of Longitudinal Velocity with respect to non-dimensional radial
 height (y/Y_{max}) for equivalent cone angle 20° and area ratio of 2 at different axial
 positions (10%, 20%, 40%, 60%, 80% and 90%).....71

Figure-6.1(b): Variation of Swirl Velocity with respect to non-dimensional radial diffuser passage heights (y/Y_{max}) for equivalent cone angle 20° and area ratio of 2 at different axial positions (10%, 20%, 40%, 60%, 80% and 90%).....73

Figure-6.2(a): Variation of Longitudinal Velocity with respect to non-dimensional radial height (y/Y_{max}) for equivalent cone angle 20° and area ratio of 3 at different axial positions (10%, 20%, 40%, 60%, 80% and 90%).....75

Figure-6.2 (b): Variation of Swirl Velocity with respect to non-dimensional radial diffuser passage heights (y/Y_{max}) by taking the cone angle of 20° , Area ratio of 3 and swirl angles of (0° to 25°) at different axial positions(10%, 20% ,40% ,60%,80% and 90%).....77

Figure-6.3(a): Variation of Longitudinal Velocity with respect to non-dimensional radial height (y/Y_{max}) for equivalent cone angle 20° and area ratio of 4 at different axial positions (10%, 20%, 40%, 60%, 80% and 90%).....78

Figure-6.3(b): Variation of Swirl Velocity with respect to non-dimensional radial diffuser passage heights (y/Y_{max}) by taking the cone angle of 20° , Area ratio of 4 and swirl angles varied from (0° to 25°) at different axial positions(10%, 20% ,40% ,60%,80% and 90%).....80

Figure-6.4(a):Variation of Longitudinal Velocity with respect to non-dimensional radial height (y/Y_{max}) for casing diverging angle of 6° , Area ratio of 2.5 and inlet swirl angles of (0° to 25°) at different axial positions(10%, 20% ,40% ,60%,80% and 90%).....81

Figure-6.4(b): Variation of Swirl Velocity with respect to non-dimensional radial diffuser passage heights (y/Y_{max}) by taking the casing diverging angle of 6° , Area ratio of 2.5 and swirl angles of (0° to 25°) at different axial positions (10%, 20%, 40%, 60%, 80% and 90%).	83
Fig.6.5 (a) Velocity streamline diagram at AR = 2 and Swirl angle = 0°	85
Fig.6.5 (b) Velocity streamline diagram at AR = 2 and Swirl angle = 7.5°	86
Fig.6.5 (c) Velocity streamline diagram at AR = 2 and Swirl angle = 12°	86
Fig.6.5 (d) Velocity streamline diagram at AR = 2 and Swirl angle = 17°	87
Fig.6.5 (e) Velocity streamline diagram at AR = 2 and Swirl angle = 25°	87
Figure-6.6 Variation of pressure recovery coefficient for area ratios of 2, 3 & 4 along the casing of annular diffuser	88.
Figure-6.7 VARIATION of pressure coefficient for area ratios of 2, 3, & 4 along the hub of annular diffuser	90
Fig. 6.8 shows the variation of pressure recovery coefficients at are area ratio of 2.5 and different swirl angles at the casing wall of axial annular diffuser	92
Fig. 6.9 shows the variation of pressure recovery coefficients at are area ratio of 2.5 and different swirl angles at the hub wall of axial annular diffuser	93

LIST OF TABLES

Table 3.1: Geometry of the diffuser.	33
Table 3.2: Dimensional details of Annular axial Diffuser with AR of 2, 3, 4 and coneAngle of 20 ⁰	35
Table 3.3: Uncertainty in measurement by different instruments	42
Table.6.1: Summary of maximum pressure recovery coefficient on the Casing wall and its nature	89
Table 6.2: Summary of maximum pressure recovery coefficient on the hub wall and its nature	90

NOMENCLATURE

A	Area
B	Blockage Factor
AR	Area Ratio
C	Constants
C_p	Pressure Recovery Coefficient
C_{pi}	Ideal Pressure Recovery Coefficient
θ	Hub angle
D	Diameter
P	Static Pressure
P_t	Total Pressure
Re	Reynolds Number
V	Velocity
x, y, z	Cartesian Coordinate System
w	Swirl velocity
G	Generation of Turbulence Kinetic Energy
Y_M	Fluctuating Dilatation in Compressible Turbulence
S	Swirl Number of Swirling flow

LIST OF SYMBOLS

μ	Dynamic Viscosity
μ_t	Turbulent Viscosity
k	Turbulent Kinetic Energy
ρ	Density of flowing fluid
θ	Wall Angle
2θ	Equivalent Cone Angle
ξ	Total Pressure Loss Co-Efficient
ν	Kinematics Viscosity
$\bar{\tau}$	Stress Tensor
ε	Turbulent Kinetic Energy Dissipation Rate
η	Diffuser Effectiveness

LIST OF SUBSCRIPTS

i	Ideal pressure
hi	Hub inlet
ho	Hub outlet
ci	Casing inlet
co	Casing outlet
r	Radial direction
m	Maximum
x	Axial direction
z	Swirl flow direction
eq	Equivalent
in	Inlet
out	Outlet

AUTHOR BIOGRAPHY

	<p>Devesh Kumar</p> <p>2K12/Ph.D./ME/11</p> <p>Department of Mechanical Engineering, Delhi Technological University, Delhi, India</p> <p>Email: dev77mmmut@gmail.com , dkme@mmmut.ac.in</p>
---	--

Devesh Kumar has received the Bachelor of Technology (B.Tech.) from Harcourt Butler Technological Institute (BHTI) Kanpur (UP), in the year 1999 now Harcourt Butler Technological University (BHTU) and the Master of Technology (M.Tech.) from Indian Institute of Technology Delhi (IITD), India in the year 2005. He is currently pursuing Ph.D. from Department of Mechanical Engineering, Delhi Technological University (DTU) Delhi, India-110042 (Formerly known as Delhi College of Engineering, DCE). Presently, he is working as Assistant Professor in Department of Mechanical Engineering, Madan Mohan Malaviya University of Technology (MMMUT) Gorakhpur (UP). His area of research includes Computational Fluid Dynamics, Fluid Engineering and Solar Energy.

CHAPTER-1

INTRODUCTION

1.1 Introduction

Diffusers are the main components for field of Fluid handling devices. Diffuser is a component which is generally used to convert the flow energy in to Pressure energy by retarding the flowing fluid. It is a typical task to obtain effective retarded flow than an effective accelerated flow. The main function of the diffuser is to obtain the high static pressure by reducing the velocity of the flowing fluid and maintain the uniform flow at the exit side of the diffuser. The uniform flow at the outlet of the diffuser can be achieved if there is no secondary flow there. But in extreme cases if the secondary flow has the magnitude less than 10 % of the average velocity, the flow can be assumed uniform.

We know that diffusion is a phenomenon in which flow retards and detach from the surface of the diffuser by reversing its direction .This separated flow with reverse direction moves in the direction of the pressure gradient. Flow separation is a phenomenon which reduces the performance of the diffuser it should be avoided due to the invoked pressure loss. The position of flow separation and flow reversal in diffuser is not defined by the geometry but entirely by the pressure gradient. It is very difficult to predict the flow through Diffuser with the help of numerical means due to sensitivity of diffuser for the flow **Kumar et al. [1 and 2]**. Formation of eddies with transfer or loss of some kinetic energy in to internal energy may result in reduction of useful pressure rise in the case of wide angle diffuser. If divergence angle is small then the length of the diffuser increases. Skin friction in the long diffuser may cause reduction in pressure rise with increase in length.

Diffusers are essential component in many fluid handling Systems such as in aircraft, gas turbine, power plant, piping industries, centrifugal compressor, axial flow compressor, combustion chamber and wind tunnel.

Flow through diffuser is described by considering a rapid growth of the boundary layer, leading to various degrees of irregularity in the flow pattern, non-uniformity of the velocity profile, total pressure loss, instability and recirculation if flow separates. Experimental observations help the researchers to reduce the unwanted effects thereby optimizing the retrieval of the static pressure rise. Experimental studies combined with the empirical relations or analytical studies help in improving the diffuser performance [1].

Geometrical and dynamical parameters affects the performance of the diffuser. Inlet length, diameter of the duct, area ratio, and angle of divergence, diverging length and geometry of the outlet by maintaining free or submerged discharge conditions controls the performance of the diffuser. Reynolds number, Mach number, boundary layer parameters and inlet velocity etc. are some dynamical parameters which also change the effectiveness of the diffuser. Geometrical parameters such as the inlet and outlet. Area ratio, inlet radius ratio, diverging length and two walls angles are the important variables which can change the performance of the diffuser and also defined the geometry of the given diffuser.

Swirling flow in the diffuser is the main parameter which controls the flow separation and therefore increasing the effectiveness of the diffuser. The swirl flow at the inlet of the diffuser can be generated with the help of compressor, pump and inlet guide vanes at the inlet of the diffuser. Swirl flow can also be produced with the rotary motion of the central shaft such as hub of the diffuser in the case of annular diffuser. The swirling flow can also be produce by rotary motion of the internal shaft inside the diffuser surface. Introduction of swirling flow

changes the direction of the velocity field too much and also changes the effectiveness of the given system.

Diffusers with inside surface i.e. annular diffusers are used in industry due to its importance in the industry have received attention in the recent years. Annular diffusers are generally used in aircraft industry due to restriction of space. Annular diffuser is generally used to increase the pressure up to maximum value in available shortest possible length. Manoj Kumar Gopaliya [14 and 48]. Better pressure recovery can be obtained in wide angle diffuser with the presence of inside surface such as hub to guide the flow outwards in the annular diffuser. There are different types of geometric combinations are possible due to presence of inner surface that can be modify independently with respect to casing of the annular diffuser. It is difficult to describe necessary geometric parameters due to the presence of large numbers of independent variables in annular diffuser Goebel and Japikse [73]. Annular diffuser effectively operates the combustor of a jet engine where pressure falls by reducing the total pressure loss. Diffusers are the required part for good turbo machinery performance because they increase the performance of a turbo machinery by increasing the pressure recovery and efficiency. It is very known fact that annular diffuser are complex in nature due to presence of inner wall which guide the flow outwards.

It is tedious and time taken to go for experiment methods in case of annular diffuser due to interconnections of various parameters. If we changed one parameter then setup will have to be modified. So experimental analysis of annular diffuser is not economic and due to this reason Computational fluid dynamic approach has become the important tool to analyze and calculate the performance of annular diffuser Arora et al [2005].

1.2 CLASSIFICATION OF DIFFUSERS

1.2.1 Axial Diffuser

In axial diffusers, fluid flow takes place along the direction of the length which is parallel to the axis of diffuser. The increase in the static pressure is achieved with reduction of kinetic energy in the diffuser. There is increase in static pressure due to the retardation of the flow velocity in the direction of fluid flow. Axial diffuser can be further divided in to the following:

- Conical diffuser
- Channel diffuser
- Annular diffuser

Types of annular diffuser

- Constant diameter central shaft and enlarging outer surface.
- Central shaft and outer surface enlarging - equal angles
- Both hub and casing diverging – Unequal angles
- Converging hub and diverging Casing.

1.2.2 Radial Diffusers

Flow along the radial outward direction in confined space between two boundaries. It can be classified in to two groups:

- Vanned diffuser
- Vane less diffuser

In Vanned diffuser curved blades are present in the diffuser but in vane less type there is no blades in the diffusing area.

1.2.3 Curved Wall Diffuser

Curved wall diffuser is generally used where space is limited. Due to curvature high turbulence and non-uniformity occur in these types of diffuser. In aircraft industry this type of diffusers are generally used. The performance of the curved wall diffuser depends on the radius of curvature, offset at the inlet or the outlet, geometric parameters and the inlet conditions provided. The curved walls diffusers are generally used where the less space is available. Due to restriction of the space, the application of curved diffuser is limited up to aircrafts, combustor of jet engines etc.

Different types of curved wall diffusers are given below:

- Y shaped diffuser
- L shaped diffuser
- S shaped diffuser

1.3 Performance of Diffuser

The performance of diffuser mainly depends on the following parameters are given below:

- Geometrical parameters
- Dynamical parameters
- Flow parameters
- Boundary layer parameter

1.3.1 Different Geometric Parameters

- Inlet length
- Outlet length

- Diffusion Length
- Equivalent Cone angle
- Non-dimensional length
- Area Ratio , $AR = A_2 / A_1$
- Aspect Ratio, $AS = b / W_1$

1.3.2 Dynamical Parameters

- Boundary layer parameter
- Reynolds Number
- Mach number
- Inlet velocity profile

1.3.3 Flow Parameters

- Aerodynamic Blockage
- Inlet Swirl
- Inlet Turbulence
- Mach Number Influence
- Reynolds Number

1.3.4 Boundary Layer Parameters

- Boundary Layer Suction
- Blowing and Injection

In the present study annular diffuser have been analyzed by studying the development of flow, flow separation, flow reversal and influence of the swirl flow on the effectiveness of the diffuser by changing the area ratio from 2 to 4 and at different swirl intensities.

1.4 Performance Calculation Parameters

Performance parameters are the parameters which determines the effectiveness of the diffuser. Performance parameters are the key to judge whether a diffuser suits for a fluid flow or not. Different performance terms are needed to calculate the different performance parameters are given below:

1.4.1 Static Pressure Recovery Coefficient

It is defined as the ratio of change of pressure between the inlet and outlet of the diffuser with respect to inlet dynamic head available at the inlet of the diffuser.

$$C_p = \frac{P_2 - P_1}{\frac{1}{2} \rho V_{avg}^2} \quad (1.1)$$

Here numbers 1 stands for inlet and 2 stands for outlet of the diffuser, V_{avg} stands for average flow inlet velocity of the diffuser. The recovery of the static pressure will be maximum by assuming the isentropic flow through the diffuser. Then, by employing the mass balance equation, the equation (1.1) can be changed in the form as shown in the equation (1.2) by assuming the incompressible flow.

$$C_{pi} = 1 - \frac{1}{AR^2} \quad (1.2)$$

1.4.2 Diffuser Effectiveness

Diffuser Effectiveness is an important parameter to judge the performance of the diffuser and it is equal to the ratio of pressure recovery coefficients in actual and ideal case. Isentropic flow is assumed in the case of ideal flow.

Diffuser effectiveness is the crucial factor for judging the effectiveness of the diffuser for Unknown conditions relative to available data.

$$\eta = \frac{C_p}{C_{pi}} \quad (1.3)$$

1.4.3 Coefficient of Total Pressure Loss

The total pressure loss coefficient reflects the efficiency of diffusion and drag of the system. The most common definition of loss coefficient is the ratio of total pressure rise to the inlet dynamic head of the diffuser. Efficiency of diffusion and drag of the system depends on the coefficient of total pressure loss.

$$K = \frac{P_{01} - P_{02}}{\frac{1}{2} \rho V_{av}^2} \quad (1.4)$$

There are the chances of flow separation, pressure loss, fall in the performance of the diffuser and damage of the downstream equipment in presence of positive pressure gradient (adverse pressure gradients). For avoiding above mentioned problems the value of the adverse pressure gradient should be below a critical limit by maintaining the divergence length and area ratio of the diffuser.

1.5 Necessary Conditions to Design a Good Diffuser:

- To move the fluid flow efficiently and effectively through the diffuser.
- Must be able to convert energy of the flowing fluid into pressure energy.
- Diffuser should be able to work effectively at various types of inlet conditions such as Extreme swirl, blockage and Mach number.
- Diffuser should be capable to discharge the fluid with reasonable velocity without Separation of flow.

- Must be able to achieve Pressure recovery over a short axial length.

1.6 Limitation of Diffuser Design

While obtaining the best possible design, some limitations are imposed on a diffuser.

- Limited length
- Specified area ratio
- Specified cross- sectional shape
- Maximum static pressure recovery
- Minimum stagnation pressure loss

So it can be stated that the performance of the diffuser directly and indirectly influences the overall efficiency of the turbo machine. Thus the detailed phenomenon which occurs in diffusing portion of diffuser must be carefully studied and thoroughly optimized if good turbo machinery performance is to be obtained.

1.7 Overview of the Thesis

The complete thesis is arranged in seven chapters.

Chapter 1: Introduction

In this chapter general concept of working, effect of area ratio, cone angle and effect of swirl on axial diffusers are introduced. The importance of the diffuser and objective of the study are briefly discussed in this chapter.

Chapter 2: Literature Survey

Chapter 2 presents a detailed literature survey of study and analysis of axial diffusers and

effect of different parameters such as swirling flow at the inlet, divergence angle, area ratio, inlet velocity profiles, blockage factor, Reynolds number and boundary layer suction and injection on the performance of the diffuser.

Chapter3: Experimental Investigation

This chapter shows the geometrical details of the axial annular diffuser which is used for experimentation. The detailed description about the experimental setup of the annular axial diffuser by mentioning the different components and the working have been shown. In this chapter the working of different instruments which are used for instrumentation are also shown.

Chapter 4: CFD Modeling

This chapter shows the CFD and Mathematical modeling of the axial annular diffuser. Here Different mathematical equations, turbulence models and .Methodology adopted to solve a problem have been also discussed in this chapter.

Chapter 5: Validation

Chapter-5 shows the validation of Computational results with the obtained experimental results.

Chapter 6: Results and Discussion

This chapter covers the study and analysis of flow through Constant diameter central shaft i.e. hub and enlarging outer surface i.e. Casing with various area ratio 2, 2.5, 3 and 4 with or without swirl for the annular diffuser. In this chapter the variation of longitudinal velocity and swirl velocity with respect to diffuser passage height have been analyzed with and without swirl. In this chapter Variation of Pressure recovery coefficients have been analyzed on the

casing and hub of the diffuser.

Chapter 7: Conclusions and Scope of the Future

This chapter shows the conclusions of the results obtained and shows the proposed future work.

CHAPTER 2

LITERATURE REVIEW

This chapter presents a detailed literature survey of study and analysis of axial diffusers and effect of different parameters such as swirling flow at the inlet, divergence angle, area ratio, inlet velocity profiles, blockage factor, Reynolds number and boundary layer suction and injection on the performance of the diffuser.

2.1 Introduction

This chapter covers the detailed literature survey of study and analysis of diffusers such as conical and annular diffuser by the different researchers. The performance of the diffuser depends on flow separation, pressure recovery coefficient, pressure loss coefficient, effectiveness, area ratio, diverging length, diverging angle and swirl flow. If the divergence angle is large, this will cause of formation of eddies with transfer of some kinetic energy into internal energy and thus reduction in useful pressure rise. When the angle of divergence will be small, diffuser will be long and therefore a high value of skin friction loss will occur. This chapter consists the study of development of flow, flow reversals, separation of flow and effect of coefficient of pressure recovery, pressure loss coefficient and effectiveness on the performance of diffuser by considering the work of different research. The literature survey of the diffusers by considering the effect of different parameters are shown below:

2.2 Geometry of the diffuser

Some of the researchers shows the geometrical parameters plays an important role in designing the axial annular diffuser because performance of diffuser depends on area ratio,

diverging length and cone angle. The literature review of the axial flow diffuser by taking area ratio, cone angle, diverging length, different shape of the diffuser and effect of strut in to consideration are shown below:

B. B. Arora and B. D. Pathak [5] performed the performance analysis of diffuser of cone angle 10° at different swirl angles by using computational approach (CFD) and Renormalization group RNG turbulence model. In the present work different geometry of the diffuser were analyzed and Pressure recovery coefficient was calculated. From the results it was clear that the pressure recovery coefficient was more for diffuser with hub and casing diverging with the same angle. The CFD results were validated with experimental work.

S. N. Singh *et al.* [7] analyzed the four diffusers PDHC, UDHC, SHDC and CHDC with cone angle of 15° , axial length 278 mm and area ratio 3. The results were presented in the forms of coefficients of pressure gain, total pressure loss coefficient, flow behavior i.e. development of flow separation and flow reversals at casing and hub walls. It was shown that the performance of PDHC and UDHC diffusers was good for the swirl 0° to 30° after that it decreases. SHDC and CHDC were highly sensitive to swirl. The optimum value of swirl was 30° and 10° for (PDHC, UDHC) and (SHDC, CHDC).

P. Phatangare *et al.* [66] analyzed the diffuser experimentally by changing the area ratio and diffuser angle. It was shown that the pressure recovery was consistently more through the diffuser with angle of divergence of 7° by considering the different Reynolds number. In this paper it was also shown that the diffuser with higher area ratio gives the higher values of pressure recovery in comparison of the diffuser with lower area ratio. The

performance of the diffuser for the angle of 7° is found higher as compared to other diffusers. 2017.

R. Coladipietro *et al.* [67] investigated the behavior of equiangular annular diffusers by considering the effects of swirl at inlet and wall layer. They analyzed the diffusers by taking different area ratios of 1.25, 1.50 and 3.0. Here the analysis was done in two methods. In the first method the thick wall layer while in the second thin wall layer was taken at the inlet of the diffuser. The blockage factors of 0.10 and 0.06 were found in the case of thick and thin wall layer respectively. The performance of each diffuser was checked by taking the different amount of swirl (from 0° to about 25°) at the inlet of the diffuser. Here it shown that by increasing the inlet swirl and diffuser diverging length, the performance of the test diffuser increases. It was found that the performance of the test diffuser with a thin wall layer for short diverging length diffusers while for long diverging length diffusers with a thick wall layer was good. It was also shown that the efficiency of the diffuser initially decreases and after that increases by the increasing the diverging path.

Manoj Kumar Gopaliya *et al.* [15] presented the effect of horizontal and vertical offset on a Y shaped duct. Here the Y shaped duct has rectangular inlet and outlet circular section with area ratio of 2, settling length of $1.5D$ for the $Re=2.74 \times 10^5$. In this paper computational Fluid Dynamics approach was used by considering $k-\epsilon$ turbulence model to analyze the problem. In this paper it was shown that the pressure recovery at the outlet of the diffuser decreases marginally due to offset effect.

Stefano Ubertini [16] analyzed the flow in an industrial gas turbine unit by taking the diffuser in to consideration. Measurements were performed on a scale model of 35% with

and without the struts. The similarity between the model and PGT10 Exhaust diffuser was maintained on the basis of Geometric and Reynold number. Total pressure, the flow angles and the wall static pressure were calculated through the diffusers. The performance of diffuser was increased with the use of strut.

Feld Camp *et al.* [68] done Experimental calculations to find the influence of struts on annular diffuser. Here it was presented that struts does not change the value of net pressure loss for flow without swirl at intake of the annular diffuser. But the pressure recovery increases with the increase of swirl up to 20° in the annular diffuser, despite increased total pressure losses. The performance of the diffuser in the presence of 40° swirl at the inlet is mainly dependent on strut profile. Minimal decrease in pressure recovery was found for the higher thickness-to-chord ratio of the strut configurations as compared to the diffuser with 20° swirl at the inlet. Significant fall of pressure was found in the lower thickness-to-chord ratio configurations due to the presence of flow separation from the struts.

Berge *et al.* [21] calculated the effectiveness of the annular diffuser by calculating the pressure recovery coefficient at the walls of the diffuser. In this paper it was shown that the increase in the pressure decreases by using the more number of struts due to increase in blockage factor. Here it was also shown that Performance parameter i.e. coefficient of Pressure recovery initially rises and then falls by the changing of swirl flow in the test diffuser

Sandip A. Kale [17] constructed the three different diffuser geometry around the micro wind turbine without flange, vertical and inclined flanges. CFD approach was used to find

the velocity and pressure variation. It was found that the diffuser with inclined flange gives better performance as compared to other diffusers.

Kamyar Mansour *et al.* [18] analyzed the structure and nature of the flowing flow around the flanged diffuser by using Computational Fluid Dynamics approach. It was found that by the use of flanged diffusers, the wind speed increases by 1 to 2.1 times of wind approaching speed. By increasing speed power also increases. Good agreements were found between CFD and Experimental approach.

Manoj Kumar and B. B. Arora *et al.* [4] analyzed the annular diffuser with area ratio 2, casing divergence angle 10.9° and Reynold number 2.25×10^5 with the help of CFD approach. Mean velocity, static pressure and total pressure were measured through the diffuser and along the walls of hub and casing of parallel hub and diverging casing annular diffuser. Flow separation and flow reversals were also checked at different swirl angles. In the last the computational results were compared with the experimental results.

Ratan Mohan *et al.* [49] analyzed the annular diffuser by varying the swirl angle at inlet ($25^\circ, 28^\circ$ and 32°) and half cone angles from 12.5° , 15° and 17.5° . Pressure recovery coefficients were calculated on the walls of the diffuser at different cone angles and different swirl intensities at the inlet of the annular diffuser. The following results were obtained in terms of pressure recovery coefficients are shown here. (I) $C_p = 0.68, 0.613$ and 0.52 for half cone angles of $12.5^\circ, 15^\circ$ and 17.5° at without swirl (ii) $C_p = 0.72, 0.69$ and 0.66 for half cone angles of $12.5^\circ, 15^\circ$ and 17.5° with swirl flow.

Ehan Sabah Shukri *et al.* [22] calculated the results in terms of velocity variations in an annular diffuser by considering the effect of area ratio. Here diffuser was fitted with square

twisted hub and it was analyzed with the help of numerical approach. In this paper it was found that the value of the velocity increases with the decrease in area ratio with the help of Computational Fluid Dynamics approach. Here area ratio was taken as 2.4, 2.8 and 3.7. 2015.

A. G. Barker [23] performed the experimental work on the diffuser which was located at the exit of compressor outlet guide vanes. The area ratio was taken as 1.45 and 1.60. In the present work static pressure and stagnation pressure were calculated on the surface of the diffuser. It was shown that static pressure increases, and stagnation pressure decreases. The static pressure increased from 0.130 to 0.520 for 1.45 area ratio diffuser and 0.130 to 0.565 for 1.60 area ratio.

S. N. Singh *et al.* [8] analyzed three diffusers A1, A2, A3 with cone angle of 20° , 25° and 30° with area ratio of 3.04, 3.5 and 4. Swirl angle was varied from 0° , 12° , 17° and 25° . The diffuser performance was presented in terms of diffuser efficiency, diffuser effectiveness and development of flow with the help of longitudinal velocity and tangential velocity. It was shown that for wide angled diffusers the flow separates both at the hub and casing while for others separation is confined mainly to the casing.

Prakash *et al.* [18] analyzed the flow through different configurations of diffusers the results were presented in the terms of static pressure recovery coefficients. In the present paper It was found that the maximum static pressure recovery occurs in the diffuser having a cone angle of 7° . In this paper the obtained Experimental results were in agreements with the available theoretical results.

Ganesh V. *et al.* [68] analyzed the problem in terms of boundary layer development in a straight core annular diffuser by using numerical approach. Results were calculated and compared for four cone angles. Velocity profile, displacement thickness, momentum thickness, Pressure recovery coefficient and effectiveness were calculated here.

Majid Nabavi [19] studied the flow through a planer diffuser numerically and validated against experimental work. The effect of divergence angle and area ratio were also observed on critical Reynold number at which asymmetric flow starts.

2.3 Effect of Flow Parameters on Diffuser Performance

2.3.1 Inlet Swirl Flow

Some of the researchers show that the swirl flow are the important parameter which can change the flow structure and shift the flow from one position to another position in the diffuser. They showed that by the changing of swirl angle or swirl velocity the performance of the diffuser increases up to some extent after that it decreases. Separation can be moved or delayed in the diffuser by introduction of swirling flow at the inlet of the diffuser.

Manoj Kumar *et al.* [1] and Singh *et al.* [8] the introduction of swirling flow produces centrifugal forces. Centrifugal forces makes the flow stronger on the casing side but increasing the separation on the hub surface.

Elkersh *et al.* [20]. Due to the swirl flow pressure recovery coefficients increase initially up to the certain value of swirl flow after that it decreases. Flow separates both at the hub and casing for wide angled diffuser while for others separation is confined mainly to the casing **S. N. Singh [7], Shrinath [25], Hoadley [26], Sovran & Klomp [24], Shaalan &**

Shabaka [39], Kumar [48] Colodipietro et al [27], Lohmann et al. [28] showed that diffuser performance increases with introduction of swirling flow. Pressure recovery of diffuser increases up to a certain value after that it deteriorated. **Japikse [14] and Yeung & Parkinson [15]** also showed that diffuser performance rises with providing the swirling flow in the diffuser up to a certain value after that it decreases.

The swirling flow is a key factor which moves the separation and reversal of the flow through the diffuser from one position to another. **Howard [34], Stevens [12, 13], Singh et al. [8]**, developed an annular diffuser without flow separation, however they become successful up to some extent. **Manoj Kumar and B. B. Arora [6]** analyzed the flow in annular diffuser by using CFD technique and they found the flow behavior of the flowing fluid through the annular diffuser by considering the effect of rotation component at the intake of the annular diffuser. In the present work it was found that the diffuser flow tends to move towards the casing side and increase the tendency of flow separation at the hub side of annular diffuser with the application of swirl flow at the inlet.

The study of diffuser research has stated that considerably more investigations have been carried out on two dimensional conical diffusers. Much of the extent data covering annular diffusers was done in the experimental laboratory.

Stafford and James [39], B. B. Arora et al. [3, 4] used the CFD approach to analyze the flow through annular diffuser. Longitudinal velocity, swirl velocity and pressure recovery coefficients were analyzed and plotted throughout the diffuser. In this paper it was shown that the value of pressure recovery coefficient depends on area ratio and swirling flow. Pressure recovery coefficient increases up to some extent by increasing the value of area ratio and swirl intensity at the inlet of annular diffuser. Here the flow was hub generated

and shift towards the casing walls with the application of swirl flow at inlet. Here the computational results were in good agreements with the obtained experimental results. **Manoj Kumar et al [11]** visualized the development of flow, flow reversals and separation through the annular diffuser. Longitudinal velocity and pressure recovery coefficient were calculated and plotted for the annular diffuser. The separation of flow was delayed by introduction of swirl. Due to delay in separation the pressure recovery coefficient at diffuser walls increases.

C. B. Ohio et al [70] performed the experimental work on a conical diffuser with cone angle 16.5° and area ratio 4.4. The swirl flow was generated with the help of swirl generator which contains 24 flat blades. Here axial velocity and static pressure were calculated at different sections 1 to 18. Here flow separation delayed and moved forward up to certain value of swirl after that performance of diffuser decreases.

D. S. Kumar et al [20] performed the Experimental work to find the performance of annular diffuser by introduction of swirl flow at inlet. Static pressure, axial velocity, tangential velocity, pressure recovery coefficient, effectiveness and coefficient of total pressure loss were calculated with the help of three-hole cobra probe at various locations in the longitudinal directions of the annular diffuser.

D S Kumar et al [73] done the experimental investigation to study and analyze the flow within the annular diffuser by taking the different intensities of swirl at the inlet. In the present work the annular diffuser with diverging hub and casing with equal angle was used. Pressure, velocity in the axial direction was measured by mounted three-hole cobra probe at many locations on the longitudinal direction with different sections. Performance measuring parameters such as coefficient of pressure recovery, effectiveness of the

diffuser, and coefficient of total pressure loss of the annular diffuser were calculated with the help of measured values of the static pressure at different locations.

Elkersh et al [20] calculated the performance of equiangular diffusers by taking the effect of geometrical parameters and swirling flow. In the present work three different annular diffuser geometry were analyzed by changing the inlet swirl angles up to 45° . Here it was shown that the centrifugal forces due to swirl flow produces the stronger flow on the outer wall i.e. on the walls of casing of the diffuser and produces the separation on the internal shaft i.e. On the walls of hub of the annular diffuser. In the present work, It was shown that by increasing the value of the inlet swirl up to 30° the performance of diffuser increases and after that performance of the diffuser decreases. It was also shown that the pressure recovery and pressure loss coefficient depends on area ratio and cant angle.

Vassiliev V [34] calculated the performance of the diffuser by considering the effect of inlet swirl and Mach number In the present work, it was shown that the performance of the diffuser only depends on the swirl at the inlet of the diffuser but not depend on the inlet Mach number for a given geometry. Computational Fluid Dynamics results were very close to the obtained experimental results in the present work. But in the case of strongest flow separation, the results of Computational Fluid Dynamics approach were not in the agreements with the measured experimental results.

Coladipietro R. et al [40] investigated the behavior of equiangular annular diffusers by considering the effects of swirl at inlet and wall layer. They analyzed the diffusers by taking different area ratios of 1.25, 1.50 and 3.0. Here the analysis was done in two methods. In the first method the thick wall layer while in the second thin wall layer was taken at the

inlet of the diffuser. The blockage factors of 0.10 and 0.06 were found in the case of thick and thin wall layer respectively. The performance of each diffuser was checked by taking the different amount of swirl (from 0^0 to about 25^0) at the inlet of the diffuser. Here it was shown that by increasing the inlet swirl and diffuser diverging length, the performance of the test diffuser increases. It was found that the performance of the test diffuser with a thin wall layer for short diverging length diffusers while for long diverging length diffusers with a thick wall layer was good. It was also shown that performance of the diffuser changes with the change of the diverging length of the test diffuser

2.3.2 Inlet Turbulence and working fluid

“**N. V. Mahalakshmi et al [9]**” analyzed the velocity variation in straight axial conical diffuser with cone angles 5^0 and 7^0 by taking two types of flow such as uniform velocity and wake type distorted flow at the intake section of the conical diffuser. Experimental work was performed in a wind tunnel which has low speed in the present work. “Hot wire anemometer was used to” calculate the mean flow in terms of velocity and the turbulent parameters.

Ubertini et al. [35] determine the different parameters such as velocity components, turbulence dissipating eddy length scales and finally the development of flow with the help of above parameters in annular exhaust diffuser.

Erica M. Cherry [37] performed the experimental work to measure the velocity of flow and its contours in two different diffusers with straight inner walls and angled outer walls. Two different inlet conditions were applied in two different diffuser segments, one

containing fully developed channel flow and the other containing the water from a row of struts. Velocity and its contours were calculated and plotted for both the diffusers.

S. J. Stevens et al [12] calculated the performance and mechanism of the flowing fluid by performing the low speed test on the annular diffuser. In the present work the pressure recovery coefficient and the total pressure loss coefficient were calculated by taking the effect of inlet turbulence. Here it was shown that with the increase in inlet turbulence the stability of outlet flow, Pressure recovery and the total pressure loss increases’.

J. Stevens [13] performed the experimental work to examine the performance of symmetrical diffuser by considering the effect of inlet conditions. The area ratio and wall angles of the diffusers was taken as (4:1) and (2.5⁰, 5⁰).In the present work, it was shown that the efficiency of the diffuser decreases with the increase in outer wall momentum thickness for the 2.5⁰ diffuser. Detailed study for the growth of boundary layer in the 5⁰ degree conical and annular diffusers operating with fully developed flow at inlet was done by taking the power law velocity profiles.

Monje B.et al [43] performed the experimental work to find the performance of conical ducts by taking air and supercritical carbon dioxide as a flowing fluid. It was observed that supercritical carbon di oxide enhances the pressure rise capability and reducing the total pressure losses with respect to air as a working fluid. 2013.

Ozturk Tatar et al. [38] analyzed the flow in centrifugal compressor vanless diffuser by using the Computational Fluid Dynamic (FLUENT.) approach. They analyzed the flow and calculated the Velocity, Pressure and turbulent kinetic energy at different hub sections

.Numerical work was carried out by taking Finite volume method assumed steady and incompressible flow here. Diffuser flow was highly non-uniform and completely mixed at the diffuser exit.

2.3.3 Mach Number Influence

Several reports have revealed measurement at different Mach number. Most annular diffuser study has been executed at low inlet Mach numbers. The research by **Wood *et al.* [44]**, **Thayer [48]**, and **Japikse *et al.* [32]** reveal virtual independence of revival with Mach number up to some stage of around 0.80 to 1.1. The actual level depends on method of measurement and the type of inlet.

Wood *et al.* [44] Show that a shock structure must be presented before the performance begins to deteriorate, but the reference Mach number may have little to do with the actual shock location and shock structure. In most cases, the reduction of performance with Mach number is very slight but in a few cases, there can be a degradation of five or ten point of performance recovery.

2.3.4 Influence of Reynolds Number

Dynamic Viscosity of a fluid is a vital constraint for the flowing fluid in any fluid system and in any fluid dynamic process. Viscosity is a very important term which generally comes in the form of important dimensionless number known as Reynolds number. Annular diffusers are not generally characterized by the non-dimensional number such as Reynolds number calculated with the help of hydraulic diameter at inlet or outlet. Reynolds number plays an important role for fluid flow problem because it tells about the nature of the flow

i.e. Laminar or Turbulent. All studies reveal that when the flow is in the fully turbulent regime, then Reynolds number is a reasonably weak parameter.

Crockrell *et al.* [46] shows that diffuser performance does not depend on Reynolds number generally if we neglect the effect of Reynolds number on the inlet boundary parameters. Whenever inlet boundary parameters remain constant, the variation of Reynolds number within the range of 2×10^4 to 7×10^5 , the diffuser performance would be nearly independent of Reynolds number. **Sharan [47]** found that when Reynolds number increases, there is no variation in pressure recovery for thick boundary layers.

2.4 Aerodynamic Blockage

Aerodynamic Blockage In comparison to channel and conical diffusers, aerodynamic blockage on annular diffuser is much less. The basic boundary layer equations disclose the consequence of the displacement thickness as a characteristic length scale of the inlet boundary layer flow.

Stratford *et al.* [86] Accepted the importance of the boundary layer displacement thickness to pressure recovery method. **Thayer [45]** reported that pressure recovery as high as 0.61 to 0.65 is possible for curved wall diffusers for an area ratio of 2.15. An extensive study by **Stevens's *et al.* [88]** found that for curved wall diffuser, fine pressure recovery was detected for a loss significantly below the level which would be expected from pressure recovery loss correlation, but pressure recovery values were lower than those which would be expected from **Sovran *et al.* [24]** as reported by him.

Klein [85] compared **Stevens *et al.* [13]** Data with the result of **Sovern *et al.* [24]** for an inlet blockage of .02 and with forecasting using the latter's method for diffuser performance for larger blockages. An inclusive study on the effect of aerodynamic blockage on annular diffuser performance carried out by **Goebel *et al.* [87]**. Similar calculations were made at 20° and 40° of inlet swirl. In all cases the data pattern was in the course of reduced pressure recovery for increased aerodynamic blockage. Upon careful examination, it was found that the boundary layers in this diffuser are different. First, the influence of inlet situation on annular diffuser performance is more complex than for channel and conical diffuser. In this case, both the hub and casing surfaces can develop boundary layers with considerably different histories. As they pass through the diffuser the two differing boundary layers will experience different growth processes. Additionally, blockage on one wall has the effect of altering the area of the flow region with also changing of flow velocity, thus influencing the growth of the boundary layer on the opposite wall. Because of this reason complex interactions can build up within the diffuser

2.5 Boundary Layer Parameter

The flow of flowing fluid in the diffuser depends on the development of boundary layer and its nature .The nature of the boundary layers regulate the flow at the diffuser walls. The change of pressure (rise) is created by slowing down the flow through the diffuser. Adverse pressure gradient or the positive pressure gradient generally acts on the wall shear layers and will cause the wall boundary layers grows in to the thickness and reduction in velocity .After some points the flow break away from the diffuser walls and forming areas of back flowing within the diffuser. The blockage of flow area is because of the net result

of thickening of the wall boundary layers or the creation of regions of backflow, which brings down the effective area existing to the flow. Drop in effective area of flow results in reduced pressure rise through the diffuser.

2.5.1 Boundary Layer Suction

The outcome of suction consists in the exclusion of decelerated fluid particles from the boundary layer before the separation.

Wilbur *et al.* [53] shown that suction control is not proficient when applied in a broad backflow region. Investigated the suction incident and found the decrease in the measured total pressure loss by 63% and a suction flow rate of 2.3% increased the static pressure rise by 25 – 60% [53]. Experiments by **Juhasz [84]** on short annular diffuser showed that the diffuser exit profiles could be shifted either towards the hub or towards the casing of annulus by bleeding off a small fraction of the flow through the inner and outer wall respectively. Boundary Layer Suction for both channel and conical diffuser with large divergence angle is also adopted by **Ackert [64]**.

2.5.2 Blowing and Injection

Wilbur *et al.* [53] show that, 33% increases in the calculated value of pressure at the exit with 50% reduction in net pressure loss can be achieved by an injection rate of 3.4%. **Juhasz [84]** conducted experiments on the consequence of injecting secondary fluid into wide angle conical diffusers through annular slot at inlet and found the result in significant enhancement in the uniformity of exit flow and in the magnitude of pressure recovery.

2.6 Research Gap

Extensive research has been carried out on the analysis of axial diffuser. Going through the literature survey, following research gaps have been found.

- (1) Most of the work has been carried out as experimental work.
- (2) Mathematical and analytical modeling is scanty available.
- (3) Work on annular diffuser is scanty available.
- (4) Study on intermediate area ratio 2.5, 3.5 and 4.5 has not been carried out.

2.7 The Objectives of the Thesis

- (1) To analyze the annular diffuser at intermediate area ratios.
- (2) To analyze the annular diffuser experimentally.
- (3) To analyze the annular diffuser computationally.
- (4) To validate the computational results with the experimental results and reported data.
- (5) To carry out the parametric investigations.
- (6) To determine the region of flow separation.

CHAPTER 3

EXPERIMENTAL INVESTIGATION

3.1 Introduction

The objective of experiment was to design and build a plenum that could be used to characterize diffuser performance, as well as, develop guidance for other designs with similar flow objectives. The primary objective was to acquire an insight into the nature of flow and its complexity in an annular test diffuser. A secondary objective was to develop and perfect the test methods for me to design experimental methods used to test or to visualize the effect of geometrical and flow parameters effects. These testing and experimental design methods were to be used for all the tests performed in this project.

As enunciated earlier the internal flow in diffuser is complex, due to presence of non-uniform velocity profile and adverse pressure gradient. The swirling flow through diffuser further augmented the flow complexity. To visualize the nature of flow or flow structure in such flows and its complexity in an annular diffuser is of basic importance. The present experimental system used for this investigation has been designed to obtain detailed performance data of mean flow quantities based on various inlet conditions in plane two dimensional axisymmetric boundary layer flows without and with swirling flow conditions at the diffuser inlet for straight core annular diffuser.

The chapter describes the test-facility, the instrumentation and the uncertainty associated with the measured quantities. It further describes pressure distribution and velocity profile measurements which were made across the annular cross-section at various longitudinal

distances along the diffuser flow passage to produces data and the results obtained with the experimentation can serve as a basis of design.

3.2 Experimental Setup

The experimental work was performed on the experimental set up as shown in plates 3.1 to 3.2 and described in Fig. 3.1 which shows the general arrangement of the experimental facility .The experimental set up has blower, diverging & settling chamber, to study the flowing fluid properties within a straight core of circular cross sectioned annular entrance passage and test diffuser.

Atmospheric air was supplied to the blower of the experimental set up at ambient temperature, pressure and maintaining the Reynolds number more than the critical value. Centrifugal blower with a single stage was used to supply the air at the rate of 1.5m³/s and pressure of 1 meter water. Centrifugal blower sucks the atmospheric air with the help of a filter containing meshing of high quality .From the filter, the air is now moved towards the settling chamber. The flow rate was controlled and maintained uniform by using the symmetrical dampers at the inlet of the blower. The gap between the settling chamber and blower was used to seal with the help of a flexible coupling. Vibrations reaching in the settling chamber from centrifugal blower were minimized and finished with the help of Flexible coupling. The length and the diameter of settling chamber was 0.5 meter and 3.5 meter. The settling chamber was attached to a uniform area annular duct by following a smooth diverging section. The fine mesh screens and a honey comb section were present in the converging section of the set up. Steady flow, straight flow with low level of turbulence and loses is maintained with the help of mesh screen. Annulus was formed with the help of two pipes of diameter 7.6 cm and 15.5 cm. The height of the annulus was 3.95

cm. The length of annulus portion was maintained about 50 times the hydraulic diameter to obtain a full developed boundary layer at the intake of annular diffuser. The fully developed turbulent flow with zero swirl shows the actual entry conditions. Concentricity between inside and outside pipes was maintained.



Plate 3.1 Traversing Mechanism for Experimental Setup



Plate 3.2 Centrifugal Blower used for Experimental Setup.

The core was placed at the right place with the help of four radial stream-lined struts, which was used at each of two axial stations. Hub section of the diffuser was manufactured by using cast aluminum and machined to maintain smooth surface. Transparent Plexiglas was used to manufacture the casing of the annular test-diffuser. Plexi glass was used as a material for the casing so that the flow visualization inside the annular diffuser could be done. After passing through the diffuser the moving air was finally discharged in to the atmosphere.

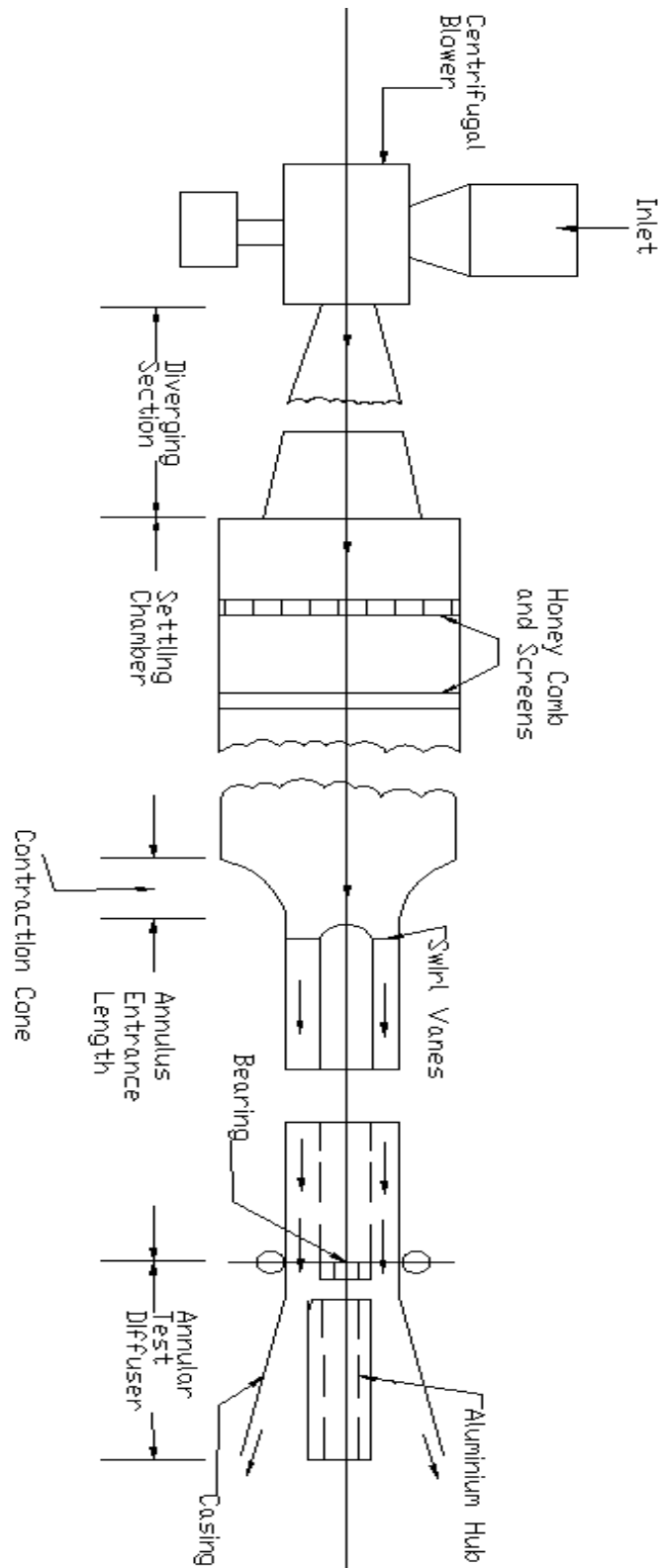


Fig. 3.1 Block diagram of Experimental setup of annular diffuser

3.3 Swirl Generation and Specification

The researchers in the past have used various methods to impart the swirl for experimental studies of swirling flow through jets, pipes and diffusers. The relevant methods as indicated in the literature are listed below for the generation of swirl

- Locating the diffuser immediately downstream of a turbo machine;
- Rotation imparted to an axial stream by means of a rotating perforated plate;
- Use of twisted tapes;
- Introduction of a tangential air stream;
- Allowing the air to flow through a set of adjustable equiangular stator vanes.

None of the methods listed above can be said to be the best method for imparting the swirl. All the methods of swirl generations has merits, demerits and limitations. In the present investigation, swirl was imparted to the air-stream by passing it through stator vanes formed by means of a flat steel plate. Twelve cuts were made on this flat steel plate to form the vanes in the radial direction. Swirl of different magnitudes were generated by setting the vanes at various angular positions. The swirl flow was generated with the help of swirl plate which was located at the preceding of the annular diffuser. This far upstream location was preferred to reduce the chances of formation of wake at the diffuser entry. Wake would have persisted in the diffuser and which would have affected its performance. Swirl can be described either in terms of the geometrical features of the device used for generating the swirl or based on the mass-averaged or area-averaged value of the swirl angle, later case is considered to be a far better method of specifying the swirl than the previous one. Averaging processes becomes necessary because the swirl angle may not be constant across a section. Swirl number is a dimensionless number which is used to define the swirl flow. It is

obtained by dividing the axial flux of the angular momentum with the axial flux of the axial momentum.

$$S = \left(\int r^2 u w dr / \int r u^2 dr \right) \cdot \frac{1}{D_{eq}} \quad (3.1)$$

Where D_{eq} is the equivalent diameter of the flow passage.

3.4 Geometry of the Test-Diffusers

Table 3.1 specifies the geometry of the annular diffuser which is used in the analysis of the flow for the present problem. The test geometry of the annular diffuser was made with an area ratio of 2.01, the other dimensions in terms of hub and casing wall angles, exit radius of hub and casing, area ratios diverging length and equivalent cone angle. The aim of the present work is to calculate the influence of the swirl flow on the development of flow, flow separation and flow reversal through diffuser and locate the zone of separation or reversal of flow if any.

Table 3.1 Dimensional details of the geometry of the annular diffuser used in experimentation.

Diffuser (Parallel Hub and Diverging Casing)	$R_h=3.8$		$R_c=7.75$		R_h/R_c 0.49		Equivalent Cone Angle
	Wall Angles		Exit Radius		AR	N	
	Hub	Casing	Hub	Casing			
	0	4.3	3.8	10.28	2.01	16	20.2

3.5 Description of Geometry of the Diffuser

A 2-D model of annular axial diffuser and meshing is generated by using Gambit software. Analysis of diffuser have been done by using Fluent. Here quadrilateral elements were used for

meshing. The size of mesh was taken as 0.07 cm. The geometry of the diffuser which is used is shown in the figure 3.1. Here

(R_{hi}) = Inlet radius of hub

(R_{ho}) = Outlet radius of hub

(R_{ci}) = Inlet radius of casing

(R_{co}) = Outlet radius of casing

(N) = Diffuser Diverging Length

(M) = Inlet Length of the diffuser

θ = Casing Divergence angle

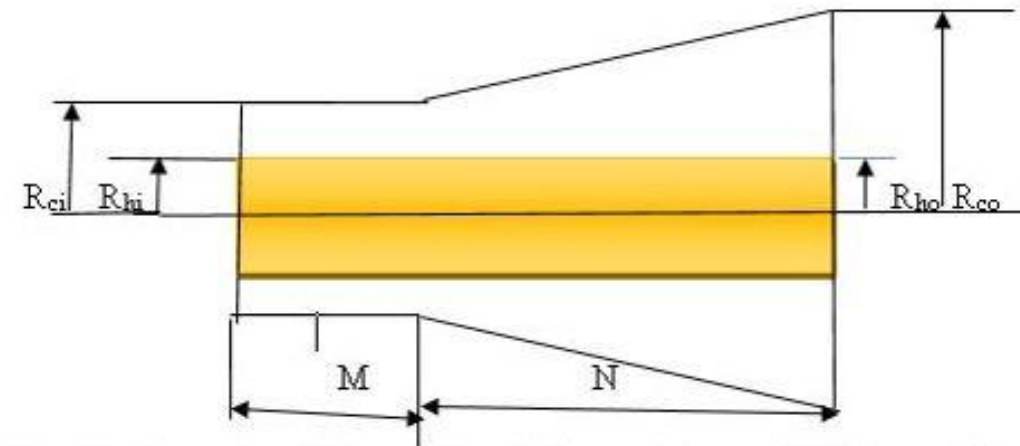


Fig. 3.2 Geometry of the annular diffuser

3.6 Dimensional Details of the Annular Diffuser for different area ratios.

Dimensional details of the different diffuser geometry with different areas ratios 2, 3 and 4 are given in the Table 3.2.

Table 3.2 Dimensional details of Annular axial Diffuser with AR=2, 3, 4 and equivalent Cone Angle of 20°

S.N.	Dimensional Parameters	Area Ratio (2)	Area Ratio (3)	Area Ratio (4)
1.	Hub radius at the inlet (R_{hi})	3.8 cm	3.8 cm	3.8 cm
2.	Hub radius at the outlet (R_{ho})	3.8 cm	3.8 cm	3.8 cm
3.	Casing radius at the inlet (R_{ci})	7.75 cm	7.75 cm	7.75 cm
4.	Casing radius at the outlet (R_{co})	10.28 cm	12.300 cm	14.3007cm
5.	Diffuser Diverging Length (N)	15.867 cm	28.042 cm	38.3063 cm
6.	Inlet Length (M)	3.95 cm	3.95 cm	3.95 cm
7.	Casing Divergence angle	4.31°	2.767°	2.113°

3.7 Diffuser Inlet Location

The flow conditions at the inlet should refer ideally to those at the actual or geometric start of the diffuser; however, placement of a pressure tap exactly at the transition being difficult, the inlet location was chosen to be a station somewhat upstream of the geometrical inlet. The inlet location so chosen entails friction loss in the length of annular ducting between the chosen inlet section and the actual diffuser entry but reduces the streamline curvature effects at the start of a geometric expansion because decrease of pressure in the vicinity of the wall below the pressure of the core

flow region. So to strike a balance the reference section was located 5 cm upstream to the geometric start of the diffuser to minimize the unnecessary penalty to the diffusion process and the friction loss is expected to be very small in comparison to the actual diffuser loss. Further the inlet velocity profile would be only marginally different from that at the geometric start of the diffuser.

3.8 Instrumentation

Cobra probe, traversing mechanism and inclined tube manometers were used to calculate the different parameters such as static pressure and yaw angle. The description of different instruments which are used are given below:

3.8.1 Three-Tube Impact Pressure Probe (Cobra Probe)

Cobra probe with three tubes was used to calculate the pressure and velocity at particular instances of time in the flowing fluid through the diffuser. The probe was fabricated from the stainless tubes with 0.16 mm outer radius. The size of a pressure probe was chosen as to balance the pressure transmission lag as well as the accuracy with which the probe can be used.

Square cut was formed on the leading edge of the center tube of a cobra probe whereas the two outer tubes were chamfered at 40° to 45° relative to the respective tube axes. This arrangement was made to achieve the maximum yaw sensitivity. As the probe assembly was to be mounted on the traversing mechanism, the three tubes were placed parallel, coplanar and then soldered into a 3 mm steel tube. The stem of the probe assembly was formed by maintaining a distance of 50mm from the tip to minimize possible errors due to interference of the flow.

3.8.2 Traversing Mechanism

Traversing mechanism was designed to have two degrees of freedom to survey the mean turbulence velocity field. This enabled the probe to be traversed as well as rotated about its

longitudinal axis. The least count for the traversing mechanism in the longitudinal direction was kept 0.1 mm while that in rotation was 0.5° . The cobra probe was first mounted on the traversing mechanism and then inserted into the flow passage to survey the flow field. The probe was aligned to be parallel to the reference direction within the accuracy of $\pm 2^\circ$, and was made to touch the surface of the diffuser hub. Readings closer than 0.5 mm from the hub as well as casing wall could not be obtained as the probe-head was 1 mm in diameter. In the boundary layer region close to the walls measurements were made in steps of 0.5 mm. However, away from the wall large steps were chosen and the step size was adjusted so as to get about 10 to 20 points at a particular traversing station depending upon the height of the diffuser passage. There was possibility of backlash error associated with the mechanisms which was overcome by moving the traversing system in the same direction while taking any one set of observations

3.8.3 Manometers

. The manometers consist of thirty six glass tube. In order to rise the effectiveness of the, it was inclined with 10 degree to the horizontal.-Distilled water was used as measuring liquid. While the manometer was in an inclined position the menisci of the tubes wore observed to be at different levels. This error, although small in magnitude, was corrected for while reducing the pressure data into the relevant flow parameters. The steady state conditioned was maintained while taking the reading with the manometers and the probe. Four to five minutes was given to take the every observation while maintaining the steady state condition. Carbon tetrachloride was used to clean the hypodermic tube frequently by removing the dust particles. The monomeric tubes were also checked to remove leakage frequently.

3.9 Initial Conditions

The initial conditions consist of the physical conditions for the flowing fluid through the annular diffuser. Flowing fluid initially passes through an annulus pipe having a length to hydraulic diameter ratio of 50 ensures the existence of fully developed flow at the intake of the annular diffuser then it passes through the diffuser. Fully developed flow with turbulence level and without swirl has been chosen as the flow at real intake condition as compared to thin boundary layer flow as proposed by other researchers. Atmospheric pressure was maintained at the exit of test diffuser by attaching no tail pipe at the exit of the diffuser. All the experimental measurements were performed by assuming incompressible flow in the present experimental setup. The value of Reynolds number was taken as 2.5×10^5 . The Reynolds number was calculated by taking equivalent flow diameter in to consideration at the intake section of the annular diffuser. The above value of Reynolds Number shows that the flow through the annular diffuser was turbulent in nature at the inlet. Before actual measurements were carried out in the test diffusers the boundary layer was checked for axial symmetry. This was done by first checking the lateral variation of the static pressure.

3.10 Experimental Procedure

For each diffuser data was measured and collected in the following

- Measurement of the static pressure at the walls
- inlet velocity profiles
- velocity profiles in the diffuser at different points using the three-hole cobra probe
- Flow visualizations

3.10.1 Measurement of the wall Static Pressure

For measuring the static pressure at the walls, the pressure tapings were used at the diffusers along the generatrix of the casing as well as on the hub wall. Holes of 6 mm in radius were carefully produced for the inserting of stainless steel tubes of 6 mm outer radius and 3 mm inner diameter. The pressure taps were then coupled to an inclined multi-limb manometer through polythene tubing. Wall static pressure was checked in diametrically opposite planes both at the first and the last measuring station at different circumferential tapings to ensure axial symmetry of the flow. The deviation in the readings to the extent of $\pm 3\%$ of the average inlet dynamic flow was recorded. The deviation being small the flow was regarded as axisymmetric.

3.10.2 Calculation of the Average Velocity Field

Mean velocity profiles were determined at various locations along the diverging length of the annular diffuser. Measurements of the velocity were made normal to the diffuser hub by means of a cobra probe. Holes of 3 mm diameter were drilled on the diffuser casing at suitable intervals along its length to introduce the probe. The free holes were plugged with carefully shaped inserts to prevent air from leaking into the flow passage. Static pressure, total pressure and yaw angle at different positions were calculated to determine the velocity profiles in the flow field. The three quantities were obtained by using of cobra probe along the different positions of the annular diffuser passage length. The following assumptions were made to analyze the flow are

- (i) Steady flow
- (ii). Incompressible flow
- (iii). Inviscid flow

The velocity U at every position in the region of flowing fluid was computed with the help of law of conservation of energy. The longitudinal and swirl velocity was then computed as follows

$$u = U \cos \varphi$$

$$w = U \sin \varphi$$

Where φ is the yaw angle with respect to longitudinal direction on the hub surface.

The longitudinal and swirl velocity were then calculated in terms of non-dimensional form with respect to the maximum longitudinal velocity U_m of any transverse. These non dimensionless velocity profiles (u/U_m) and (w/U_m) for longitudinal and swirl respectively were plotted as a function of non-dimensional diffuser passage radius r/R_m . Non-dimensional diffuser passage radius (r/R_m) was obtained by dividing the diffuser passage radius r at any location of the traverse measured from the hub surface to the maximum diffuser passage radius R_m . Flow field measurements were carried out at various transverses of the diffuser passage length for different inlet swirls, turbulent intensity etc.

3.10.3 Flow Visualization

Small wool tufts, 2.5 cm long and capable of rotating freely in any direction, were used to observe the flow pattern in the test-diffusers. These tufts were mounted along four generatrices, approximately 90° apart, on both the hub and casing walls of the diffusers. The movement of the tufts could be viewed through, the transparent casing of the diffuser test section. Classification of flow regimes in accordance with the movement of the wool tufts is liable to considerable subjective interpretation. However, a survey of the existing literature on the subject indicates that, a classification suggested by Carlson and Johnston [1967].

3.11 Uncertainty in Measurements

Despite the utmost care and precautions an experimenter may take to eliminate all possible errors from his observations, certain experimental errors are likely to be caused by geometrical inaccuracies of the test apparatus while the others may be due to inaccuracies in the measuring instruments.

Perspex sheet of 4 mm thickness was used to make the outer surface i.e. casing of the annular diffuser. Oil bath was used to heat the Perspex sheet initially and that Perspex sheet was rolled on the conical shaped block made from wood of the desired necessary dimension. Then the roll sheet was butt joined along the length to make the casing with the help of a Perspex strip. After that flanges was applied at the two corners. The flange at the inlet end of the diffuser also served as the joint between the casing and the straight annular passage preceding it. The operation of rolling produced error in creating desired roundness in the casing of the annular diffuser. Due to the operation of rolling the casing diameter deviated from that of a perfect cone thereby resulting in an error in the divergence angle of the casing. The hub, on the other hand, was made from aluminum by using the casting and machining process. As a result, it had a good accuracy with regards to the diameter and the divergence angle. The variations stated above affected the flow passage height through the annular diffuser. This passage height was also influenced by the positioning of the hub inside the casing. Likewise, the height of the straight annular ducting was affected by irregularities in the dimensions of the pipes comprising it and by any maladjustment introduced while mounting one pipe inside the other.

The number of factors such as leaking in the tubes of manometers ,alignment problem in the probe, variations in the surface condition of the inclined manometers , changing of weather conditions and flow stream pressures may affects the readings of the probe.

Table 3.3 Uncertainty in measurement

Physical Quantity	Uncertainty in Measurement
Hub Radius of the hub (R_h)	$\pm 0.6\%$
Radius of the casing (R_c)	$\pm 0.1\%$
Velocity (U)	$\pm 1.2\%$
Swirl angle (Φ)	$\pm 1.5\%$
Angle of Divergence (Θ)	$\pm 0.5\%$
Pressure Recovery Coefficient (C_p)	$\pm 5\%$
Total Pressure (P_t)	$\pm 1.2\%$
Static Pressure (P_s)	$\pm 1.5\%$
Dynamic head (\bar{q}_1)	$\pm 4.5\%$
Mean Velocity (\bar{U})	$\pm 2\%$
Reynolds Number (Re)	$\pm 5\%$
Atmospheric Pressure (P_{atm})	$\pm 1\%$
Annular Height (Y_m)	$\pm 1\%$
Traverse position (y)	± 0.05 mm

There is a possibility of near wall displacement. Due to wall displacement, the probe gives the readings at other locations away from the wall as compared to the real probe position. Moreover, as the probe used had small size its response to the applied pressures was slowly.

Even though considerable care was taken to provide adequate time before recording a reading due to slow response of the probe, there was always a possibility of human error in recording a reading without stabilizing the pressure. Backlash effect in the micrometer screw cannot be fully ruled out in spite of recording all the readings in the same direction. The uncertainties associated with the measured quantities are given in the Table. 3.3.

CHAPTER 4

COMPUTATIONAL AND MATHEMATICAL MODELLING

This chapter shows the Computational Fluid Dynamics approach for modeling and Mathematical modeling of the axial annular diffuser. Here Different mathematical equations such as continuity equation, Momentum equation and energy equation are used. In this chapter the different turbulence models and Methodology adopted to solve present problem have been also discussed.

4.1 Introduction

Now days Computational Fluid dynamics approach has become a necessary tool to solve any physical problem of fluid flow in a short time with the help of high-speed computers. It is due to the fact that to solve any physical flow problem with the help of experimental set up takes lot of time and lot of cost is involved there. Any computational code for any fluid flow problem generally solve the three types of equation such as Continuity equation, Momentum equation and energy equation by converting these equations in algebraic forms.

The results of any computational code depend on the type of mesh and convergence criteria. Fluent is a well-known fact which is mostly used to solve the fluid flow problems with and without heat transfer. Turbulent models are also required to solve the turbulent flow problems due to large number of variables. The objective of our research work is to analyze and visualize the flow through the axial annular diffuser of parallel hub with diverging casing and find the development of flow by considering the effect of swirl.

Experimental velocity profiles are used to supply the amount of swirl at the entry section of diffuser. Finally, the obtained computational results have been validated with respect to obtained experimental results. The different types of meshes which can be used in Computational Fluid Dynamics are given below:-

- (a) Two dimensional triangular/quadrilateral
- (b) Three dimensional tetrahedral / hexahedral / pyramid/ wedge,
- (c) Mixed (hybrid) meshes.

In the present problem we have used the two-dimensional quadrilateral elements of size 0.07cm for meshing of the axial annular diffuser geometry.

4.2 Planning of CFD Analysis

4.2.1 Geometry Creation

The geometry of the diffuser has been created with the help of Gambit by taking the dimensions of the diffuser from the experimental setup. We have developed 2-dimensional model of the axial annular diffuser with the help of Gambit Design modular for the present problem.

4.2.2 Grid Generation and its Independence:

FLUENT has been used to generate the grid. In the present analysis two-dimensional quadrilateral meshing elements with 0.07 cm mesh size have been used. Here we performed the grid independence test by varying the mesh size and compute the results by calculating the computational time. Mesh independence test is generally used to obtain an optimum size grid which is less time consuming and gives accurate results. Grid sensitivity and independence tests were performed on different diffuser geometry by taking the grid size

and different turbulence models. Different models of turbulence were checked with the help of experimentally obtained velocity profile for fully developed flow through the axial annular diffuser with area ratio of 2.0 and equivalent cone angle of 20 degree.

4.2.3 Boundary Conditions

After meshing of the diffuser geometry, we have defined the different surfaces of the axial diffuser and flow region, which are given below:

(i) Velocity Inlet (ii) Pressure Outlet (iii) Hub surface of the diffuser (iv) Casing of the diffuser (iv) Flow domain

Operating and boundary conditions at different sections of the annular axial diffuser were used to solve present fluid flow problem. Different conditions were used on the boundary i.e. (boundary conditions) of annular diffuser are given below:

4.2.3.1 Inlet boundary Condition

The present analysis involves the axial velocity with swirl. Turbulence intensity is specified as $I = 0.16 (Re_{DH})^{-1/8} \times 100$

Here, Re_{DH} stands for Reynolds number calculated with the help of the hydraulic diameter. For defining the Swirling flow tangential components of velocity along with axial component of velocity have to be taken into consideration. Tangential Velocity components have been calculated on the basis of inlet swirl angle. In the present case swirl angle of 5° , 7.5° , 12° , 17° , 25° have been considered. Here we have inserted the inlet velocity profile in the axial and tangential direction with 3% turbulence.

4.2.3.2 Outlet Boundary Condition

Atmospheric pressure or zero-gauge pressure condition has been applied at the exit of the

annular diffuser and set a “back flow” conditions for considering and allow the possibility of back flow at the exit section of the diffuser. In the “back flow” condition turbulence intensity is specified based on the equivalent flow diameter.

4.2.3.3 Surface or Wall Boundary Conditions

For binding the solid and fluid regions, Wall boundary conditions are applied at the walls. No slip i.e. zero velocity is defined for the fluid at the walls in viscous flows. Drag resistance and roughness of the wall are the major factors for calculating the Heat and mass transfer on the walls. Hence roughness effects were considered for the present analysis and a specified roughness based on law of wall modified for roughness is considered. For defining the wall, two inputs to be defined are the value of roughness height and it's constant. Roughness constant value of 0.5 is entered to indicate the smooth surface with uniform grain roughness.

4.2.4 Choice of Physical Models:

In the present Physical model, following conditions have been taken are given below:

- Two-dimensional fluid flow
- Steady flow
- Incompressible fluid flow
- Turbulent fluid flow

4.2.5 Determination of the Solution Procedure:

FLUENT code was used to solve the present fluid problem by taking convergence criteria of 10^{-6} for X velocity. The differential equations were converted in to algebraic equations

in the present problem by using computational Fluid Dynamics approach. Finite volume scheme was used to discretize the flow domain in to cells and nodes. The algebraic equations are solved by considering two levels of iterations which are required to solve the problem of the non-linearity and coupling of the equations. We have to decide to stop the iteration at the right time on each level so that accuracy and efficiency could be obtained. Any computational model will give the accurate results if the solution of the discretized differential equations tends to exact solution of the differential equation at zero grid spacing for obtaining the convergence. We have set the convergence criteria around 10^{-6} for X velocity the results are in the stable conditions for the present problem.

4.3 Mathematical Modeling

The present study uses different models and basic laws of Fluid mechanics to obtain the outputs. FLUENT has the capability to solve the various types of the problem with the help of modeling and simulation. In the present problem Fluent have solved the two differentials equations of mass conservation and conservation of the momentum by considering the turbulent flow. FLUENT uses four equations to model a 2-D flow problem in addition to the turbulence modeling equations. These four equations are

➤ **Conservation Principle**

- Momentum conservation or Moment balance equation
- Continuity equation or Mass balance equation

➤ **Velocity Equations**

- X- velocity equation
- Y- velocity equation

4.4 Conservation Principles

Conservation laws are the laws which are based on the conservation principles of species such as Mass, Momentum and Energy. This Conservation principles contains the three equations of conservation such as

(1) Continuity equation based on mass conservation

(2) Momentum conservation based on momentum balance

(3) Energy conservation equation based on energy balance Mass conservation and

Momentum conservation equations are preferred for the fluid flow problems without heat transfer. Energy conservation problem is preferred for the fluid flow problems by considering the heat transfer. The above equations can be derived on the basis of control mass and control volume approach. For solving the fluid flow problems by taking heat transfer into consideration one more equation of conservation of energy are to be solved. If the number of variables are large as compared to governing equations in the case of turbulent flow, Additional equations are necessary by considering the different turbulence models. In the present problem two equations of mass conservation and momentum conservation were solved by taking the RNG k- ϵ model in to consideration.

4.4.1 The Mass Conservation Equation (Continuity Equation)

The mass balance equation in the generalized form is represented as follows:

$$\frac{\partial \rho}{\partial t} + \nabla \cdot (\rho v) = 0 \quad (4.1)$$

The above equation is the generalized equation for conservation of mass whether the flow is steady, unsteady, compressible or incompressible. The mass conservation equation for two dimensional axisymmetric geometries is given below:

$$\frac{\partial \rho}{\partial x} + \frac{\partial(\rho v_x)}{\partial x} + \frac{\partial(\rho v_r)}{\partial x} = 0 \quad (4.2)$$

Here x and r show the axial and radial direction and v_x and v_r stands for the velocities in the axial and the radial directions

4.4.2 Equation for Conservation of Momentum

Momentum Conservation equation for non-accelerating reference of frame can be presented as follows:

$$\frac{\partial \rho \vec{v}}{\partial x} + \nabla \cdot (\rho \vec{v} \vec{v}) = -\nabla P + \nabla \cdot (\bar{\tau}) + \rho \vec{g} + \vec{F} \quad (3.3)$$

where

p = static pressure,

τ = the stress tensor as shown

ρg = body force due to the gravitational effects

F = body force due to the external effects. External effects come in to picture due to interaction. The last term in equation 3.3 has porous-media and user-defined sources, which depend on the source.

The stress tensor (τ) is given below as shown by the equation (3.4)

$$\bar{\tau} = \mu \left[\left(\nabla \vec{v} + \nabla \vec{v}^T \right) - \frac{2}{3} \nabla \cdot \vec{v} I \right] \quad (3.4)$$

Here μ stands for molecular viscosity, I stand for unit tensor, and the second term in equation (3.4) shows the volume dilation effect.

Momentum conservation equations for 2-D Flow in axial and radial directions is given by equations (3.5) and (3.6).

$$\begin{aligned}
 & \frac{\partial(\rho v_x)}{\partial x} + \frac{1}{r} \frac{\partial (r\rho v_x v_x)}{\partial x} + \frac{1}{r} \frac{\partial (r\rho v_r v_x)}{\partial r} \\
 &= -\frac{\partial P}{\partial x} + \frac{1}{r} \frac{\partial}{\partial x} \left[r\mu \left(2 \frac{\partial v_x}{\partial x} \right) - \frac{2}{3} (\nabla \cdot \vec{v}) \right] + \frac{1}{r} \frac{\partial}{\partial r} \left[r\mu \left(\frac{\partial v_x}{\partial r} + \frac{\partial v_r}{\partial x} \right) \right] + F_x
 \end{aligned}
 \tag{3.5}$$

and

$$\begin{aligned}
 & \frac{\partial(\rho v_r)}{\partial t} + \frac{1}{r} \frac{\partial (r\rho v_x v_r)}{\partial x} + \frac{1}{r} \frac{\partial (r\rho v_r v_r)}{\partial r} \\
 &= -\frac{\partial P}{\partial r} + \frac{1}{r} \frac{\partial}{\partial r} \left[r\mu \left(2 \frac{\partial v_r}{\partial r} \right) - \frac{2}{3} (\nabla \cdot \vec{v}) \right] - 2\mu \frac{v_r}{r^2} + \frac{2\mu}{3r} (\nabla \cdot \vec{v}) + \rho \frac{v_z^2}{r} \\
 &+ \frac{1}{r} \frac{\partial}{\partial x} \left[r\mu \left(\frac{\partial v_x}{\partial r} + \frac{\partial v_r}{\partial x} \right) \right] + F_r
 \end{aligned}
 \tag{3.6}$$

Where $\nabla \cdot \vec{v} = \frac{\partial v_x}{\partial x} + \frac{\partial v_r}{\partial r} + \frac{v_z}{r}$

Where V_z stands for the swirl velocity

Momentum equation for 2D swirling flows in tangential direction are shown by the equation (3.7) as shown below:

$$\begin{aligned}
 & \frac{\partial}{\partial x} (\rho v_z) + \frac{1}{r} \frac{\partial}{\partial x} (r\rho V_x V_z) + \frac{1}{r} \frac{\partial}{\partial r} (r\rho V_r V_z) \\
 &= \frac{1}{r} \frac{\partial}{\partial x} \left[r\mu \frac{\partial V_z}{\partial x} \right] - \rho \frac{V_r V_z}{r} + \frac{1}{r^2} \frac{\partial}{\partial r} \left[r^3 \mu \frac{\partial}{\partial r} \left(\frac{V_z}{r} \right) \right]
 \end{aligned}
 \tag{3.7}$$

4.5 Turbulence Modelling

Fluctuating velocity components are the main source of the turbulent flows. These fluctuations velocity components couple with the quantities such as momentum, energy, and species concentration. Due to mixing or coupling of these fluctuating components the transported quantities such as momentum and energy also fluctuate. It is very difficult to simulate the practical engineering problem by taking the effect of these fluctuation because of small scale and high frequency. The simulation of the above-mentioned type of flow involves lot of time and cost. So time average and ensemble average have been performed on the exact governing equations to remove the small scales quantities and resulting in a set of modified equations that are computationally less costly and easy to solve with less time taken to solve as compared to exact governing equations. Some additional unknown variables come in to picture by taking the average of the above mentioned equations. Turbulence models are generally used to calculate the values of these unknown variables in terms of known quantities

4.5.1 Selection of a Turbulence Model

It is very difficult to choose an optimum turbulence model which can solve any type of turbulent flow problem. For selecting a turbulence model following considerations should be taken in to account are given below:

- (1) Type of the phenomenon or physics involved in the given problem
- (2) Specific class of problem such as flow with swirl or without swirl
- (3) The level of quality is required
- (4) Existence of computational resources
- (5) Computational time required

Selection of a best turbulence model for a physical flow problem is very difficult. Because every model has its merits, demerits and limitations. The description of most famous models is given below:

4.5.2 Simplest Turbulence Two Equation Model (Standard k- ϵ Model)

The Standard k- ϵ Model is a simplest two equations model for the variables k and ϵ *i.e.* turbulent kinetic energy and its dissipation effects are generally preferred to find the value of the turbulent velocity and length scales. Now the Standard k- ϵ Model is a role model for different types of problems because it is simple, takes less computational time and gives the accurate results. Launder and Spalding are the researchers who derived the Standard k- ϵ Model. It is an economical model for different types of engineering problems. Robustness, economy, and reasonable accuracy are the key factors due to which this model is mostly used and preferred in the industry. This model is basically a semi-empirical model and is mostly used in Industry due to a wide range of turbulent flows.

Two transport equations for the turbulence kinetic energy (k) and turbulence kinetic energy dissipation rate (ϵ) are used with this model. Two transport equations for the turbulence kinetic energy (k) and its dissipation rate (ϵ) are derived with the help of physical and mathematical interpretation. The standard k- ϵ model was only preferred to solve the practical and industrial flow problems, which are totally turbulent in nature. In this model the effect of molecular viscosity is not taken in to consideration.

(a) Transport Equations for the Standard k- ϵ Model

The following Transport Equations for calculating the value of turbulence kinetic energy, k, and its rate of dissipation, ϵ , are given below:

$$\begin{aligned} \frac{\partial}{\partial t}(\rho k) + \frac{\partial}{\partial x_i}(\rho k u_i) \\ = \frac{\partial}{\partial x_j} \left[\left(\mu + \frac{\mu_t}{\sigma_k} \right) \frac{\partial k}{\partial x_j} \right] + G_k + G_b - \rho \varepsilon - Y_M + S_k \end{aligned} \quad (4.7)$$

$$\begin{aligned} \frac{\partial}{\partial t}(\rho \varepsilon) + \frac{\partial}{\partial x_i}(\rho \varepsilon u_i) = \frac{\partial}{\partial x_j} \left[\left(\mu + \frac{\mu_t}{\sigma_\varepsilon} \right) \frac{\partial \varepsilon}{\partial x_j} \right] + G_{1\varepsilon} \frac{\varepsilon}{k} (G_k + C_{3\varepsilon} G_b) - C_{2\varepsilon} \rho \frac{\varepsilon^2}{k} + S_\varepsilon \\ \dots\dots (4.8) \end{aligned}$$

In the equations (4.7) and (4.8) G_k stands for turbulence kinetic energy generation due to the mean velocity. Gradient. G_b stands for generation of kinetic energy by considering the buoyancy effect into consideration. Y_M stands for the ratio between compressible turbulence and the net dissipation rate in the presence of the fluctuating dilatation. Here the terms $C_{1\varepsilon}$, $C_{2\varepsilon}$, and $C_{3\varepsilon}$ are the model constants for the standard k- ε Model. σ_k and σ_ε in the above-mentioned transport equation show the turbulent Prandtl number for kinetic energy of the moving fluid due to turbulence and kinetic energy dissipation effects.

(b) Modeling the Viscous Parameter (Viscosity due to turbulence)

The equation for calculating the viscosity due to turbulence (μ_t) is achieved by taking the kinetic energy and its dissipation rate due to turbulence is given below. This equation is known as the modeling equation of turbulent viscosity for the standard k- ε Model.

$$\mu_t = \rho C_\mu \frac{k^2}{\varepsilon} \quad (4.9)$$

Where, C_μ shows a constant.

Here $C_{1\varepsilon}$, $C_{2\varepsilon}$, C_μ , σ_k , and σ_v are known as model constants. The values of the model constants are given below:

$$C_{1\varepsilon} = 1.44, \quad C_{2\varepsilon} = 1.92, \quad C_\mu = 0.09, \quad \sigma_k = 1.0, \quad \sigma_\varepsilon = 1.3$$

The above defined values have been determined by performing the experiments with air and water.

4.5.3 RNG k-ε Model

The Renormalization group k-ε turbulence model is obtained with the help of Navier-Stokes momentum equations at an instant and a mathematical method based on “renormalization group”. The transport equations for the **(RNG)** k-ε Model are given below: k-ε model. The Model for Renormalization group has some refinements with respect to the standard k-ε model are given below: Transport Equations for turbulent kinetic energy and its dissipation rate in the Renormalization group (RNG) k-ε Model are given below:

$$\frac{\partial}{\partial t}(\rho k) + \frac{\partial}{\partial x_i}(\rho k u_i) = \frac{\partial}{\partial x_j} \left[(\alpha_k \mu_{eff}) \frac{\partial k}{\partial x_j} \right] + G_k + G_b - \rho \varepsilon - Y_M + S_k \quad (4.10)$$

$$\frac{\partial}{\partial t}(\rho \varepsilon) + \frac{\partial}{\partial x_i}(\rho \varepsilon u_i) = \frac{\partial}{\partial x_j} \left[(\alpha_k \mu_{eff}) \frac{\partial \varepsilon}{\partial x_j} \right] + C_{1\varepsilon} \frac{\varepsilon}{k} (G_k + C_{3\varepsilon} G_b) - C_{2\varepsilon} \rho \frac{\varepsilon^2}{k} - R_\varepsilon + S_\varepsilon \quad (4.11)$$

In the equations (4.10) and (4.11) G_k stands for turbulence kinetic energy generation due to the mean velocity Gradient. G_b stands for generation of kinetic energy by considering the

buoyancy effect in to consideration. Y_M stands for the ratio between compressible turbulence and the net dissipation rate in the presence of the fluctuating dilatation α_k and α_ε show the inverse effective Prandtl numbers for kinetic energy and its dissipation rate due to turbulence respectively. S_k and S_ε show the user-defined source terms .in the above equations. (4.10) and (4.11).

Modeling the Viscous Parameter (Viscosity due to turbulence)

Differential Equation for turbulent viscosity can be obtained by using the method of scale elimination in Renormalization group turbulence model is shown below:

$$d \left(\frac{\rho^2 k}{\sqrt{\varepsilon \mu}} \right) = 1.72 \frac{\hat{\nu}}{\sqrt{\hat{\nu}^3 - 1 + C_\nu}} \quad (4.12)$$

Where

$$\hat{\nu} = \frac{\mu_{eff}}{\mu} \quad C_{\hat{\nu}} \approx 100$$

For calculating the changes in effective turbulent transport can be calculated by integration of the above equation with taking the effect of Reynolds number (or eddy scale) This Equation better solve the low-Reynolds-number flows and the flow near the wall, where viscosity plays a major role and Reynold number is less there.

Following equation for turbulent viscosity at the high value of the Reynolds-number is obtained is given below:

$$\mu_t = \rho C_\mu \frac{k^2}{\varepsilon} \quad (4.13)$$

Here $C_\mu = 0.0845$ comes by using Renormalization Group (RNG). Theory. The value of C_μ from RNG k- ϵ Model is approximately equals to 0.09 as in the case of the standard k- ϵ model.

4.5.4 The Recent Developed Turbulence Model (Realizable k- ϵ Model)

The realizable k- ϵ model is a relatively recent development and differs from the standard k- ϵ model in two important ways:

- The turbulent viscosity in the realizable k- ϵ model has the new mathematical equations for as compared to the standard k- ϵ model.
- The new equation for the dissipation rate in realizable k- ϵ model can be derived with the help of an exact equation for the transport of the mean-square vorticity fluctuation.

Transport Equations for the Realizable k- ϵ Model

Model transport Equations for the turbulent kinetic energy and its dissipation rate in the in the realizable k- ϵ model are given below:

$$\frac{\partial}{\partial t}(\rho k) + \frac{\partial}{\partial x_i}(\rho k u_i) = \frac{\partial}{\partial x_j} \left[\left(\mu + \frac{\mu_t}{\sigma_k} \right) \frac{\partial k}{\partial x_j} \right] + G_k + G_b - \rho \epsilon - Y_M + S_k \quad (4.14)$$

and

$$\frac{\partial}{\partial t}(\rho \epsilon) + \frac{\partial}{\partial x_i}(\rho \epsilon u_i) = \frac{\partial}{\partial x_j} \left[\left(\mu + \frac{\mu_t}{\sigma_\epsilon} \right) \frac{\partial \epsilon}{\partial x_j} \right] + \rho C_{1\epsilon} S_\epsilon + C_{1\epsilon} \frac{\epsilon}{k} (C_{3\epsilon} G_b) - C_{2\epsilon} \rho \frac{\epsilon^2}{k + \sqrt{\nu \epsilon}} + S_\epsilon \quad (4.15)$$

Where

$$\eta = \max \left[0.43, \frac{\eta}{\eta+5} \right] \quad \eta = S \frac{k}{\varepsilon}$$

Modeling equation for calculating the Turbulent Viscosity in a turbulent flow by considering the turbulent kinetic energy and turbulent kinetic energy dissipation rate is given below:

$$\mu_t = \rho C_\mu \frac{k^2}{\varepsilon} \quad (4.16)$$

The value of the C_μ is no longer constant in this turbulence model as compared to the others models such as standard and Renormalization group. The value of this constant C_μ can be calculated with the help of the equation is given below:

$$C_\mu = \frac{1}{A_0 + A_s \frac{kU^*}{\varepsilon}} \quad (4.17)$$

Where

$$U^* = \sqrt{S_{ij}S_{ij} + \tilde{\Omega}_{ij}\tilde{\Omega}_{ij}}$$

$$\tilde{\Omega}_{ij} = \Omega_{ij} - 2\varepsilon_{ijk}\omega_k$$

and $\tilde{\Omega}_{ij} = \bar{\Omega}_{ij} - \varepsilon_{ijk}\omega_k$

Model Constants in the realizable k-ε model

Following model constants have been established for the better performance of the realizable k-ε model in certain canonical flows. The values of the model constants are given below.

$$C_{1\varepsilon} = 1.44; \quad C_2 = 1.9; \quad \sigma_k = 1.0; \quad \sigma_\varepsilon = 1.2$$

4.5.5 Turbulence Modeling in Swirling Flows

If you are modeling turbulent flow with a significant amount of swirl (e.g., cyclone flows, swirling jets), you should consider using one of FLUENT's advanced turbulence models: the RNG k- ϵ model, realizable k- ϵ model, or Reynolds stress model. The appropriate choice depends on the strength of the swirl, which can be gauged by the swirl number. The swirl number is defined as the ratio of the axial flux of angular momentum to the axial flux of axial momentum

$$S = \frac{\int r\omega\vec{v}\cdot d\vec{A}}{R \int u\vec{v}\cdot d\vec{A}} \quad (4.18)$$

Where R is the hydraulic radius.

For swirling flows encountered in devices such as cyclone separators and swirl combustors, near-wall turbulence modeling is quite often a secondary issue at most. The fidelity of the predictions in these cases is mainly determined by the accuracy of the turbulence model in the core region. However, in cases where walls actively participate in the generation of swirl (i.e., where the secondary flows and vertical flows are generated by pressure gradients), non-equilibrium wall functions can often improve the predictions since they use a law of the wall for mean velocity sensitized to pressure gradients.

4.6 Simulation Procedure

STEP 1: Modeling

- Diffuser geometry is created
- Stabilizing length equal to D was attached at inlet.
- Boundary layer was attached to both the hub and casing wall with growth factor 1.1 and 10 rows.

- Quadrilateral elements were used to mesh the diffuser geometry by taking mesh size of 0.07 cm. The number of elements in the mesh were 12000 – 75000 elements.
- Different Boundary conditions were taken are given below:
 - (i) velocity profile with axial and swirl components was entered at the inlet of the diffuser (ii). Atmospheric pressure was enter at the outlet of the diffuser (iii). No slip conditions was provided at the wall of the hub and casing.Air was chosen as a working fluid.
- After that the model geometry with proper meshing was exported to Fluent for post processing.

STEP 2: Solving the Problem by using Fluent

- In this step we checked the grid quality and its dimension.
- After that two-dimensional axisymmetric solver was taken.
- Then segregated solution procedure was taken.
- In this step atmospheric air was taking as the moving fluid and after that the values of different properties were selected
- Renormalization K- ϵ turbulence model was selected.
- Inlet velocity profile for axial and swirl velocity with and without swirl was entered at the inlet section.

- Turbulence intensity of 3% was entered at the intake of the present problem. The turbulence intensity was mentioned on the basis of flow diameter at the intake section of the test diffuser with constant diameter hub and diverging casing.
- Zero gauge pressure was mentioned at the exit of the test diffuser with constant diameter hub and diverging casing.
- Second order upwind scheme was used. For solving the mass balance and momentum conservation equations.
- Convergence criteria of 10^{-6} was used to minimize the error.
- After giving the convergence, Solution was initialized at inlet of the annular diffuser.
- Finally, iterations were given to iterate up to convergence of the solution.

Finally, longitudinal velocity, swirl velocity and pressure recovery coefficients were calculated and plotted after converging the solution.

4.7 Methodology adopted

We have used the different steps to solve the present problem of axial annular diffuser. The given block diagram shows the different steps which are used to solve the problem as shown in the Figure

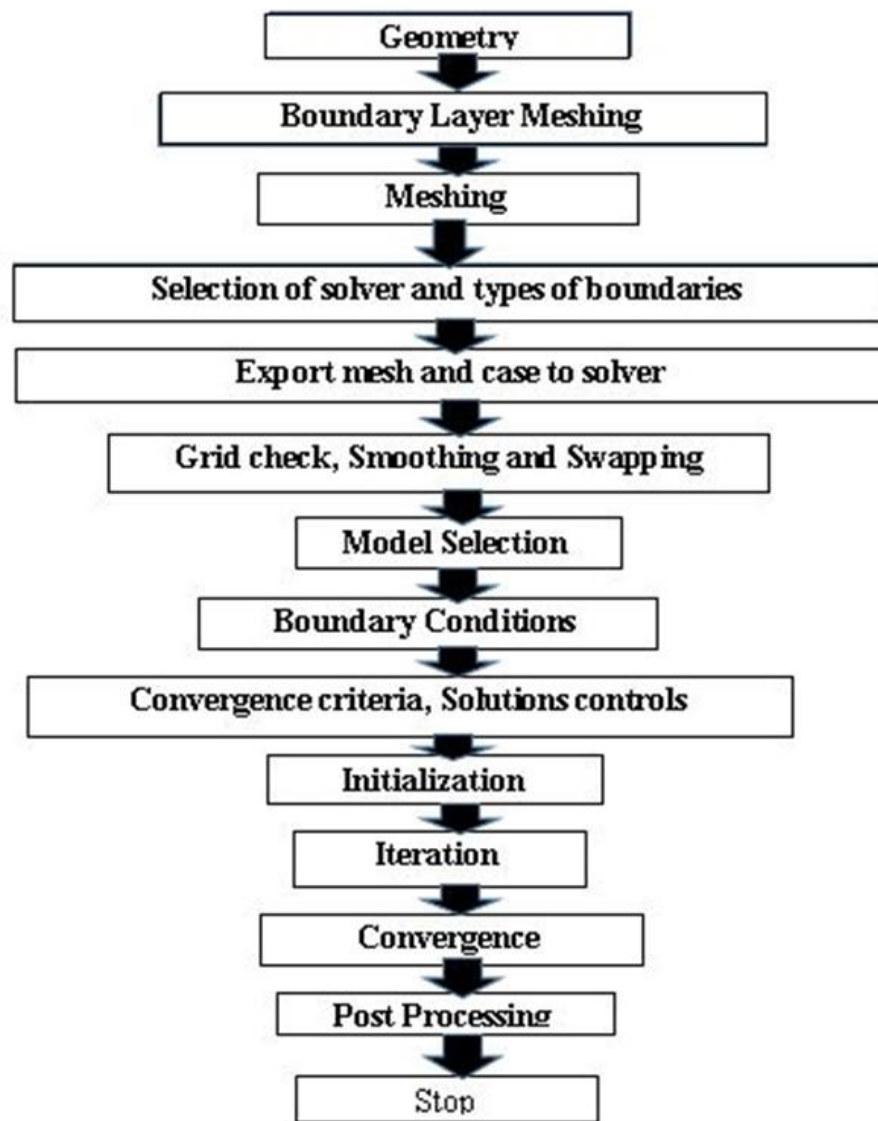


Fig. 4.1 Flow-Chart for CFD Modeling and Simulation.

CHAPTER 5

VALIDATION

This chapter shows the validation of Computational results with the obtained experimental results. In this chapter we have compared the computationally obtained longitudinal and swirl velocity with the experimentally obtained longitudinal velocity and swirl velocity at different axial locations along the annular diffuser passage height.

5.1 INTRODUCTION

Experimental and computational methods to obtain detailed performance data of mean flow quantities in plane two dimensional axisymmetric boundary layer flows without and with swirling flow conditions at the diffuser inlet for axial annular diffusers have been explained in the previous chapters. However to analyze the correlation between the two methods and their interdependence needs to be checked for further investigation. Present study in this chapter demonstrates the comparison of the results obtained with the computational method and with the experimental methods. The validation has been carried out to check the grid independence, best model suited for the present investigation based upon the close proximity of the computational results with those of experimental results in terms of inlet flow conditions, development of velocity profile and pressure recovery coefficients.

5.2 Grid Independence

The outcomes of any numerical turbulence model based on the quality of meshing chosen *i.e.* coarser, finer and the finest for a prescribed geometry in 2D or 3D. The meshing of any

geometry whether in 2D or 3D contains nodes. Cells and grid generally. The results of any computational model depend on the size of grid. Meshing is done to break the computational region into the very small regions of the physical problem. The grids which are used in Computational Fluid Dynamics may be coarser and finer. The results obtained from the coarser mesh are not accurate due to less number of meshing elements. On the other hand finer mesh gives the better results due to large number of meshing elements. Finer mesh takes a lot of computational time as compared to coarser mesh. So we have to choose the optimum grid size which takes the less computational time without sacrificing the accuracy.

Grid independence test was performed on different geometries by using different turbulence models. Here we have performed the grid independence test on the diffuser geometry for which the experimental results were obtained. Grid independence test has been performed on annular diffuser with constant diameter central shaft and diverging outer surface. We have used the same velocity profile, which was obtained experimentally for solving the computationally. The results of Renormalization- group $k-\epsilon$ model were much closer with the experimental results. Grid sensitivity was checked by taking four mesh sizes. The different geometries of annular diffusers have different dimensions and different number of grids. Grid size and computational time have been taken as parameters to obtain the optimum grid size. In the present problem quadrilateral elements have been used for meshing the different geometries of the diffusers. The dimension of one side of the quadrilateral cell represents the grid size in the present problem. Four grid sizes 0.6, 0.7, 0.8 and 0.9 mm were taken to analyze the effect of mesh size and computational time required on the accuracy obtained with respect to experimental results. Table 5.1 shows

details description about the different type of meshing with their elements and the computation time required in convergence the solution for different types of meshes.

Table 5.1 Mesh Size

	Shape of the element	Grid Size (mm)	Number. of Cells	Number. of Face	Number. of Nodes	Calculation Time (minute)
Non-refine mesh	Quadrilateral.	0.9	70614	142218	71606	150
Fine mesh	Quadrilateral.	0.8	127536	256181	128646	489
Finer mesh	Quadrilateral	0.7	234096	469454	235359	1152
Finer mesh	Quadrilateral.	0.6	410331	822131	411801	2994

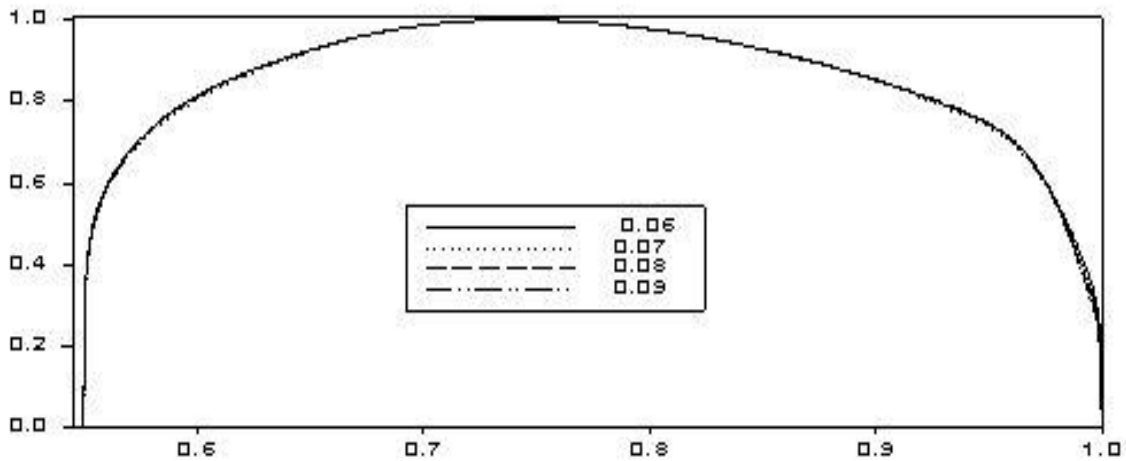


Fig. 5.1 Grid independence test at different mesh size for longitudinal velocity versus non-dimensional height at axial position $(x/L) = 10\%$

Figure 5.1 depicts that the findings of the grid size 0.6, 0.7, 0.8 and 0.9 mm with the help of Renormalization Group (RNG) k-ε model. The findings of grid sizes 0.6 and 07 mm

shows the same results approximately. So the grid size 0.7 mm has been selected for the given Computational Fluid Dynamics analysis to minimize the calculating time without neglecting the accuracy.

5.3 Validation of Different Turbulence Models

It is very difficult to choose an optimum turbulence model due to variations of physical conditions in various processes where we have to handle different types of Parameters. An optimum model is a model which gives the results very close to the experimental results under given conditions. The different types of model which were used are given below:

- **k- ϵ model**
 - Standard **k- ϵ Model**
 - Renormalization-group (RNG) **k- ϵ Model**
 - Realizable **k- ϵ Model**
- **The Spalart-Allmaras Model**
 - Vorticity Based Production
 - Strain/ Vorticity Based Production
- (SST) **k- ω Model**
- Reynolds Stress Model (RSM)
- Standard **k- ω Model**

The above mentioned turbulence models investigated by using experimentally obtained inlet velocity profile for a fully developed velocity profile on a diffuser with central shaft. Fig. 5.2 and Fig.5.3 shows the Non-dimensional longitudinal velocity and Non-dimensional swirl velocity variations with respect to radial passage heights.

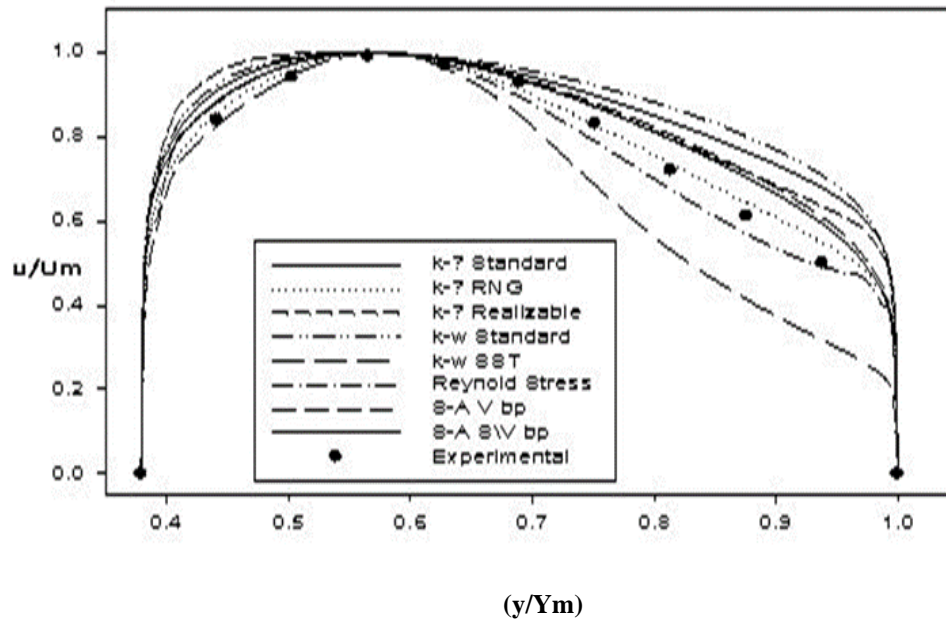
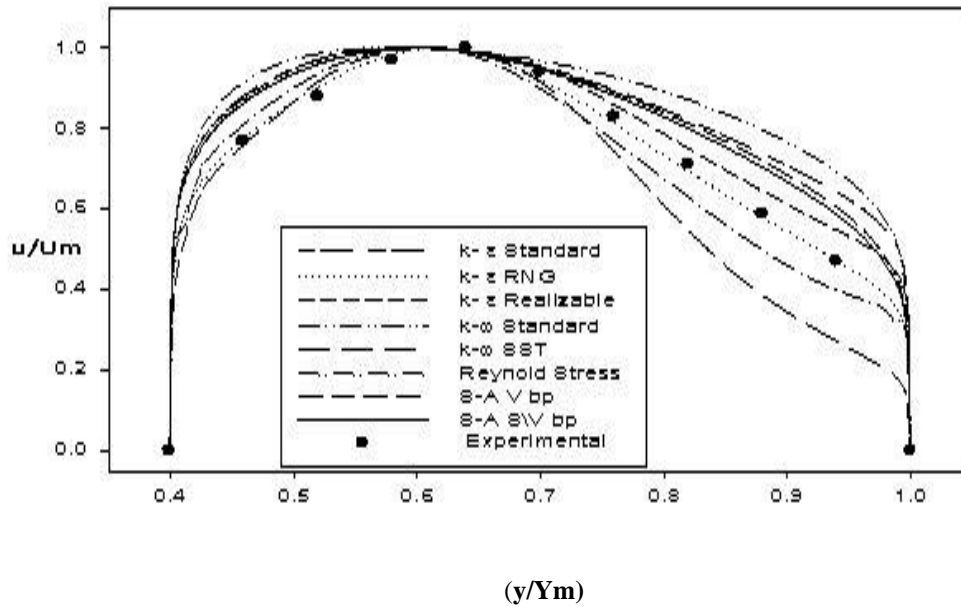


Fig. 5.2 Validation of Turbulence Model with Experimental Results in terms of Longitudinal Velocity of annular diffuser with AR=2, equivalent cone angle 20° along non-dimensional diffuser passage height at axial locations of 80% and 90% respectively.

Figures 5.2 and 5.3 shows that the results of (RNG) $k-\epsilon$ model were very closed to the experimental results. Finally, we have analyzed the flow through annular diffuser by varying the area ratio and swirl angles at the inlet by taking Renormalization-group (RNG) $k-\epsilon$ turbulence model.

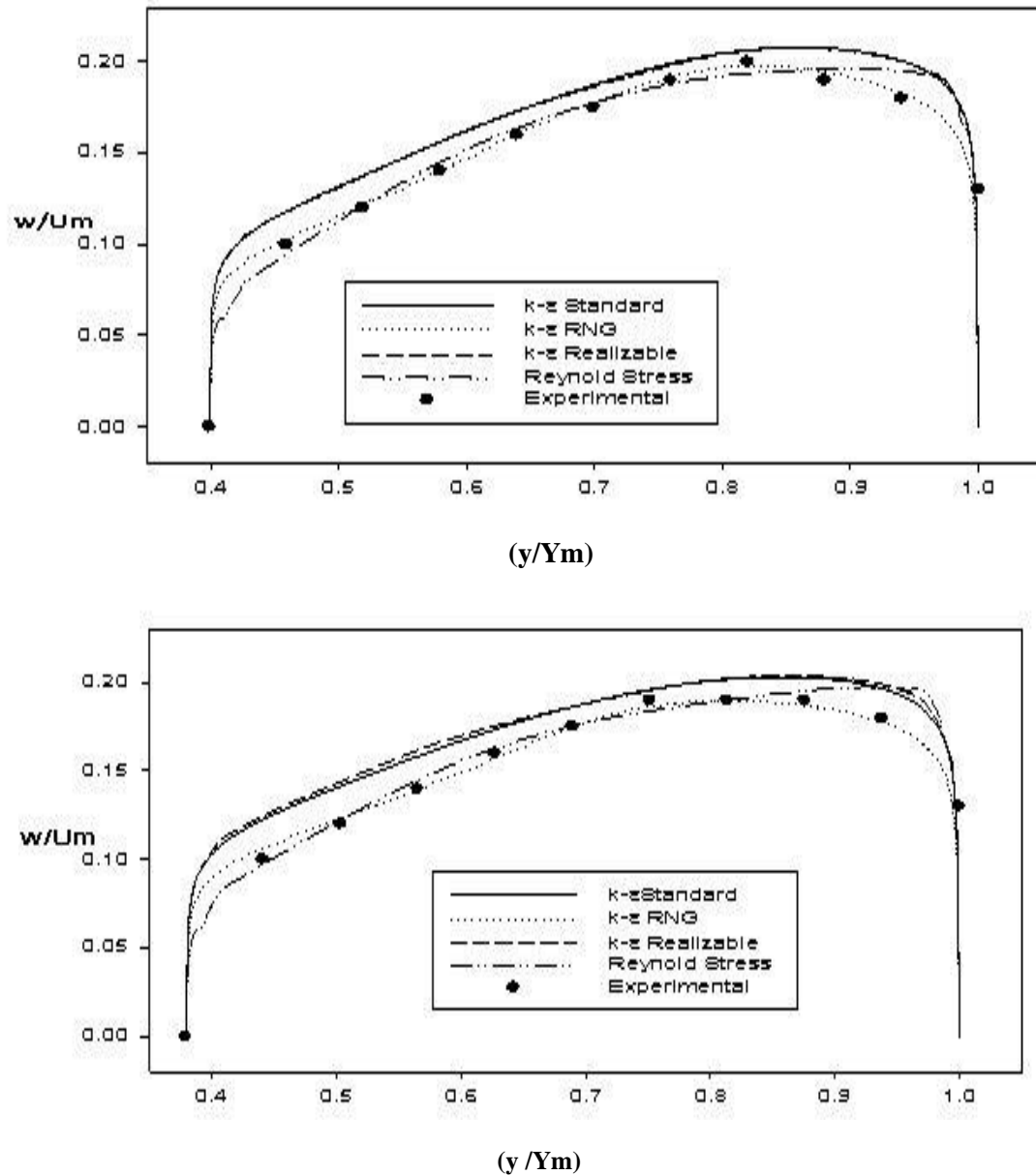


Fig. 5.3 Validation of Turbulence Models with Experimental Results of Swirl Velocity of annular diffuser of AR=2, equivalent cone angle 20° along non-dimensional diffuser passage height at the lengths of $(x/L) = 0.6$ and 0.9 .

CHAPTER 6

RESULTS AND DISCUSSION

This chapter covers the study and analysis of flow through Constant diameter central shaft i.e. hub and enlarging outer surface i.e. Casing with various area ratio 2, 2.5, 3 and 4 with or without swirl for the annular diffuser. In this chapter the variation of longitudinal velocity and swirl velocity with respect to diffuser passage height have been analyzed with and without swirl. In this chapter Variation of Pressure recovery coefficients have been analyzed on the casing and hub of the diffuser.

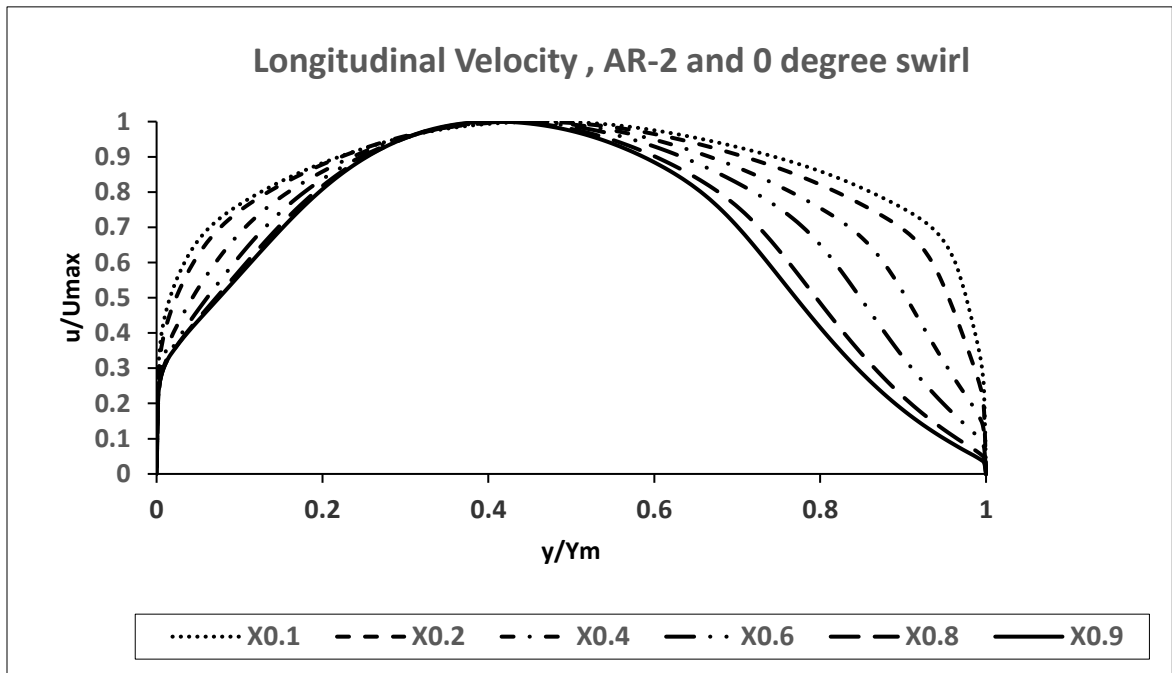
6.1 Introduction

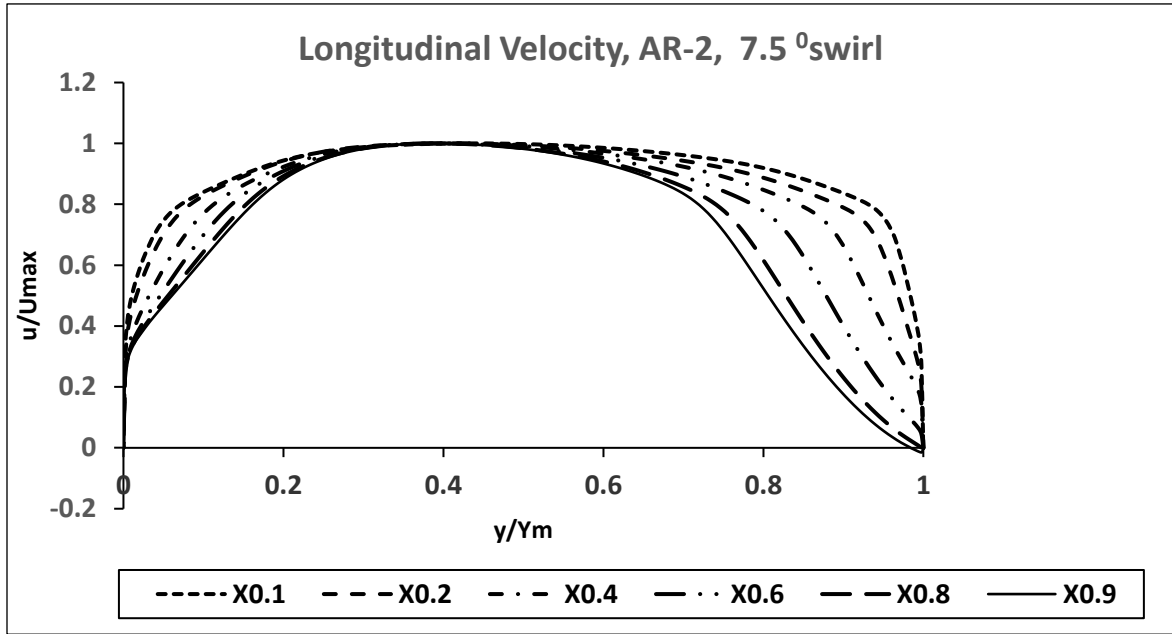
The present work in this chapter relates to the analysis of flow through the constant diameter hub and enlarging outer surface of annular diffuser in the presence and absence of rotary flow at the inlet. In this analysis development of flow, flow reversals and separation of flow have been visualized in the annular diffuser. Here longitudinal velocity and Swirl velocity have been plotted and analyzed along different diffuser passage heights at different traverses along axial direction at 10% , 20 % , 40 % , 60% , 80% and 90% with the A.R. of 2, 3 and 4. All the longitudinal velocity and swirl velocity variations are presented with respect to maximum longitudinal velocity i.e.in the non-dimensional form. Longitudinal velocity and swirl velocity have been plotted with respect to radial passage heights (y/Y_{\max}) at a particular location along the axial direction in the annular diffuser. Here y is the distance perpendicular to the axial direction and Y_{\max} is the maximum distance at traverse. $(y/Y_{\max}) = 0$ shows the central shaft position and $(y / Y_{\max}) = 1$ shows the outer

surface location of given annular diffuser. The values of swirl angle have been taken as 0° , 7.5° , 12° , 17° and 25° at the inlet of the diffuser. Computational results in terms of longitudinal velocity, swirl velocity and pressure recovery coefficient were analyzed through the annular diffuser by using Renormalization group RNG k- ϵ Turbulence model. The graphs of longitudinal and swirl velocity are presented on different movements along radial direction of the annular diffuser at various axial locations of 10%, 20%, 40%, 60%, 80% and 90% for the area ratio of 2, 3 and 4 with inlet swirl angles of 0° , 7.5° , 12° , 17° and 25° .

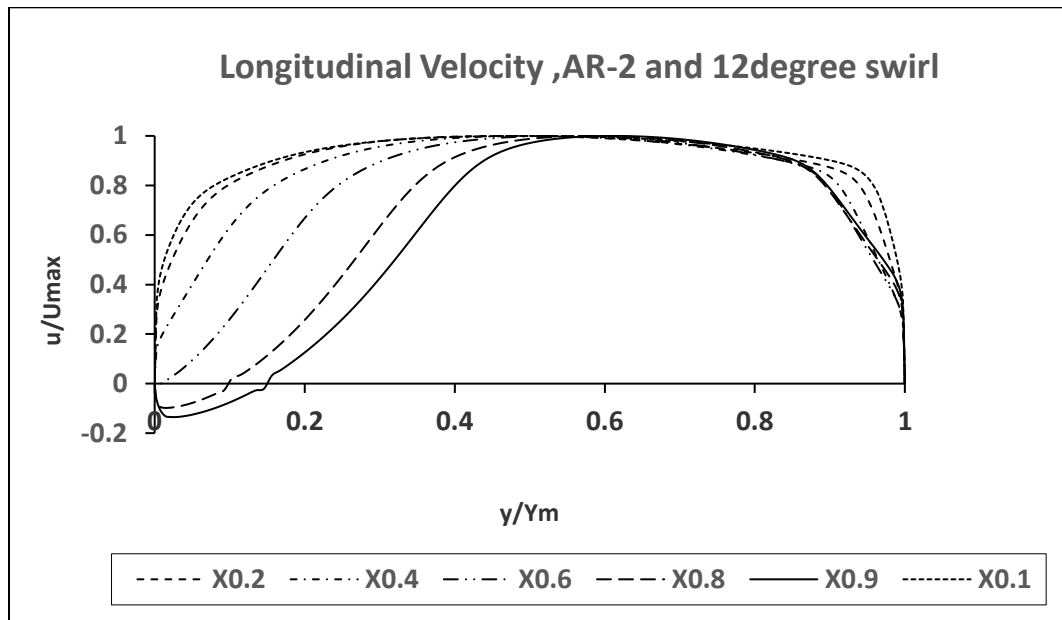
Figure 6.1 to 6.4 illustrate the velocity profiles by taking different Area ratio 2, 2.5, 3 and 4 for 20° equivalent cone angle Parallel hub and diverging casing annular diffuser. Fig.6.1 (a) to 6.4 (a) shows the Non-dimensional longitudinal velocity with respect to diffuser passage height. Whereas 6.1(b) to 6.4(b) shows the non-dimensional swirl velocity with respect to diffuser passage height. It is clear from the Fig.6.1 (a) to 6.4(a) that diffuser flow is produced at the hub for 0 degree swirl at inlet and the flow shifts towards the hub side by changing the area ratio for the given experimental velocity variation.. The maximum value of longitudinal velocity with swirl angles of 0° , 7.5° , 12° , 17° and 25° occurs at $(y/Y_{max}) = 0.4, 0.48, 0.64, 0.68$ and 0.8 respectively for AR=2. For AR=3 the peak value of longitudinal velocity for inlet swirl angles of 0° , 7.5° , 12° , 17° and 25° occur at $(y/Y_m) = 0.34, 0.44, 0.72, 0.88$ and 0.92 respectively along diffuser passage heights. For AR=4, the peak of longitudinal velocity for inlet swirl angles of 0° , 7.5° , 12° , 17° and 25° occur at $(y/Y_m) = 0.32, 0.36, 0.84, 0.86$ and 0.96 respectively along the diffuser passage height. It is clear from the Fig.6.1 (a) that the flow changes its direction in the backward direction at the outer wall of the diffuser for 7.5 degree swirl at inlet up to $(y/Y_{max}) = 0.98$ along

90% axial location for area ratio of 2. Whereas flow changes its direction at the surface of the hub for inlet swirl of 12, 17 and 25 degree. The flow changes its direction at $x/L = 80\%$ along the axial direction for 12° swirl at inlet. It also takes place at $x/L = 60\%$ along the axial direction for 17 inlet swirl and at $x/L = 80\%$ for 25° inlet swirl. For 12 degree swirl at inlet the flow changes its direction up to $(y/Y_{max}) = 0.1$ and 0.16 along axial location of 80% and 90%. For 17 degree swirl at inlet the flow changes its direction up to $(y/Y_{max}) = 0.08, 0.18$ and 0.24 along axial location of 60, 80 and 90% respectively. Whereas reversal of flow takes place up to $(y/Y_{max}) = 0.06$ and 0.1 along axial location 80 and 90% of the axial annular diffuser for 25° swirl at the inlet.





(ii)



(iii)

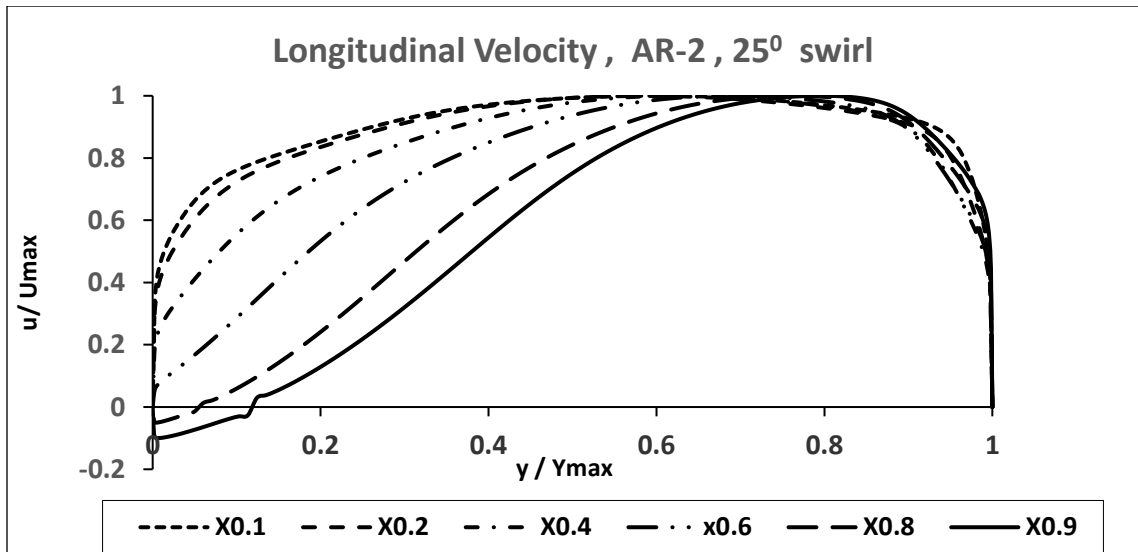
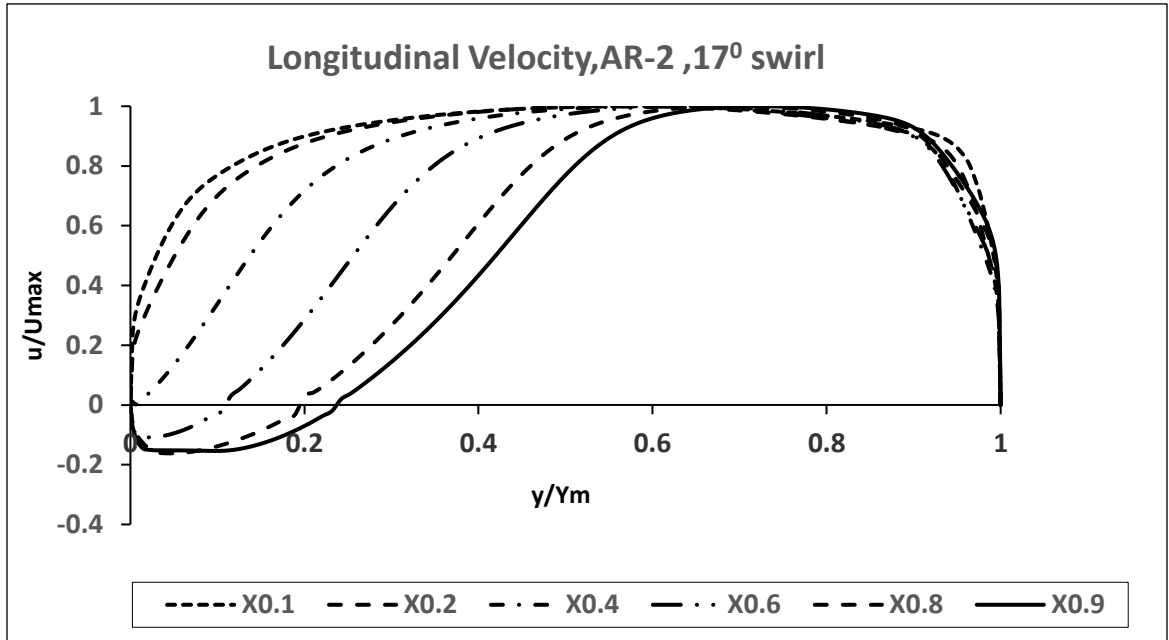


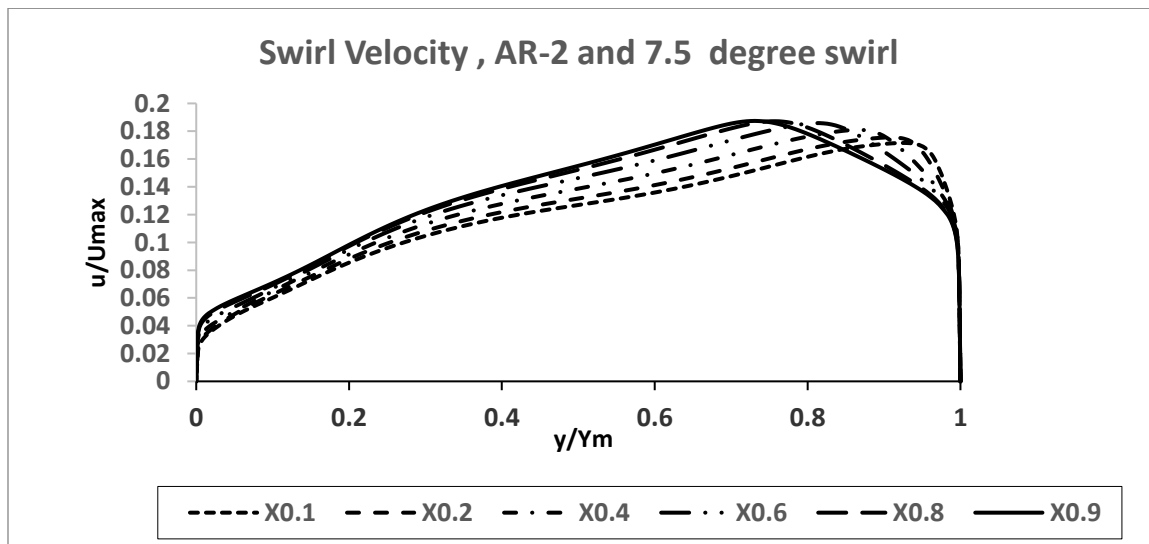
Fig. 6.1 (a) Variation of Longitudinal Velocity with respect to non-dimensional radial passage height (y/Y_{max}) for equivalent cone angle of 20° at different axial positions of 10%, 20%, 40%, 60%, 80% and 90% with swirl angles (i) 0° , (ii) 7.5° , (iii) 12° , (iv) 17° and (v) 25° .

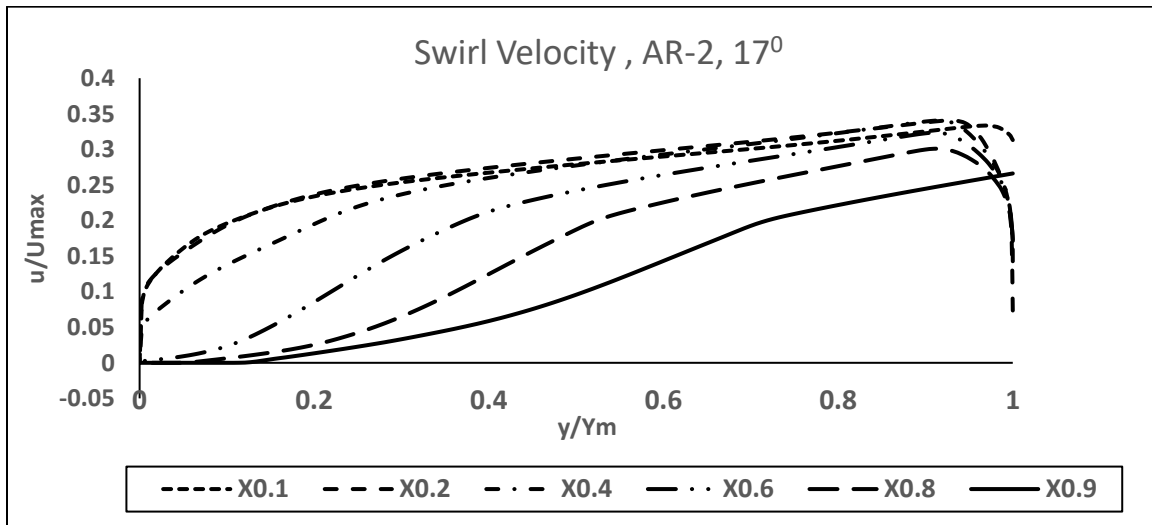
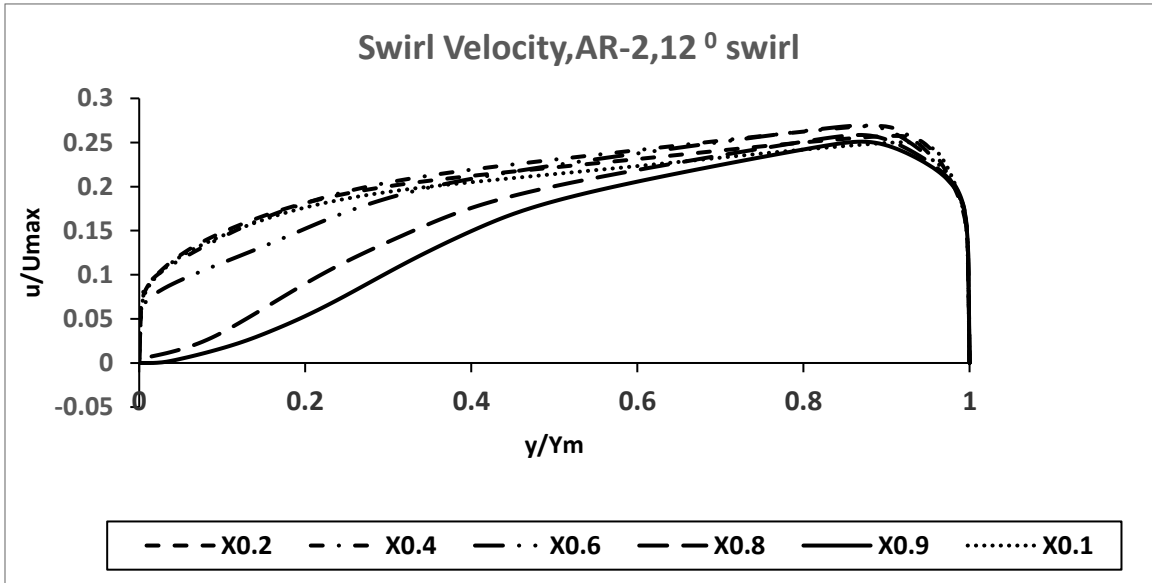
Figure. 6.2 (a) shows that the moving fluid changes its direction at the outer wall of the annular diffuser with 0° and 7.5° swirl along axial position of 60, 80 and 90% for area ratio of 3. For 7.5° swirl at inlet it occurs from outer wall surface up to $(y/Y_{max}) = 0.92, 0.9$ and 0.84 along axial position of 60, 80 and 90 % along the length of the diffuser. Flow changes its direction at the hub wall for $12^\circ, 17^\circ$ and 25° swirl at the inlet. The direction of the flow changes up to $(y/Y_{max}) = 0.06, 0.2, 0.3$ and 0.34 at axial position of 40, 60, 80 and 90% along the axial position for 12° swirl at the inlet. Diffuser flow also changes its direction up to $(y/Y_{max}) = 0.16, 0.28, 0.36$ and 0.38 at axial location 40, 60, 80 and 90 % along the length of the diffuser for 17° swirl at the inlet. Whereas diffuser flow changes its direction in the backward direction up to $(y/Y_{max}) = 0.08, 0.26, 0.36$ and 0.42 at axial location 40, 60, 80 and 90% along the diffuser for the area ratio of 25 degree respectively. Fig.6.3 (a) shows that the direction of flow changes in the backward direction at the outer surface of the annular diffuser with 7.5° inlet swirl and without swirl for area ratio 4. The flow at the casing reverses its direction at 60% , 80 % and 90% along the length of the annular diffuser. Flow reversal occurs at $(y/Y_m) = 0.95, 0.92$ and 0.9 . towards the outer wall without swirl flow. Flow reversal also occurs at $(y/Y_m) = 0.88, 0.84$ and 0.82 towards the casing wall with 7.5° swirl flow. The flow reversal moves from the casing side towards hub at swirl angle of 12° and more. The direction of flow changes in the backward direction at $x/L = 40\%$ for $12^\circ, 17^\circ$ and 25° inlet swirl angles. Flow changes its direction up to $(y/Y_{max}) = 0.16, 0.32, 0.38$ and 0.48 at axial position of 40%, 60%, 80% and 90 % respectively with inlet swirl of 12° . Flow changes its direction up to $(y/Y_{max}) = 0.16, 0.30, 0.40$ and 0.48 at 40%, 60%, 80% and 90 % along the axial direction of the diffuser for 17-degree swirl angle.

Flow changes its direction up to $(y/Y_{max}) = 0.16, 0.34, 0.42$ and 0.48 at 40%,60%,80% and 90 % along the axial direction of the diffuser for 25^0 swirl angles respectively.

It was clear from the Figure 6.4 (a) that the flow does not change its direction in the backward direction on the outer wall of the annular diffuser for $0^0, 7.5^0$ and 12^0 inlet swirl. Flow changes its direction at the hub surface for $17^0, 25^0$ swirl at the inlet. The flow changes its direction at 30% and 70% along the axial direction for 17^0 and 25^0 swirl at the inlet. The flow changes its direction up to $(y/Y_{max}) = 0.12, 0.22$ at $x/L = 70\%$ and 90% for 17^0 swirl at inlet. Whereas flow changes its direction up to $(y/Y_{max}) = 0.4, 0.22, 0.3$ and 0.34 at axial positions of 30 %, 50%, 70% and 90% for 25^0 swirl at the inlet of the diffuser.

Figure 6.5 (a) , (b), (c), (d) and (e) shows the velocity stream line diagram for area of 2 and at different swirl angles of $0^0, 7.5^0, 12^0, 17^0$ and 25^0 for the constant diameter hub and diverging casing annular diffuser. This diagram shows the directions of fluid flow, separation of flow and flow reversal.





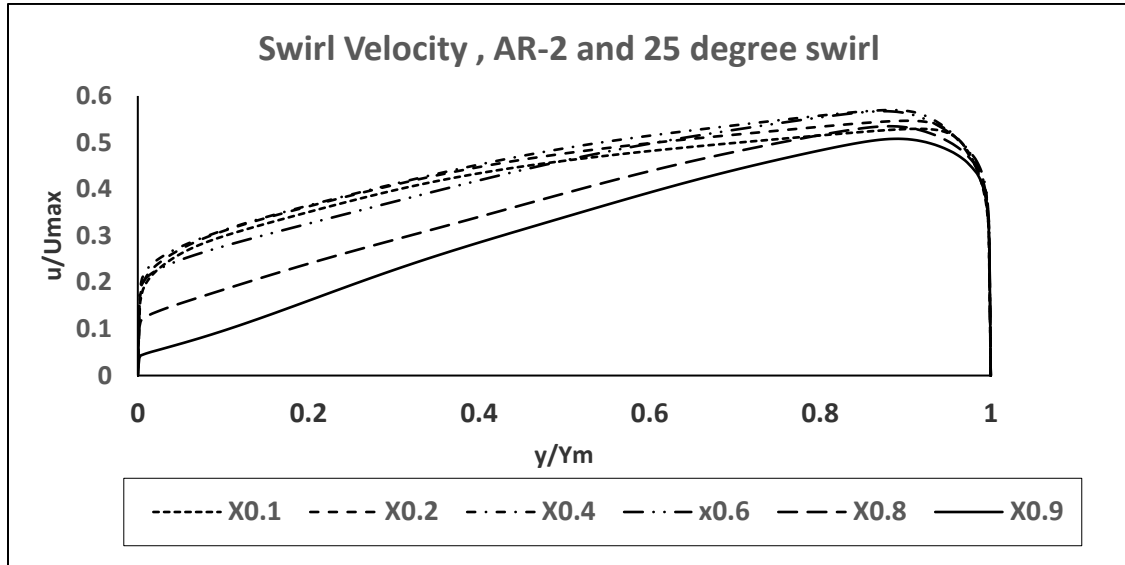
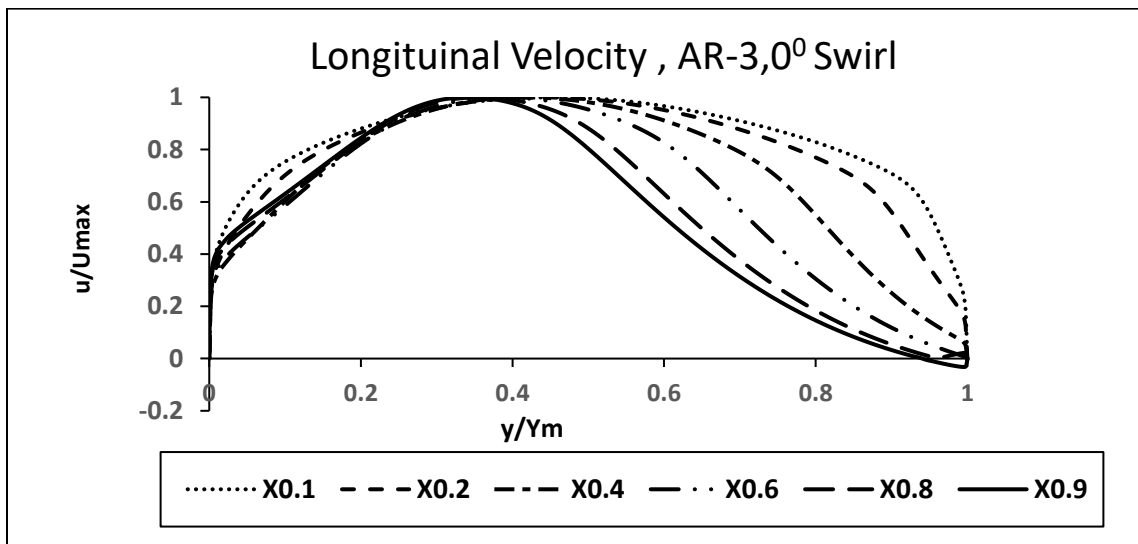
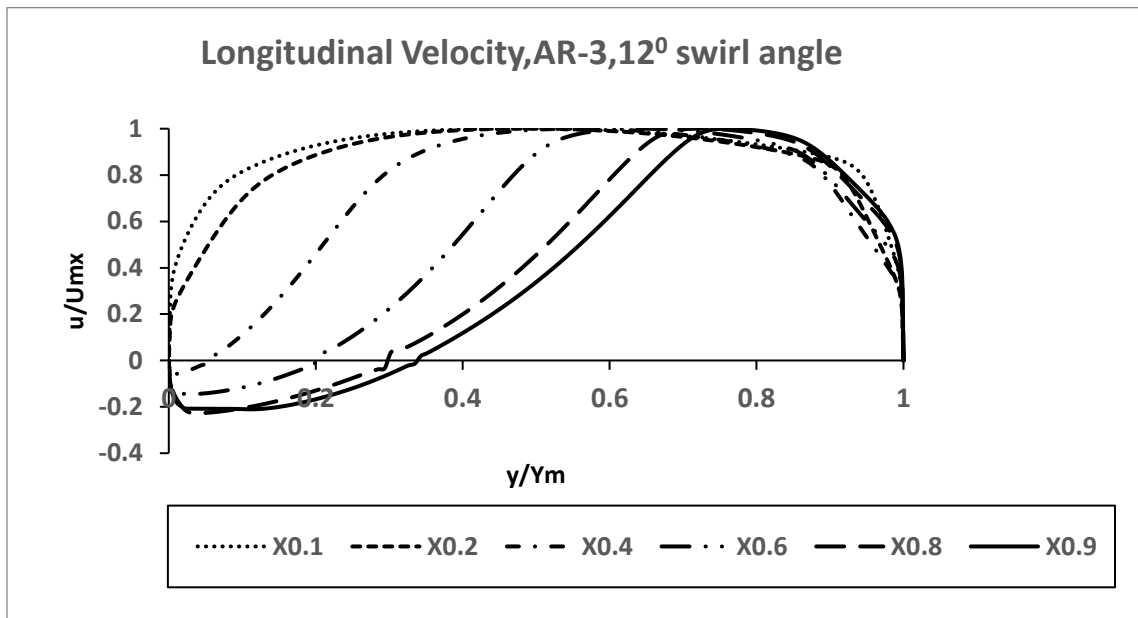
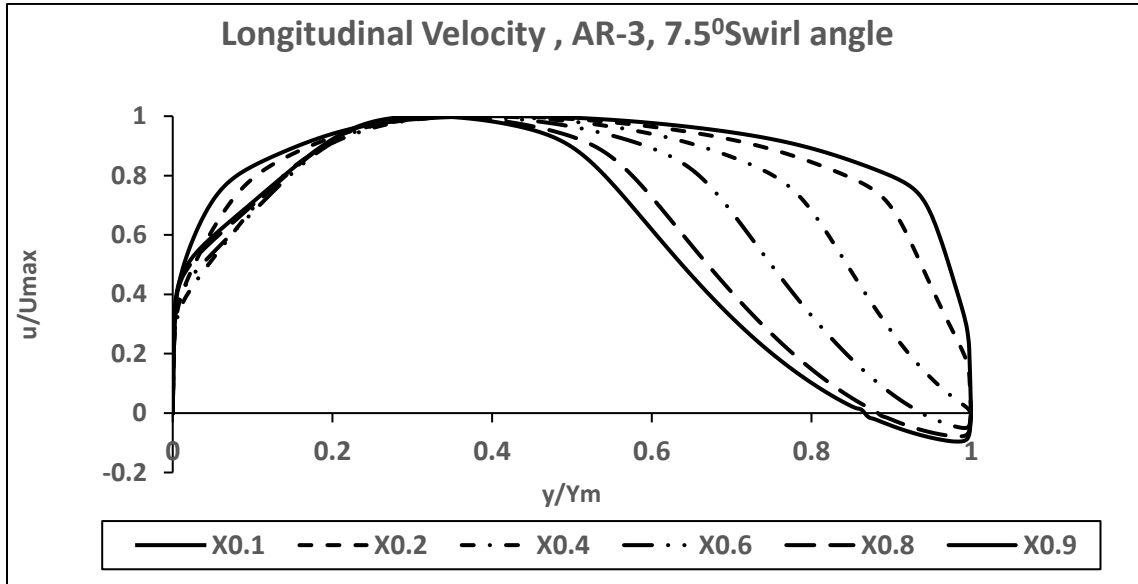


Fig. 6.1 (b) Variation of Swirl Velocity with respect to non-dimensional radial diffuser passage heights (y/Y_{max}) at different axial positions (10%, 20%, 40%, 60%, 80% and 90%).





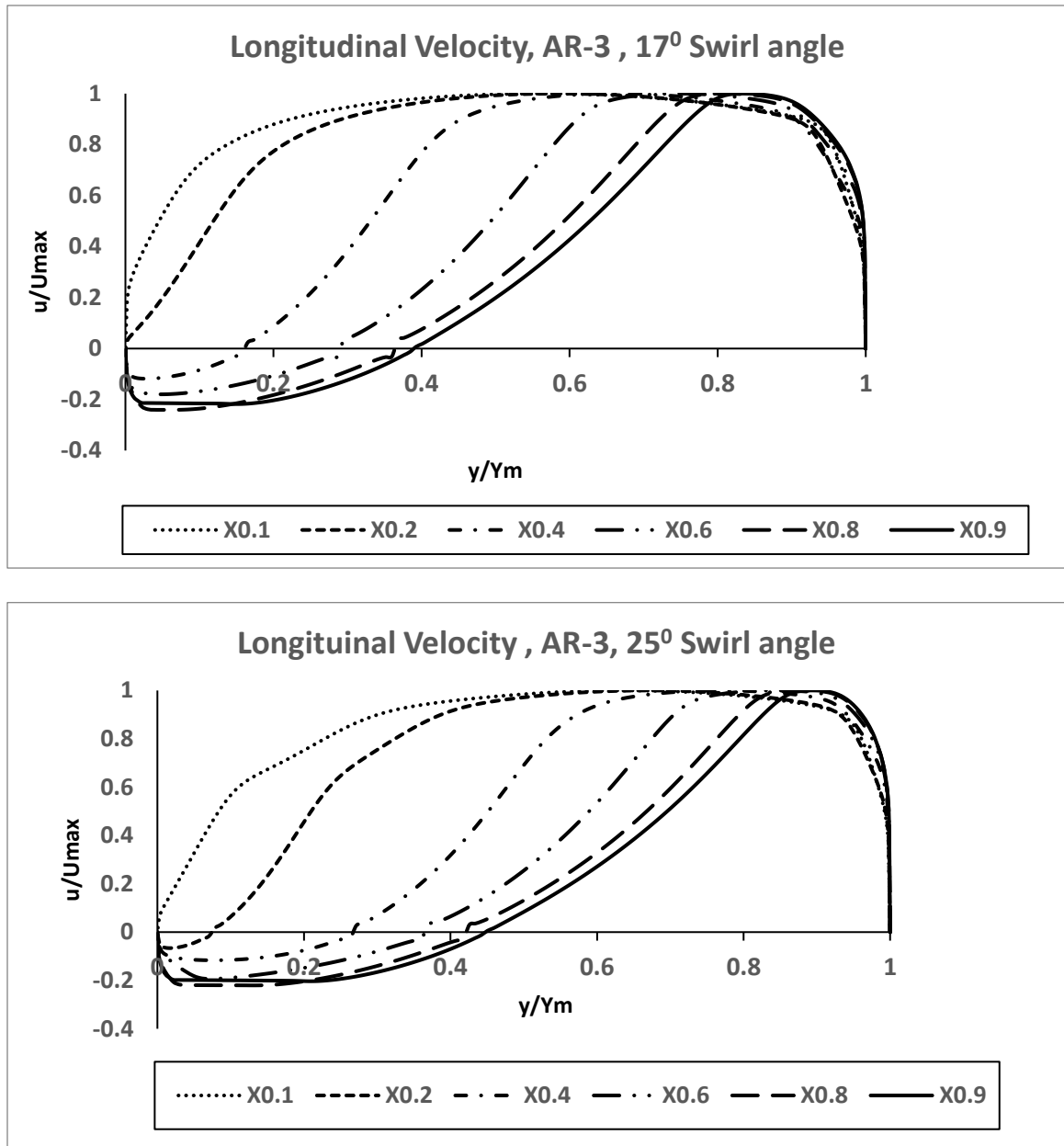
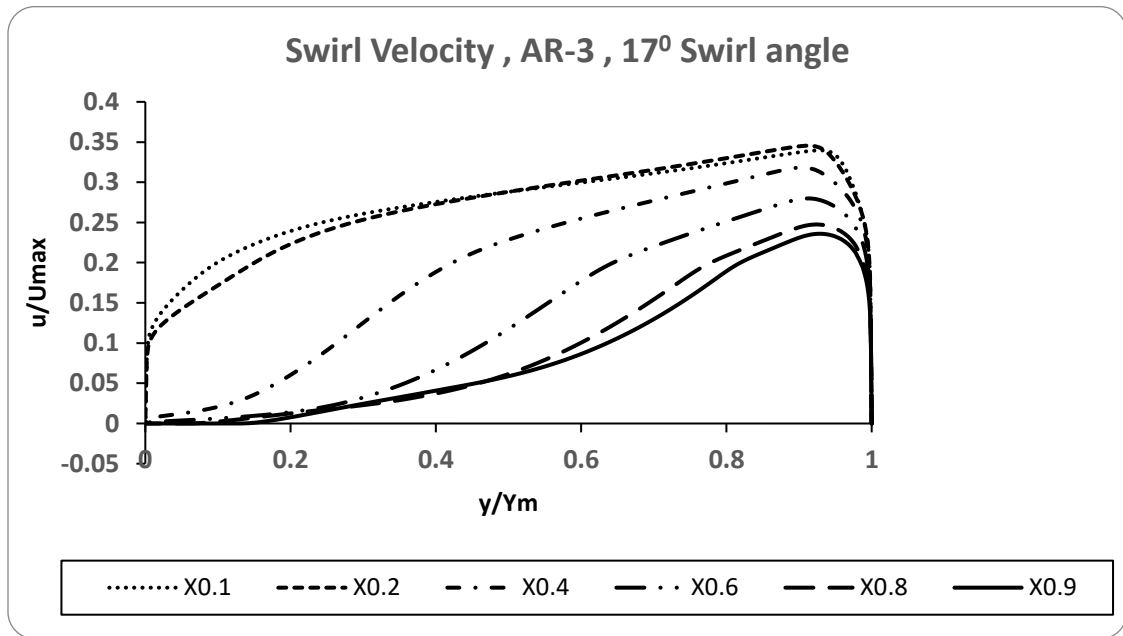
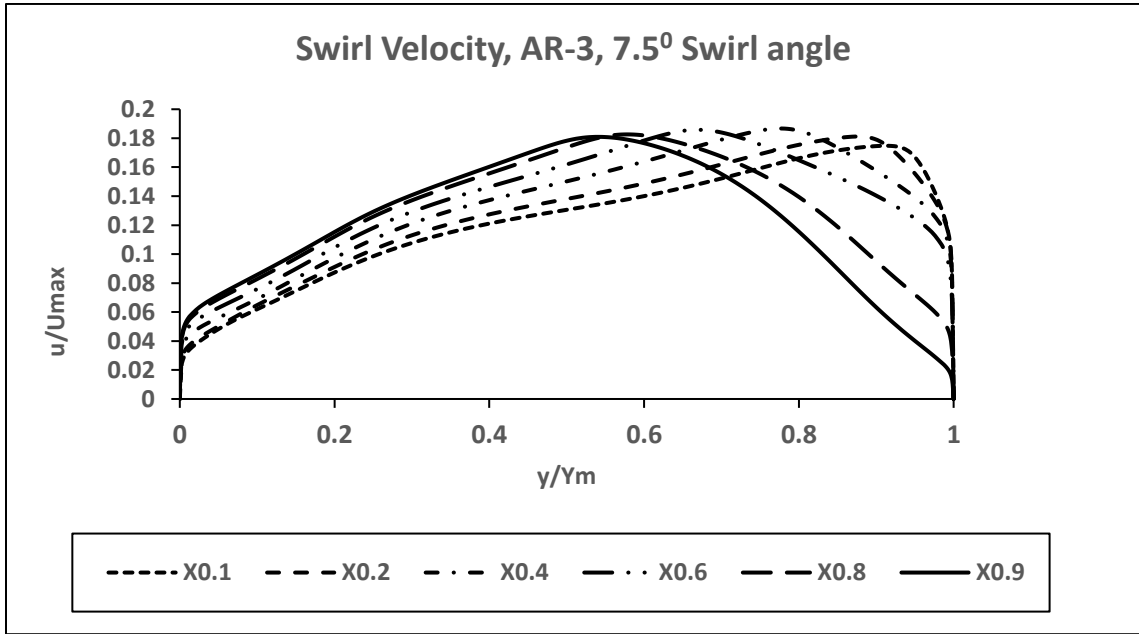


Fig. 6.2 (a) Variation of Longitudinal Velocity with respect to non-dimensional radial height (y/Y_{max}) at different axial positions (10%, 20%, 40%, 60%, 80% and 90%).



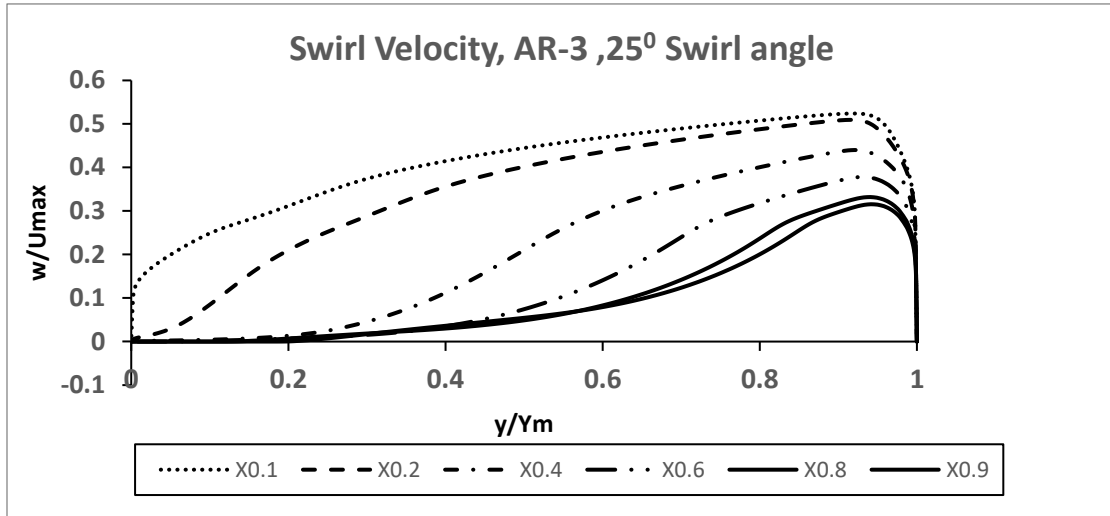
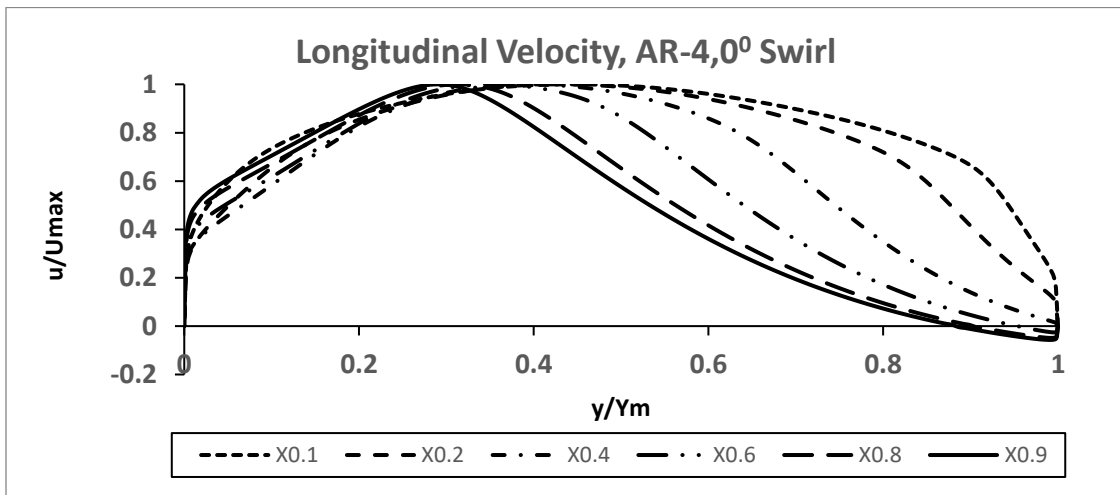


Fig. 6.2(b) Variation of Swirl Velocity with respect to non-dimensional radial diffuser passage heights (y/Y_{max}) by taking the cone angle of 20° , Area ratio of 3 and swirl angles of (0° to 25°) at different axial positions(10%, 20% ,40% ,60% ,80% and 90%).



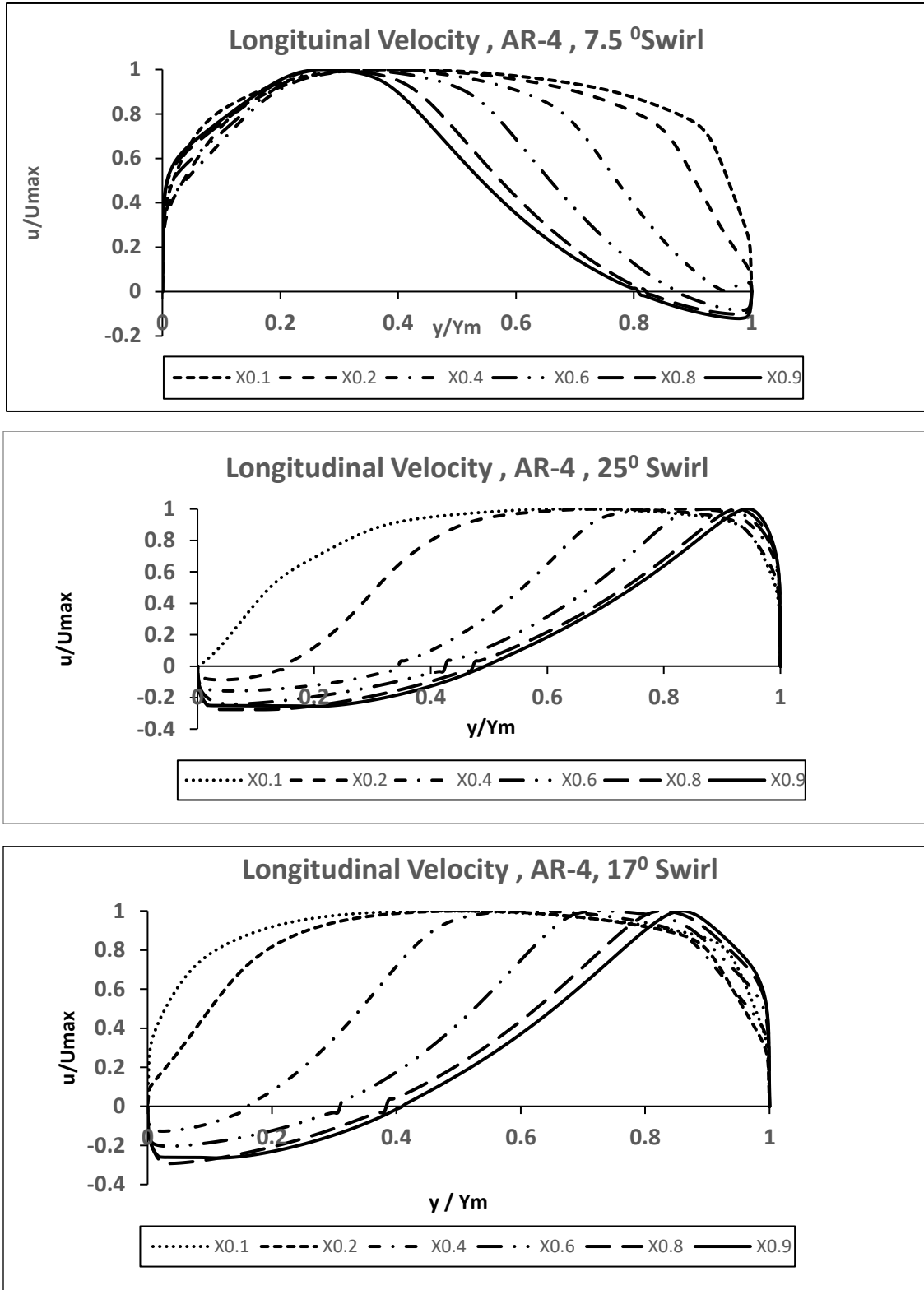
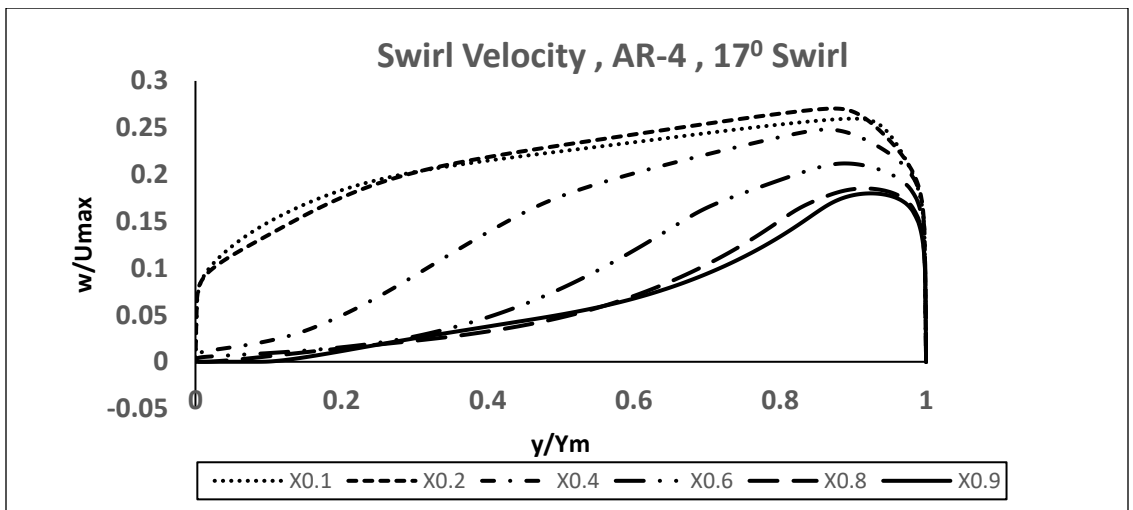
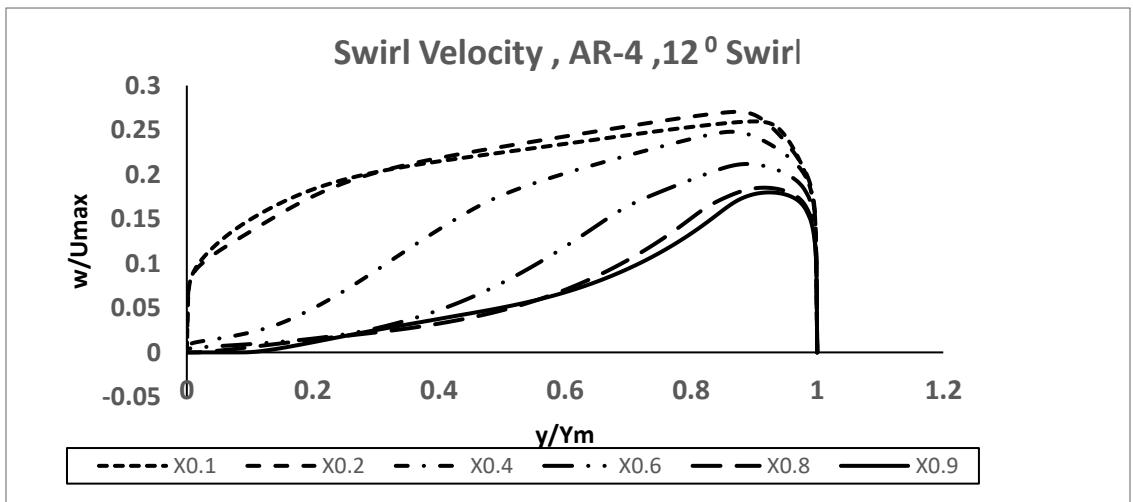
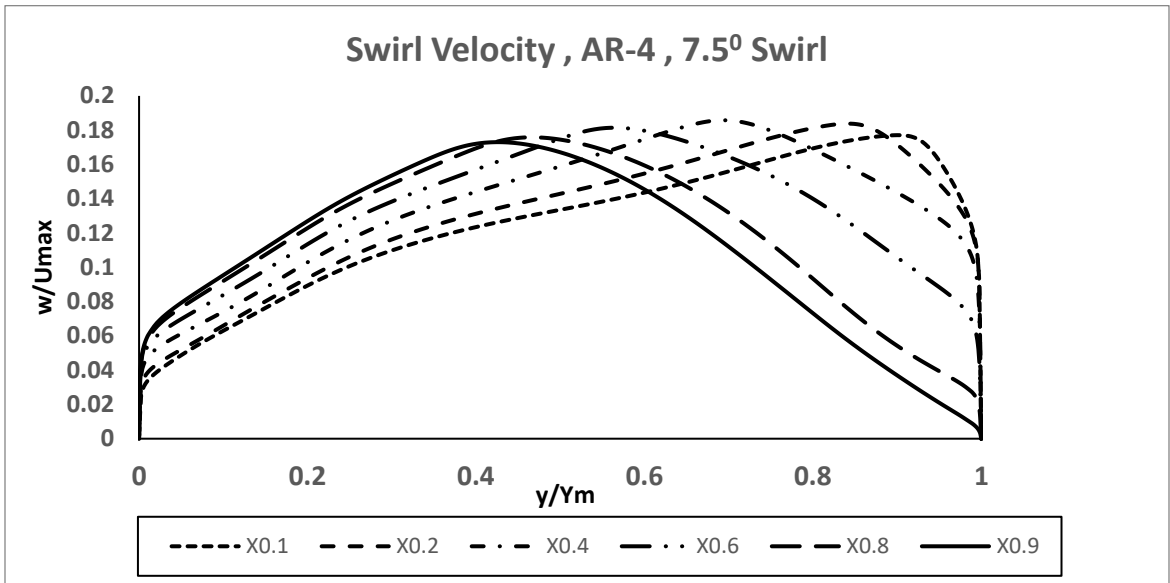


Fig. 6.3(a) Variation of Longitudinal Velocity with respect to non-dimensional radial height (y/Y_{max}) at different axial positions (10%, 20%, 40%, 60%, 80% and 90%).



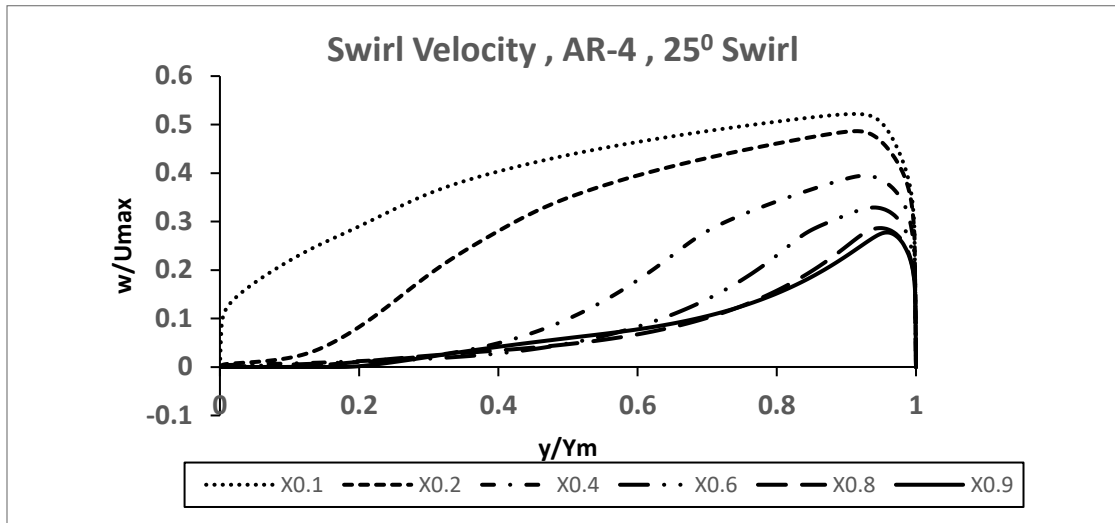
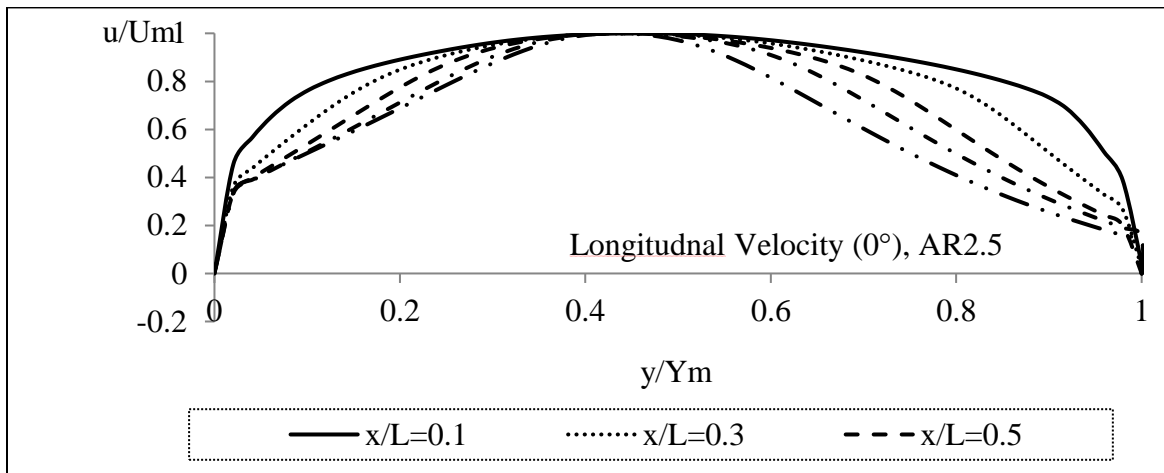
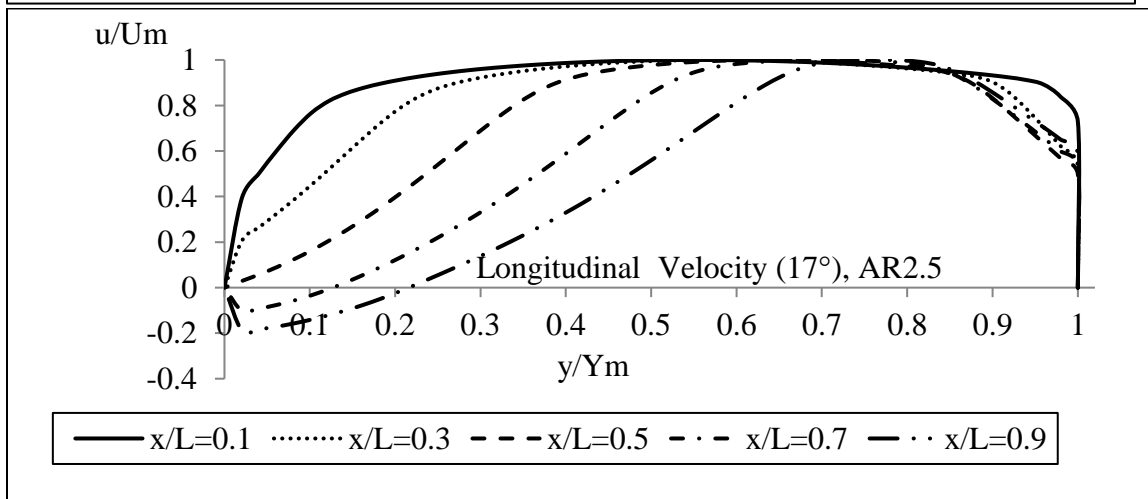
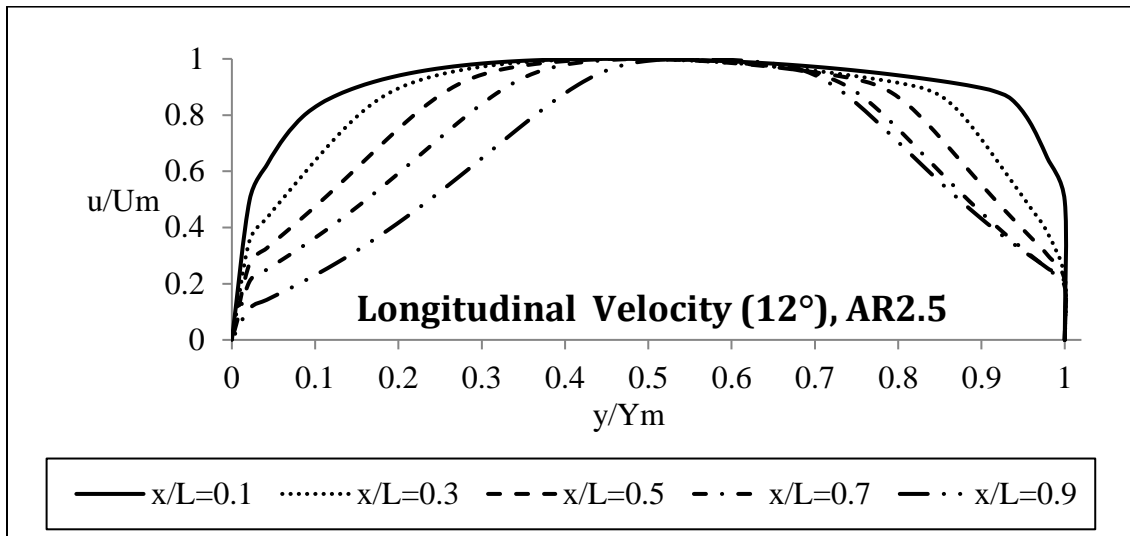
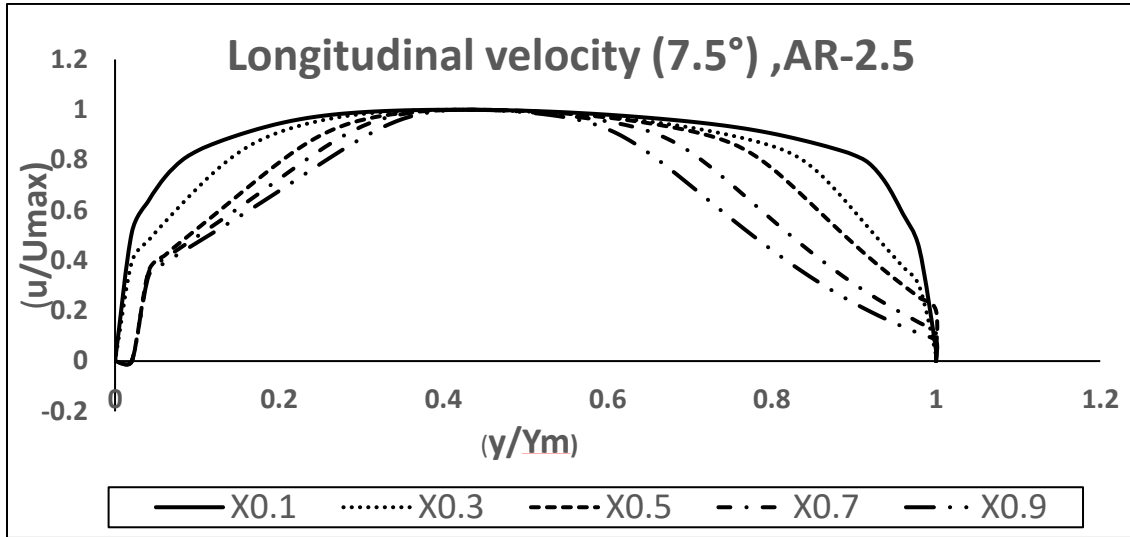


Fig. 6.3 (b) Variation of Swirl Velocity with respect to non-dimensional radial diffuser passage heights (y/Y_{max}) by taking the cone angle of 20° , Area ratio of 4 and swirl angles varied from (0° to 25°) at different axial positions (10%, 20%, 40%, 60%, 80% and 90%)





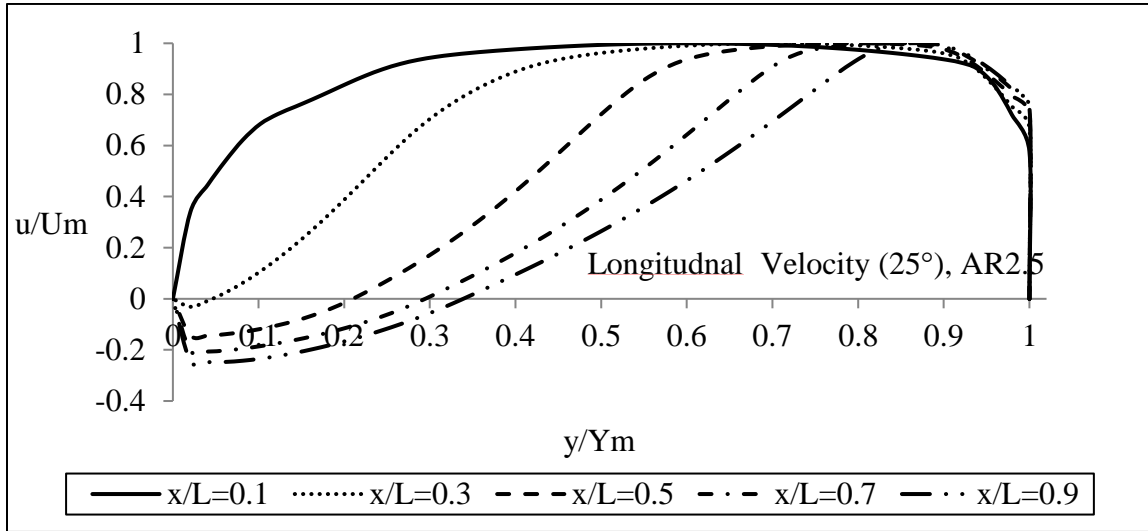
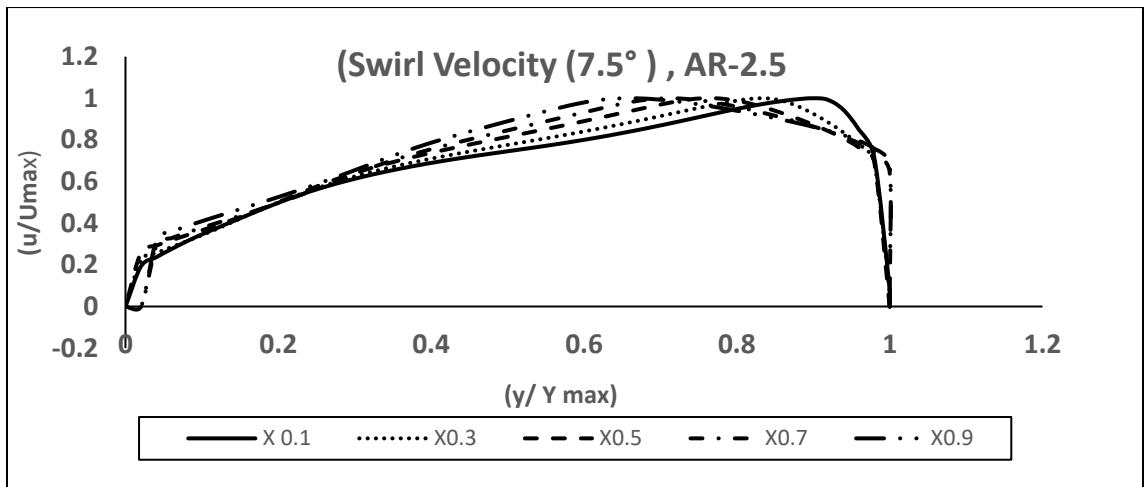


Fig. 6.4(a) Variation of Longitudinal Velocity with respect to non-dimensional radial height (y/Y_{max}) for casing diverging angle of 6° , Area ratio of 2.5 and inlet swirl angles of (0° to 25°) at different axial positions(10%, 20% ,40% ,60%,80% and 90%).



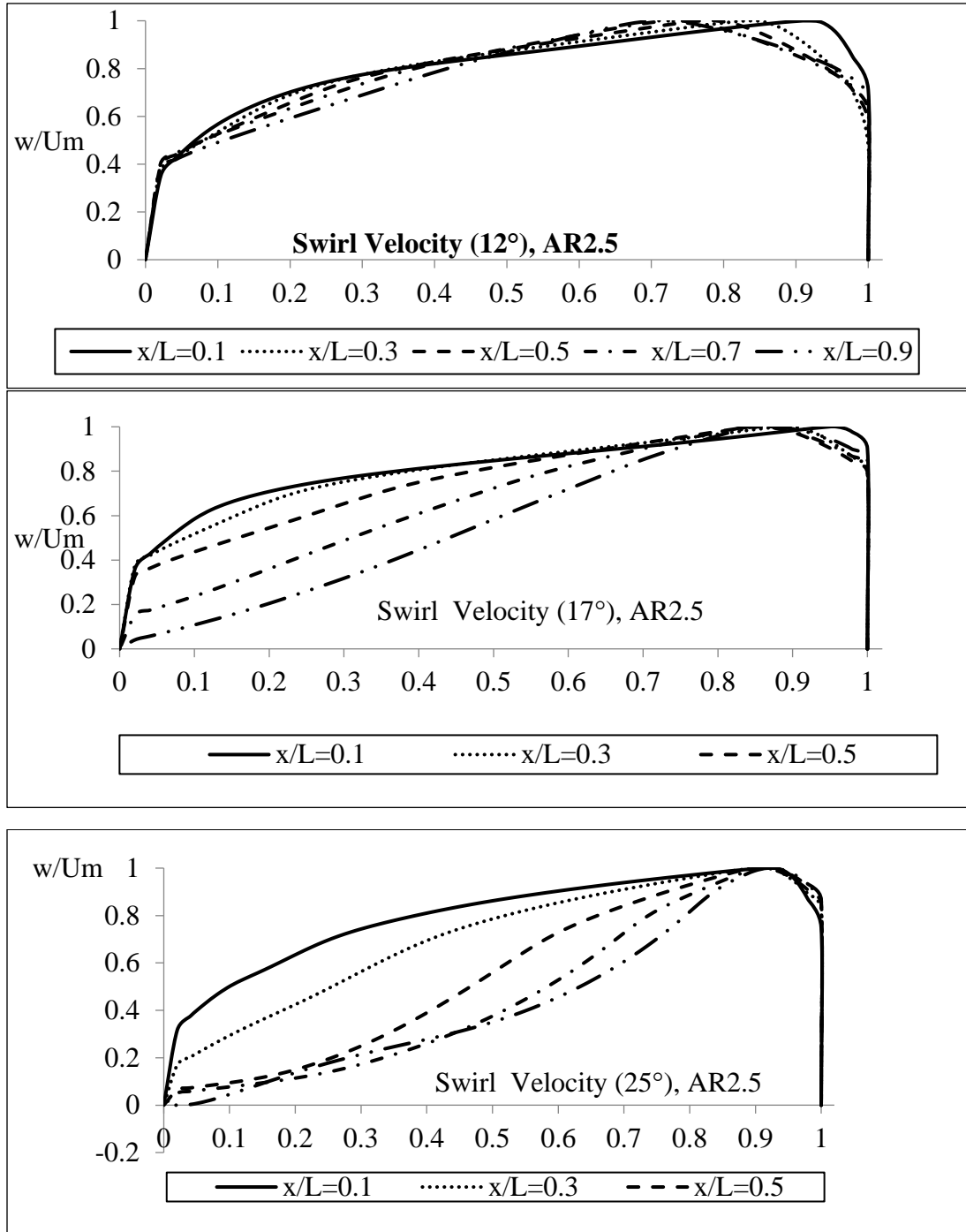


Fig. 6.4 (b) Variation of Swirl Velocity with respect to non-dimensional radial diffuser passage heights (y/Y_{max}) by taking the casing diverging angle of 6° , Area ratio of 2.5 and swirl angles of (0° to 25°) at different axial positions (10%, 20%, 40%, 60%, 80% and 90%).

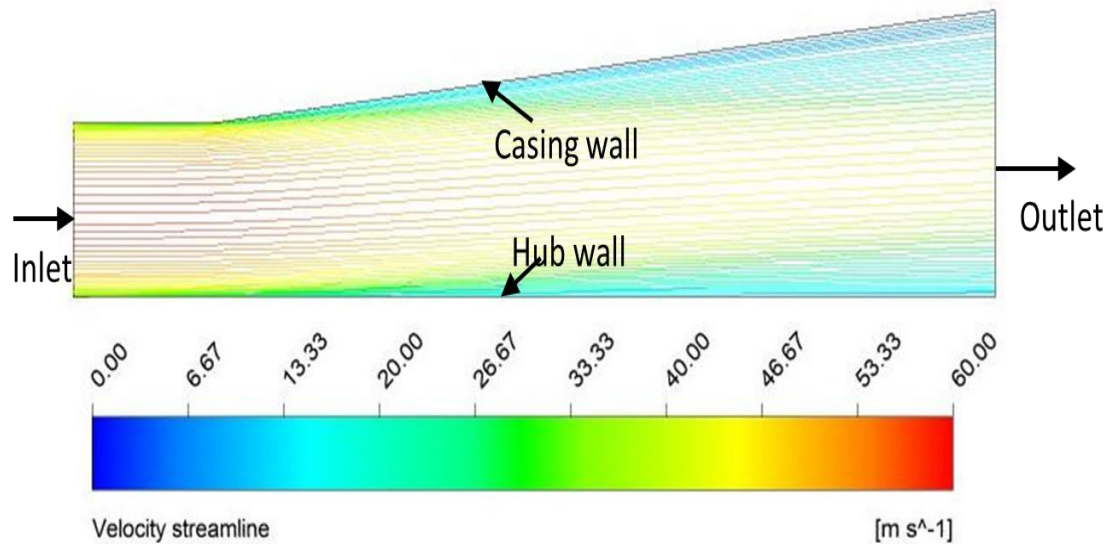


Fig.6.5 (a) Velocity streamline diagram at AR = 2 and Swirl angle = 0°

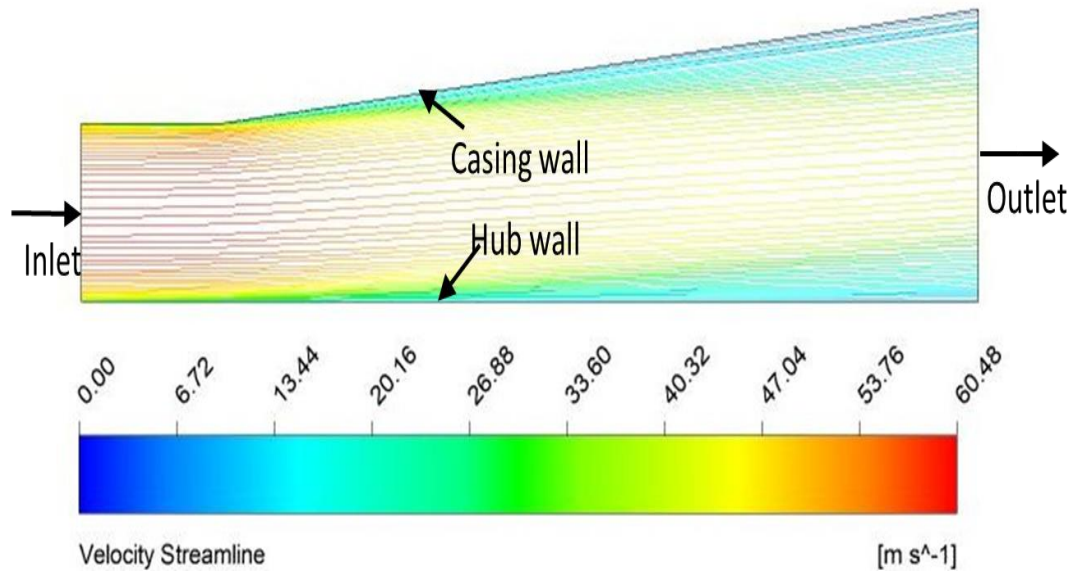


Fig. 6.5 (b) Velocity streamline diagram at AR = 2 and Swirl angle = 7.5°

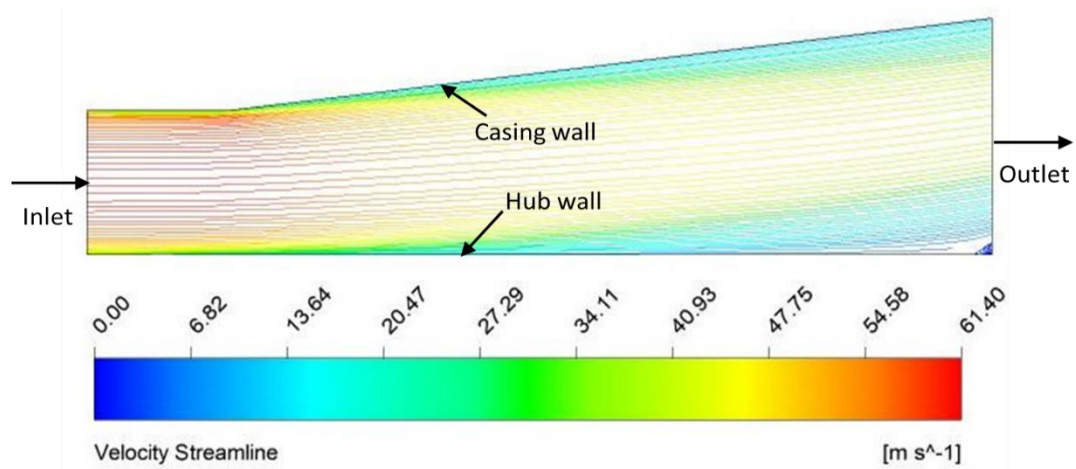


Fig.6.5 (c) Velocity streamline diagram at AR = 2 and Swirl angle = 12°

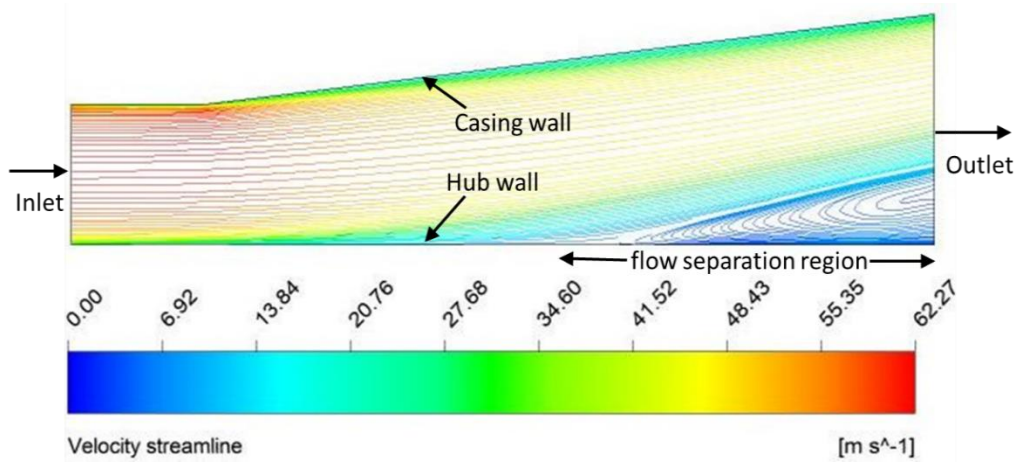


Fig.6.5 (d) Velocity streamline diagram at AR = 2 and Swirl angle = 17°

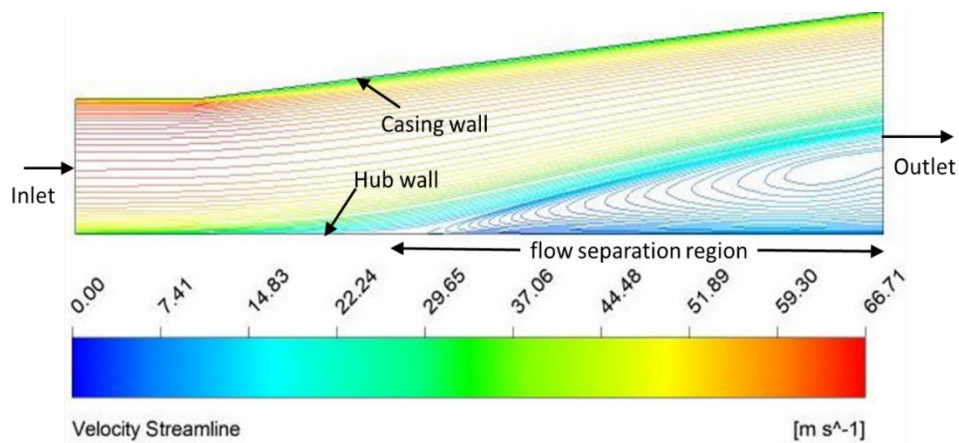
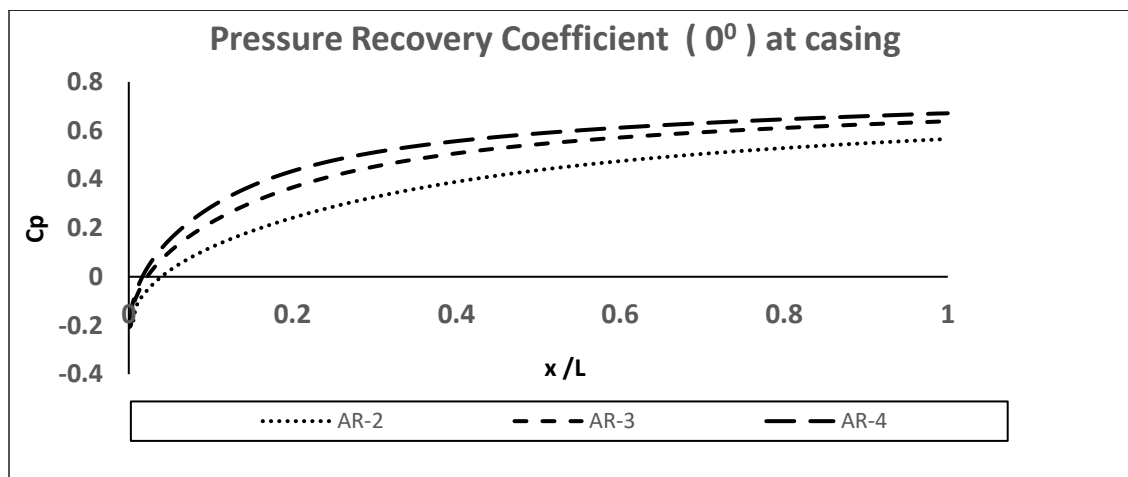
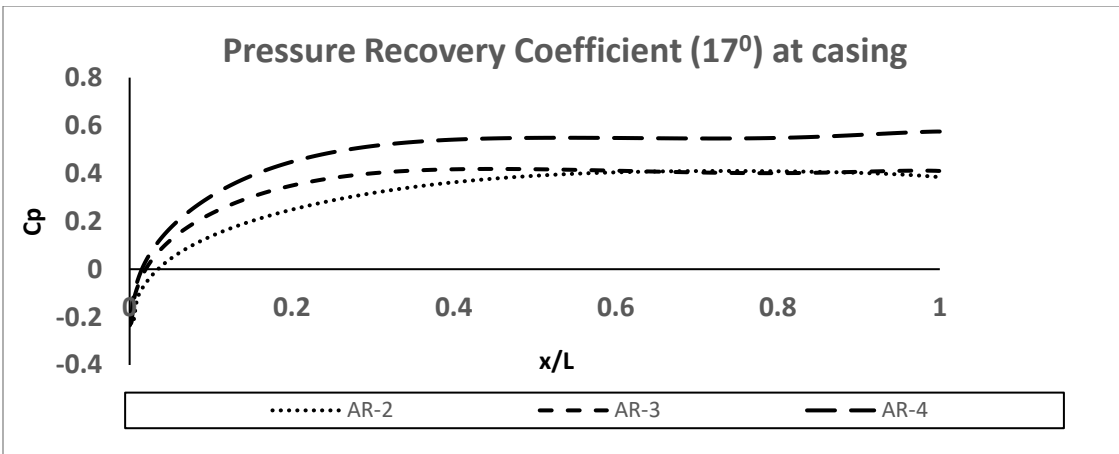
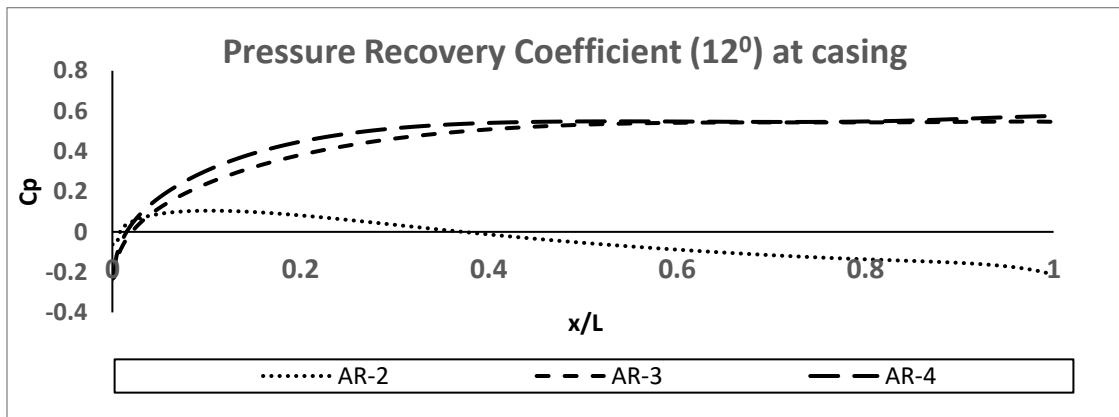
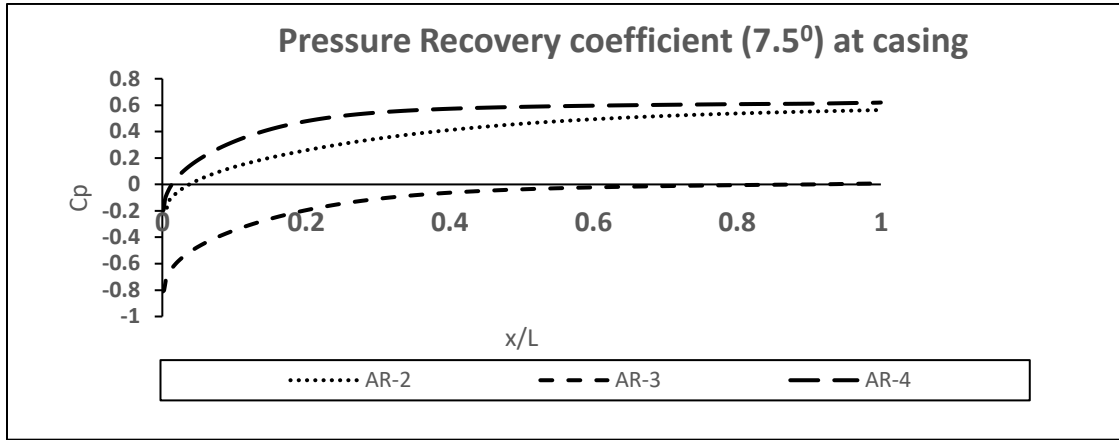


Fig.6.5 (e) Velocity streamline diagram at AR = 2 and Swirl angle = 25°

Fig. 6.6 and 6.7 represents the change of pressure recovery coefficient along the walls of casing and the hub of the annular diffuser for area ratio of 2, 3 and 4 with various swirl angles of 0, 7.5, 12, 17 and 25 degree.

Figures 6.6 and 6.7 shows that the coefficient of pressure rises by changing the area ratio from 2 to 4 without swirl at casing and hub. Figures 6.7 shows that coefficient of pressure increases along the downstream side of the diffuser. Figures 6.6 and 6.7 shows that coefficient of pressure gain decreases along the downstream side at hub and casing for 12° swirl angle and for other area ratio of 3 and 4 it increases at the downstream side of the annular diffuser. Figures 6.6 shows that the coefficient of pressure rise initially increases at high rate but at the downstream side the increase decreases at hub and casing for 17° swirl angle and area ratio of 2, 3 and 4. It is also clear from the Figures 6.6 that pressure recovery coefficient for 25° swirl angle and area ratio 2 increases continuously along the casing and hub of the diffuser but for area ratio of 3 & 4 it initially increases then decreases and finally further increases along the downstream side of the diffuser.





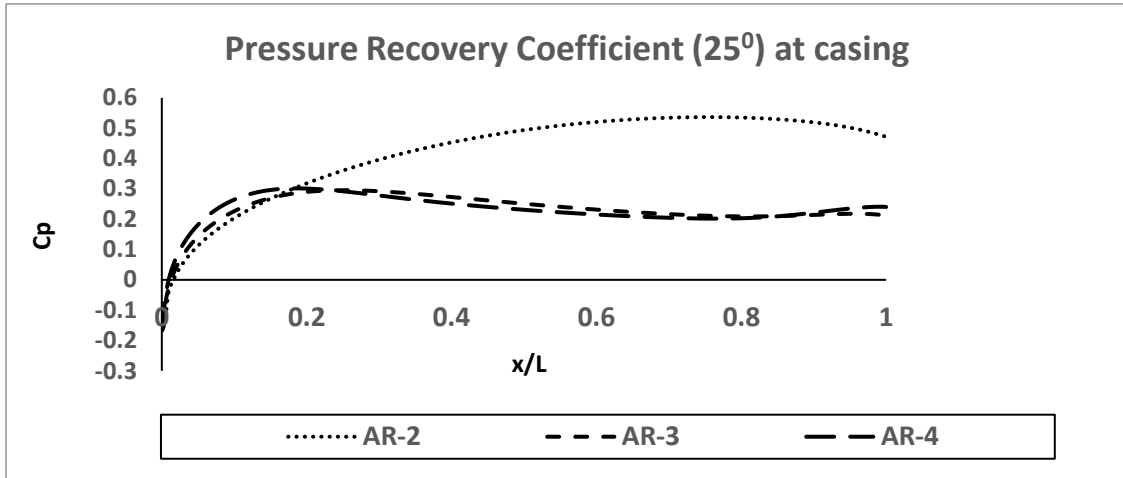
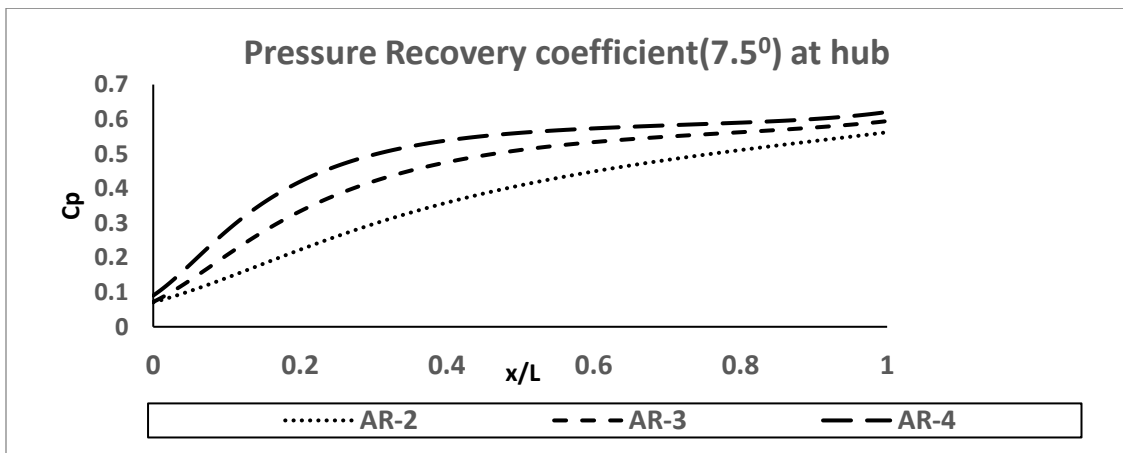
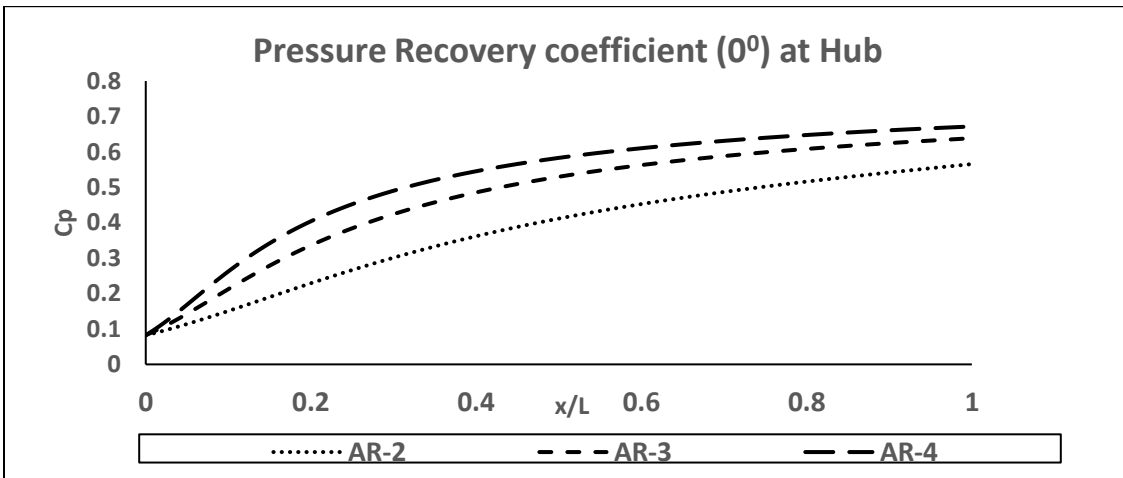


Fig. 6.6 Variation of pressure coefficient for area ratios of 2, 3, &4 along the casing for annular diffuser.



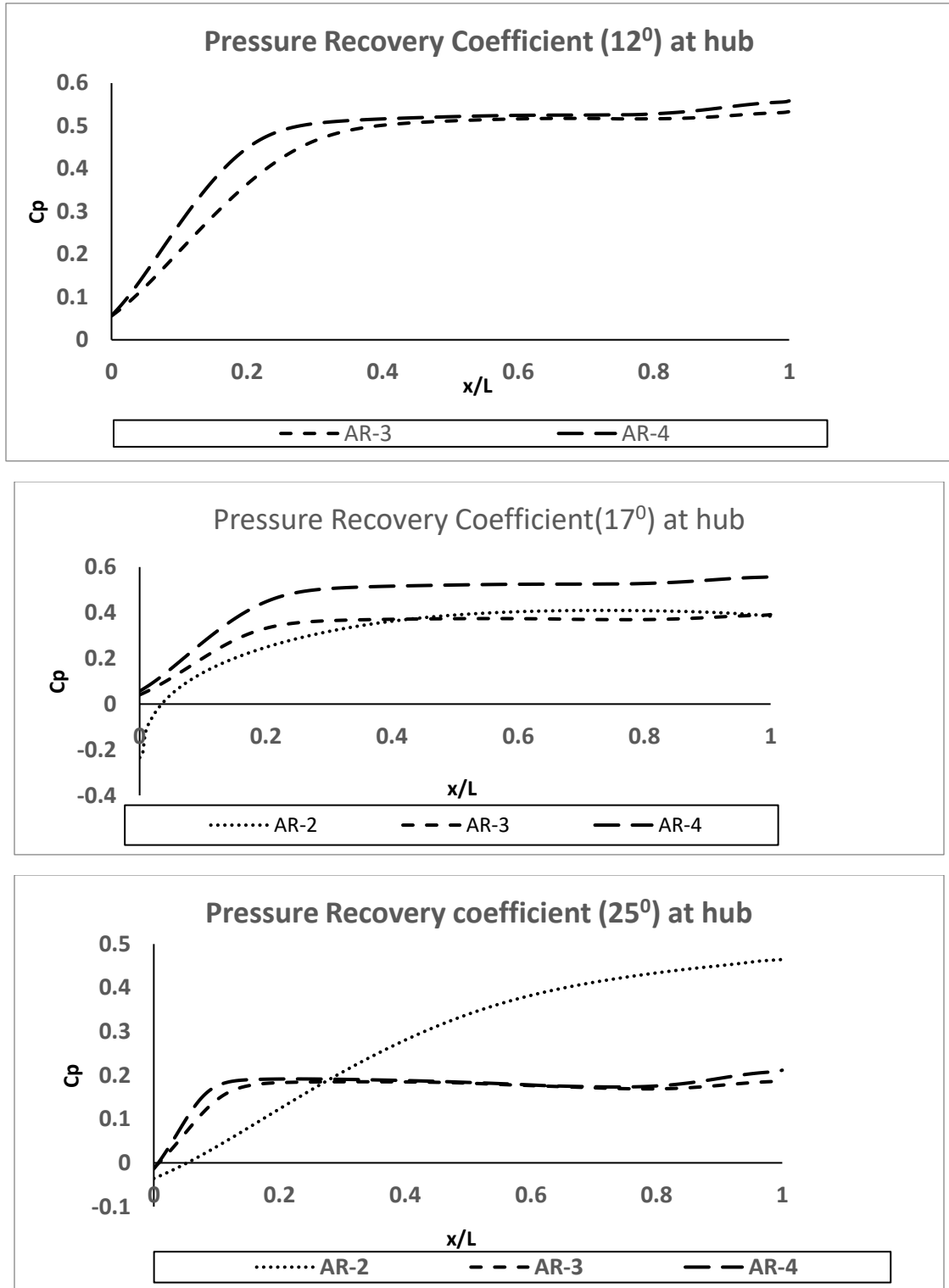


Fig. 6.7 Variation of pressure coefficient for area ratios of 2, 3, & 4 along the hub for annular diffuser.

Figure 6.8 represents the variations of pressure recovery coefficients with area ratios of 2.5 along the casing of axial annular diffuser. These pressure coefficients are shown for inlet swirl angles of 0° , 7.5° , 12° , 17° and 25° . The maximum values of pressure recovery coefficient and its variation on the casing walls is shown in Table 6.1

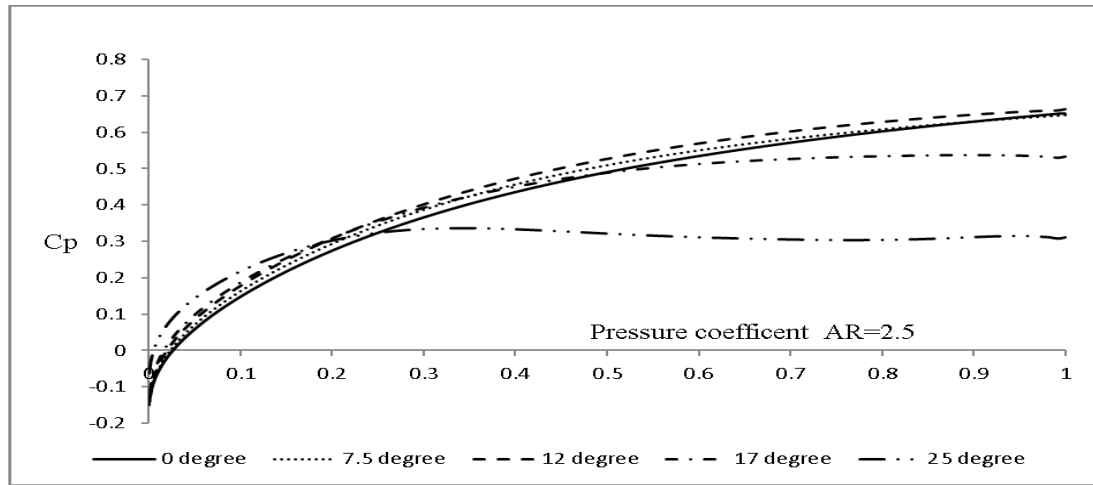


Fig. 6.8 shows the variation of pressure recovery coefficients at different swirl angles at the casing wall of axial annular diffuser.

Table 6.1 Variation of the pressure recovery coefficient along the length and Maximum value of pressure recovery coefficient $(C_p)_{max}$ on the walls of casing of annular diffuser.

S.N.	Swirl angle	$(C_p)_{max}$	Nature
1	0°	0.651155	Increases as the length increases
2	7.5°	0.646819	Increases as the length increases
3	12°	0.664129	Increases as the length increases
4	17°	0.538173	Increases as the length increases
5	25°	0.336835	Initially increases then decreases

Figure 6.9 shows the variations of pressure coefficients for the area ratios of 2.5 along the hub of axial annular diffuser. These variations of pressure coefficients are shown for inlet swirl angles of 0° , 7.5° , 12° , 17° and 25° . The maximum values of pressure recovery coefficient and its variation on the hub is shown in Table 6.2.

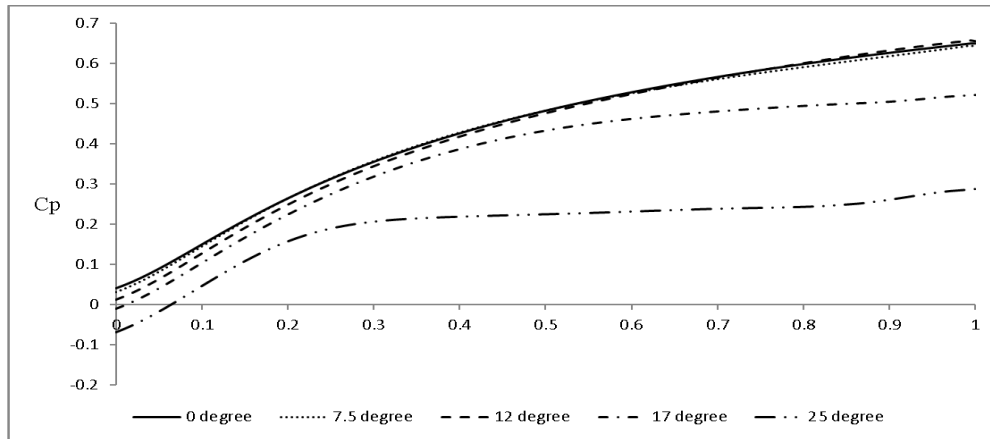


Fig. 6.9 shows the variation of pressure recovery coefficients at different swirl angles at the hub wall of axial annular diffuser.

Table 6.2 Variation of the pressure recovery coefficient along the length and Maximum value of pressure recovery coefficient $(C_p)_{max}$ on the walls of Hub of annular diffuser.

S.N.	Swirl angle	$(C_p)_{max}$	Nature
1	0°	0.650812	Increases as the length increases
2	7.5°	0.64384	Increases as the length increases
3	12°	0.657989	Increases as the length increases
4	17°	0.521246	Increases as the length increases
5	25°	0.287723	Increases as the length increases up to some length then constant and at last further increases.

CHAPTER 7

CONCLUSIONS AND FUTURE SCOPE

7.1 Conclusions

Following conclusions have been withdrawn from the analysis by changing the area ratio from 2 to 4 (2, 2.5, 3 & 4) by taking different swirl angles (0° , 7.5° , 12° , 17° and 25°) at the inlet of axial annular diffuser are given below:

- Results obtained from RNG k- ϵ model were very much near to the experimentally obtained results.
- Analysis shows that the regions of flow separation increase by increasing area ratio in the annular diffuser without swirl.
- As the swirl increases, the region of flow separation shifts from casing towards hub.
- With the introduction of swirl up to 12 degree, there is increase on pressure recovery coefficient and beyond that there is decrease in pressure recovery coefficient.
- By changing the area ratio from 2 to 4 (2, 2.5, 3, & 4) and swirl flow from 12° , 17° and 25° , the pressure recovery coefficient increases initially at the faster rate then this increase decreases at the downstream side of casing and hub of the annular diffuser.

7.2 Future Scope

1. Annular diffuser with constant diameter hub and casing diverging is considered in the present study. Future work can be done on other diffusers like rectangular, conical, radial type diffusers etc.
2. Area ratio and angle of divergence are the important parameters and hence further studies can be extended by varying these parameters.
3. This work was done for sub-sonic incompressible flow only. The additional range of work can be extended to sonic flow, hypersonic flow and compressible flow.
4. This investigation is done for a diverging section of diffuser. Because the geometry is a significant parameter and hence geometry variation can be done for further studies.
5. The analysis is performed with RNG k- ϵ model for swirling flows. Higher order discretization schemes and better turbulence models can be used for further studies.
7. The present analysis is done for stationary hub and casing. Further studies can be done on rotating hub and casing diffuser.
8. Suction, blowing and injection of boundary layer can decrease the flow separation at diffuser walls. These property can be incorporated for further studies.

REFERENCES

- [1] Manoj Kumar, B. B. Arora, Subhashish Maji and S. Maji, “Effect of Inlet Swirl on the Flow Behavior Inside Annular Diffuser”, *International Journal of Dynamics of Fluids*, vol. 7, no. 2, pp. 181-188, 2011.
- [2] Manoj Kumar, B. B. Arora, Subhashish Maji and S. Maji, “Effect of Area Ratio and Inlet Swirl on the Performance of Annular Diffuser,” *International Journal of Applied Engineering Research*, vol. 7, no. 13 pp. 1493-1506, 2012.
- [3] B. B. Arora, “Performance Analysis of Parallel Hub Diverging Casing Axial Annular Diffuser with 20° Equivalent Cone Angle”, *Australian Journal of Mechanical Engineering*, vol. 12, no. 2, pp. 179-194, April 2014.
- [4] Manoj Kumar, B. B. Arora , Maji Subhashis, “Analysis of Flow Separation in Wide Angle Annular Diffusers,” *International Journal of Applied Engineering Research*, vol.5, no.20, pp. 3419-3428, ISSN 0973-4562,2010.
- [5] B. B. Arora, B. D. Pathak, “Effect of Geometry on the Performance of Annular Diffuser,” *International Journal of Applied Engineering Research*, vol.5, no.20. pp. 2639- 2652, ISSN 0973-4562, 2009.
- [6] Hardial Singh and B. B. Arora, “Effect of Area Ratio on Flow Separation in Annular Diffuser” © Springer Nature Singapore Pte Ltd. 2019 P. Saha et al. (eds.), *Advances in Fluid and Thermal Engineering, Lecture Notes in Mechanical Engineering*, pp.297-305, April 2019.
- [7] S. N. Singh , D. P Agarwal, R. N. Sapre, and R. C Malhotra, “Effect Of Inlet Swirl on The Performance of Wide Angled Diffusers”, *Indian journal of Engineering & Materials Sciences*, vol. 1, pp. 63-69,1994.

- [8] S. N, Singh., V. Seshadri et al, “Effect of Inlet Swirl on the Performance of Annular Diffusers Having the Same Equivalent Cone Angle”, *Proceedings of the Institution of Mechanical Engineers, Part G, Journal of Aerospace Engineering*, vol. 220, pp. 129-143,2006.
- [9] N. V. Mahalakshmi , G. Krithiga , S Sandhya , J Vikraman and V. Ganesan , “Experimental Investigations of Flow Through Conical Diffusers with And Without Wake Type Velocity Distortions at Inlet” *Experimental Thermal and Fluid Science* , vol.32,no.1,pp.133-157,October 2007.
- [10] D.S. Kumar, “Effect of Swirl on Flow Through Annular Diffusers”, Ph.D. Thesis, I.I.T. Delhi, 1977.
- [11] M. Kumar , B. B. Arora, Sagar Maji , S Maji S, “Effect of Equivalent Cone Angle on the Performance of Parallel Hub Diverging Casing Annular Diffuser,” *International Journal of Fluids Engineering*, ISSN 0974-3138, vol. 4, No.2.,pp. 97-10, 2006.
- [12] S.J. Stevens and G. J. Williams, “Measurements of the Overall Performance And Boundary Layer Growth in An Annular Diffuser,” *Symposium on Internal Flows*, Salford University, England, 1971.
- [13] S. J. Stevens and G. J. Williams, “The Influence of Inlet Conditions on the Performance of Annular Diffusers,”, *Journal of Fluids Engineering*, vol. 102, no. 3, pp. 357-363, Sept. 1980.,
- [14] Manoj Kumar Gopaliya , Mahesh Kumar, Shailendra Kumar and Shiv Manjaree Gopaliya , “Analysis of performance of S shaped diffuser with offset”, *Aerospace Science and Technology*, vol.11, no.2-3,pp.130-135, March-April 2007.

- [15] Manoj Kumar Gopaliya , K. K. Chaudhary, “CFD Analysis Of Y-Shaped Diffuser with Combined Horizontal and Vertical Offsets”, *Aerospace Science and Technology* ,vol.14, no.5, pp. 338-347, July-August 2010.
- [16] Stefano Ubertini, Umberto Desideri, “Experimental Performance Analysis of an Annular Diffuser with and without Struts”, *Experimental Thermal and Fluid Science*, vol.22, no.3-4, pp-183-195,September 2000.
- [17] Sandip A. Kale, Rushikesh V. Godse, Haribhau G. Phakatkar “Performance Evaluation of Small Wind Turbine Diffuser with Different Diameters”, *International Journal of Innovative Technology and Exploring Engineering*, vol.8, no-6S4, pp.1077-1080, April 2019.
- [18] R Prakash, Karthik Srinivas V, Anand H, Adithya G, Lakshmi Narayanan N “Effect of Swirl on The Performance of an Annular Diffuser” *Applied Mechanics and Materials*, Vol. 787, , ISSN: 1662-7482, pp 318-321 , August 2015.
- [19] Majid Nabavi, “ Three-Dimensional Asymmetric Flow Through a Planer Diffuser”, *Journal of Heat and Mass Transfer*, vol.37, pp-17-30,2010.
- [20] A M Elkersh, AH Elgammal , “An Experimental Investigation of the Performance of Equiangular Annular Diffuser with Swirled Flow”, *Proceedings of Institutions of Mechanical Engineers*, vol. 199, October 1985.
- [21] Berge Djebedjian and Jean-Pierre Renaudeau, “Numerical and Experimental investigation of the flow in the annular diffuser”, *Proceedings of FEDSM 98-4967*, pp.1-6 , June 1998.
- [22] Ehan Sabah Shukri , Wirachman Wisnoe “Numerical Study on Temperature Distribution in an Annular Diffuser using Twisted Rectangular Hub / Pimpeled Hub

- as Swirl Generators”, *Journal Teknologi (Sciences & Engineering)*, vol. 75:8, pp. 19–23. March 2015.
- [23] A. G. Barker and J. F. Carotte, “Influence of Compressor Exit Condition on Combustor Annular Diffuser, part I: diffuser performance”, *J. Propul. Power*, vol.17, no.(3), pp. 678 –686, 2001.
- [24] G. Sovran and E. D. Klomp, “Experimentally Determined Optimum Geometries for Rectilinear Diffusers with Rectangular, Conical or Annular Cross-section”, *Fluid Mechanics of Internal Flow*, Sovran, G. (editor), Elsevier, Amsterdam, pp. 270-319, 1967.
- [25] T. Srinath, “An Investigation of The Effects of Swirl on Flow Regimes and Performances of Annular Diffuser with Inner and Outer Cone Angles”, *MASc Thesis, University of Waterloo, Canad*, 1968.
- [26] D. Hoadley, “Three-Dimensional Turbulent Boundary Layers in an Annular Diffuser”, *PhD Thesis, Department of Engineering, University of Cainbridge, London*, 1970.
- [27] R. Coladipietro, J. H. Schneider and K. Shridhar, “Effects of Inlet Flow Conditions on the Performance of Equiangular Annular Diffusers”, *CSME*, pp. 7384, 1974.
- [28] R. P. Lohmann, S. J. Markowski and Prookman, E. T., “Swirling Flow Through Annular Diffusers with Conical Walls”, *Journal of Fluids Engineering*, vol. 101, pp. 224-229, 1979.
- [29] R. N. Sapre, S. N. Singh, D. P. Agrawal and R. C. Malhotra, “Flow Through Equiangular Wide-Angle Annular Diffusers”, *15th NCFMFP, Srinagar*, July 1987.

- [30] D. P. Agrawal , S. N. Singh , R.N. Sapre, R. C. and Malhotra , "Effect of Hub Rotation on the Mean Flow of Wide-Angle Annular Diffusers", *HydroTurbo* 1989, Czechoslovakia, 1989.
- [31] R. Mohan , S. N. Singh, and D. P. Agrawal , "Optimum Inlet Swirl for Annular Diffuser Performance Using CFD", *Indian Journal of Engineering and Materials Sciences*, vol. 5, pp. 15- 21, 1998
- [32] D. Japikse , "Correlation of Annular Diffuser performance with Geometry, Swirl, and Blockage", *Proceedings of the 11th Thermal and Fluids Analysis Workshop (TFAWS), Cleveland, Ohio, , pp. 107-118, 21-25 August 2000.*
- [33] P. K. Yadav, Dr. B. B. Arora "Analysis of Flow Separation in Annular Diffuser" Master of Technology in Thermal Engineering of Delhi Technological University, Delhi 2016.
- [34] J. H. G. Howard , A. B. Thorriton Trurnp .and H. J. Henseler, "Performance and Flow Regimes for Annular Diffusers", ASME Paper No. 67 WA/FE 21, 1967.
- [35] S. Ubertini and U. Desideri , "Experimental performance analysis of annular diffuser with and without struts," *Elsevier, J. Experimental Thermal and Fluid Science* ,vol. 22, no. 3, , pp. 183- 195 ,September 2000
- [36] S. J. Stevens , "The Performance of Annular Diffusers". *Proc. Instn. Mech. Engrs.*, vol. 182, Part 3D, pp.58-70, 1968.
- [37] Erika M. Cherry, Angilina M. Padiligs, John K. Eaton, "Three-dimensional velocity measurements in annular diffuser segments including the effect of upstream struts wakes", *International Journal of Heat and Fluid Flow*, Volume31, Issue4,2010, PP. 569-575.

- [38] Ozturk Tatar and Ali Pinarbasi, “Flow Analysis in Centrifugal Compressors Vaneless Diffusers”, *Journal of Scientific and Industrial Research*, vol. 67, pp-348-354, 2008.
- [39] M. R. A. Shaalan, I. M. M. Shabaka , “An Experimental Investigation of the Swirling Flow Performance of an Annular Diffuser at Low Speed”, *ASME Paper No. 75WA/FE17*, 1975.
- [40] R. Coladipietro, J. H. Schneider and K. Shridhar, K., "Effects of Inlet Flow Conditions on The Performance of Equi Angular Annular Diffusers", *CSME Paper no. 73 84*, 1974.
- [41] M. R. A. Shaalan and I. M. M. Shabaka., "An Experimental Investigation of the Swirling Flow Performance of an Annular Diffuser at Low Speed", *ASME Paper No. 75 WA/FE 17*, 1975.
- [42] A. N. Kochevsky , “Numerical Investigation of Swirling Flow in Annular Diffusers with a Rotating Hub Installed at the Exit of Hydraulic Machines”, *Journal of Fluids Engineering, Trans. ASME*, vol. 123, pp.484-489, 2001.
- [43] B. Monje , D. Sánchez , R. Chacartegui a , T. Sánchez a , M. Savill b and P. Pilidis “Aerodynamic Analysis of Conical Diffusers Operating with Air and Supercritical Carbon Dioxide ”, *Internal journal of heat and flow*, vol.44,pp. 542-553, 2013.
- [44] C.C. Wood and J.R. Henry ,“Effects of Shock Boundary Layer Interaction on the Long and Short Subsonic Annular Diffuser” .*NACA RM L58A31*,1958.
- [45] S. N. Singh , V. Seshadri , K. Saha , K. K. Vempati, and S. Bharani , “Effect of Inlet Swirl on the Performance of Annular Diffusers Having the Same Equivalent

- Cone Angle”, *Proceedings of the Institution of Mechanical Engineers, Part G, Journal of Aerospace Engineering*, vol. 220, pp. 129-143, 2006.
- [46] D. J. Cockrell , E. Markland , “A Review of Incompressible Diffuser Flow” *Aircraft Engg. , volume 35*, pp 286 , 1963.
- [47] V. K. Sharan , “Diffuser Performance Co-Relations”. *JASI*, vol. 24, pp. 415, 1972.
- [48] Manoj Kumar Gopaliya , K. K. Chaudhary, “CFD Analysis of Y-Shaped Diffuser with Combined Horizontal and Vertical Offsets, *Aerospace Science and Technology*, vol.14, pp.338-347, 2010.
- [49] Manoj Kumar Gopaliya, Mahesh Kumar, Shailendra Kumar and Shiv Manjar” Gopaliya, “Analysis of Performance of S Shaped Diffuser with Offset”, *Aerospace Science and Technology*, pp-130-135, 2007.
- [50] Rita J. Schnipke , James G Rice and Ronald D. Flack, “Finite Element Analysis of Viscous Flow in a Vaned Radial Diffuser”, *Department of Mechanical and Aerospace Engineering, University of Virginia*, 2010.
- [51] Basarat Salim, “Effect of geometric parameters on the performance of wide-angle Diffusers”, *International Journal of Innovative research in science, Engineering and Technology*, vol.2, no. 9 , pp-4178-4191, 2013.
- [52] R. Keerthana, G. Jamuna Rani, “Flow Analysis of Annular Diffusers”, *International Journal of Engineering Research and Applications*, vol.2, no.3, pp-2348-2351, 2012.
- [53] S. W. Wilbur and J. T. Higginbotham, “Investigation of Two Short Annular Diffuser Configurations Utilizing Suction and Injection as a Means of Boundary Layer Control”, *NACA RML54K18*, 1955.

- [54] Alysson Kennerly Colaciti , Luis Migual Valdes Loez, “Numerical Simulation of a Radial Diffuser Turbulent Airflow”, *Applied Mathematics and Computations*, vol.189, no.2,pp.1491- 1504 , June 2007.
- [55] P.M Ligrani and M. Rouster et al, “Measurements in the Vaneless Diffuser of a Radial flow”, *Journal of Heat and Fluid Flow*, vol.4,pp.103-106, 1983.
- [56] D. P. Agarwal and S.M. YAHYA, “Velocity Distribution in Blade To Blade Plane Of A Vaned Radial Diffuser”, *International .Journal of .Mechanical Science*, vol.23 , pp-359-366, 1981.
- [57] F. Durst, A. Melling, J .H. Whitelaw, ”Low Reynolds Number Flow Over A Plane Symmetric Sudden Expansion”. *Journal of Fluid Mechanics*, vol.4 , pp.111-128, 1974.
- [58] D. J. Cerantola, A. M. Birk, “Investigation of Tabs in Short Annular Diffusers with Swirling Flow” Department of Mechanical and Materials Engineering , *Journal of Engineering for Gas Turbines and Power* , vol. 137 / 092601-1, September 2015.
- [59] Marcus Kuschel, Bastian Drechsel and Joerg R. Seume, ” Influence of Turbulent Flow Characteristics and Coherent Vortices on the Pressure Recovery of Annular Diffusers” ASME Turbo Expo 2015: Turbine Technical Conference and Exposition GT2015 June 15 – 19, 2015, Montréal, Canada
- [60] M. M. Venugopal , V Somashekar, “Design and Analysis of Annular Exhaust Diffuser for Jet Engines” *International Journal of Innovative Research in Science, Engineering and Technology* (An ISO 3297: 2007 Certified Organization), vol. 4, no. 7, July 2015.

- [61] Maqsood Mohammed, B. A. Kailash , Subramanya Gowreesh , “Design and Optimization of Flow Performance for Annular Curved Diffusing Duct Using CFD” *International Research Journal of Engineering and Technology (IRJET)* e-ISSN: 2395 -0056 , vol.02 , no. 09 Dec-2015.
- [62] A.E. Zaryankin, I.V. Garanin, V.P. Khudyakova, V.O. Kindra1 and E.M. Lisin “CFD Investigation of Flow in Finned Plane and Conical Diffusers” *International Journal of Applied Engineering Research*, ISSN 0973-4562 ,vol.11, no. 22 , pp. 11081-11088, 2016.
- [63] Ehan Sabah Shukri, Dr. Wirachman Wisnoe and Dr. Ramlan Zailani “Numerical Analysis of Temperature Distribution Enhancement in Conical and Annular Diffusers Fitted with Swirl Generators”, vol. 9, no. 9, April,2016
- [64] J. Ackert , “Aspect of Internal Flow”, *Fluid Mechanics of Internal Flow*, Ed. Sovaran G., Elsevier Amsterdam, pp 1 ,1967.
- [65] Gotfredsen, Erik , Agular Knudsen , Christian Kunoy, Jens Dahl Meyer Knud Erik Walther and Jens Honore “Adjoint Optimisation of The Turbulent Flow In An Annular Diffuser” *30th Nordic Seminar on Computational Mechanics NSCM-30 J H_sberg , N.L. Pedersen (Eds.) , Department of Mechanical Engineering, Technical University of Denmark , 2017.*
- [66] Pravin Phatangare , Tushar Raskar , Mahesh Salunke and Prof. S.B.Tawar , “Experimental Study of Aerodynamics Through A Conical Annular and Axial Flow Runner”, *International Journal of Innovative Research in Technology*, vol.3, no.11, pp.43-48, 2017.

- [67] Nagendra K. Sharma and Ashish Dixit " Validation of Standard K-E model for the Analysis of Annular Diffuser" *International Journal for Research in Applied Science & Engineering Technology (IJRASET)* , vol. 5 , no. V, IC Value: 45.98 ISSN: 2321-9653, May 2017.
- [68] Sharan Padashetty, Pravin Honguntikar and K. Rajagopal "Effect of Divergence Angle on the Performance and Flow Analysis of 3D Annular Diffuser of an Aircraft Engine using CFD Technique" *International Journal of Engineering Trends and Technology (IJETT)* , vol.49, no. 6 , ISSN: 2231-5381, July 2017.
- [69] Sangappa Hadapad , Basavaraj Dotihal "Analysis of Flow on Annular Curved Diffuser by using CFD" *IJRET: International Journal of Research in Engineering and Technology* ISSN: 2319-1163 | pISSN: 2321-7308 ,vol. 06, no. 02 , Feb-2017.
- [70] Ehan Sabah Shukri "Numerical Comparison of Temperature Distribution in an Annular Diffuser Fitted with Helical Screw-Tape Hub and Pimpled Hub".4th *International Conference on Power and Energy Systems Engineering, CPESE 2017* , Berlin, Germany, 25-29 September 2017.
- [71] Vasant Patel , D. C. Gosai and Dr. K. V. Chaudhari , "Design, CFD Analysis And Numerical Optimization of Diffuser Used In Annular Type Combustion Chamber For Small Gas Turbine Engine" *International Journal of Advanced in Management, Technology and Engineering Sciences* ,vol. 8, no. III, ISSN NO : 2249-7455, , March 2018.
- [72] R. Prakash "Investigation on the Flow Structure and the Performance of an Annular Diffuser with Two Different Types of Struts" *Journal of Informatics and Mathematical Sciences*, vol. 10, No. 3, pp. 479–488, 2018.

- [73] P. K. Yadav, Dr. B. B. Arora “Analysis of Flow Separation in Annular Diffuser” Master of Technology in Thermal Engineering of Delhi Technological University, Delhi 2016.
- [74] S. N. Singh, V. Seshadri, K. Saha, K. K. Vempati and S. Bharani, “Effect of Inlet Swirl on the Performance of Annular Diffusers Having the Same Equivalent Cone Angle”, *Proceedings of the Institution of Mechanical Engineers, Part G, Journal of Aerospace Engineering*, vol. 220, pp. 129-143, 2006.
- [75] R. Keerthana, G. Jamuna Rani, “Flow Analysis of Annular Diffusers”, *International Journal of Engineering Research and Applications (IJERA)* ISSN: 2248-9622 www.ijera.com, vol. 2, no. 3, pp.2348-2351, May-Jun 2012.
- [76] R. Hesterman, S. Kim, A. Ben Khalid, S. Wittig, “Flow Field and Performances Characteristics of Combustor Diffusers A Basic Study”. *Trans. ASME Journal Engineering for Gas Turbine and Power*, vol.117, no.4, pp.686-694, October 1995.
- [77] D. Hoadley, D. W. Hughes, “Swirling Flow in an Annular Diffuser”. University of Cambridge, Department of Engineering, Report CUED/A Turbo / TR5. 24, 1969.
- [78] J. H. G. Howard, A. B. Thornton Trump, H. J. Henseler, “Performance and Flow Regime for Annular Diffusers”. ASME Paper No. 67-WA/FE-21, 1967.
- [79] R. Prakash, N. V. Mahalakshmi, “Experimental Investigations of Flow Through Annular Diffuser with and Without Struts”, *European Journal of Scientific Research*, vol.52, pp.366-384, May 2011.
- [80] S. N Singh, V. Seshadri, Sunil Chandel and Mahendra Gaikwad, “Analysis of the Improvement in Performance Characteristics of S-Shaped Rectangular Diffuser by

- Momentum Injection Using Computational Fluid Dynamics”, *Engineering Applications of Computational Fluid Mechanics* ,vol. 3, no.1, pp.109-122 , 2009.
- [81] S. Singh, V. N. Seshakiri, K. Saha, K. K. Vempat and S. Bharani, “Effect of Inlet Swirl On The Performance Of Annular Diffusers Having The Same Equivalent Cone Angle”, *Proceedings of IMechE. Part G, Journal of Aerospace Engineering* , vol.220, pp. 129 – 143, December 2005.
- [82] D.S. Kumar and K.L. Kumar, “Effect of Swirl on Pressure Recovery in Annular Diffusers”, *Journal of Mechanical Engineering Science* , vol.22, pp. 305 – 313, 1980.
- [83] R. Prakash, V. K. Srinivas, H. Anand, G. Adithya and N. L. Narayanan, “Effect of Swirl on the Performance of An Annular Diffuser”, *International Journal of Applied Mechanics and Materials*, vol.787, pp.318 – 321, 2015.
- [84] A. J. Juhasz , “Performance of An Asymmetric Annular Diffuser with Non-Diverging Inner Wall Using Suction”, *NASA TN -7575*, vol. 85,1974.
- [85] D. Choudhury D., “Introduction to the Renormalization Group Method and Turbulence Modeling.” *Fluent Inc. Technical Memorandum TM-107*, 1993.
- [86] A. Klein , “Characteristics of Combustor Diffusers.” *Progress in Aerospace Science* ,vol. 31, no.3, pp.171-271,1995.
- [87] B. S. Stratford and H. Tubbs, "The Maximum Pressure Rise Attainable in Subsonic Diffusers", *Journal of the Royal Aeronautical Society*, Technical Note, April 1965.
- [88] J. H. Goebel and D. Japikse , “The Performance of an Annular Diffuser Subject to Various Inlet Blockage and Rotor Discharge Effects “. *Consortium Final Report, Creare TN-325*, 1981.

- [89] S. J. Stevens and G.J. Williams , 1980. “The Influence of Inlet Conditions on the Performance of Annular Diffuser”. *Trans. ASME Journal Fluids Eng* , vol.102, pp.357-363,1980.
- [90] S.J. Stevens, G.J. Williams, “Performance of Annular Diffusers” *Gas Turbine Collaboration Committee Report No. 299,1969.*
- [91] E.M. Cherry, M. Angelina, J. E.P. Christopher and J.K. Eaton, “Three-dimensional velocity measurements in annular diffuser segments including the effects of upstream strut wakes”, *International Journal of Heat and Fluid Flow* , vol.31 , pp. 569 – 575 , 2010.